POLITECNICO DI MILANO

M.Sc. in Civil Engineering for Risk Mitigation

Prediction of Clear-water Local Scour at Bridge Piers

Supervisors

Dr. Alessio Radice

Prof. Silvio Franzetti

Thesis by

Seyed Kamran Jalali 780545

July 2014

POLITECNICO DI MILANO

Prediction of Clear-water Local Scour at Bridge Piers

A Master thesis submitted to Department of Civil and Environmental Engineering in partial fulfillment of the requirements for the degree of Master of Science in Civil Engineering for Risk Mitigation.

Submitted by:

Seyed Kamran Jalali

Student ID: 780545

Supervised by:

Dr. Alessio Radice

Dept. of Civil and Environmental Engineering
Politecnico di Milano
Piazza L. da Vinci, 32, I-20133 Milan

Co-supervised by:

Prof. Silvio Franzetti

Dept. of Civil and Environmental Engineering
Politecnico di Milano
Piazza L. da Vinci, 32, I-20133 Milan

Abstract (English)

The major damage to bridges at river crossings occurs during floods. Damage is caused by various reasons, one of the main ones being riverbed scour at bridge foundations (piers and abutments). The damage can range from minor erosion to complete failure of the bridge structure or its road approach. Complete failure results in severe disruption to local traffic flows.

The localized scour phenomenon and specifically scour at bridge piers has been the subject of extensive investigations by many researchers and vast literature exists on the topic. In spite of this big research effort, comprehensive design approaches are still missing due to a general inability of predictive equations to fit data from different authors. In this thesis, a relatively large amount of local scour data (516 experiments) has been collected from literature works on clear-water scour at cylindrical piers. A great deal of work has been devoted to selecting experiments that were not evidently flawed by some irregularity that could be due to any problem occurred during performance of the tests.

An appropriate dimensionless framework has been introduced to steer the following analysis of literature scour values. It was recognized that different authors made different choices performing their experiments, therefore one of the most important actions undertaken here has been making all the tests homogeneous. The treatment of flow velocity was evidently a crucial factor, thus it was considered with highest attention. In this context, an analysis of threshold condition has been conducted to find a suitable criterion for defining a threshold for sediment movement and the one proposed by Melville & Coleman (2000) was finally chosen as the most suitable one among the other available criteria in literature. In this way the critical velocity for sediment motion of all the experiments was computed by a unique criterion. On the other hand, all the measured upstream flow velocities were unified by converting all the declared values by the different authors to depth-averaged velocity at the channel axis. Thanks to these strategies, all the experiments could be used as a unique, homogeneous database.

The dimensionless scour depth (the ratio between the scour depth and the pier diameter) was investigated in terms of its dependence on flow intensity, sediment coarseness and nondimensional time. A formula has been proposed for prediction of the scour depth. The equation consists of an exponential factor for considering the effect of sediment coarseness and a 3rd order polynomial for the effect of flow intensity; a multiplicative constant accounts for different times. The proposed model is valid for a vast range of flow intensities ($0.48 \leq U \leq 1.39$) and sediment coarseness ratios ($2 \leq D_{50} \leq 325$). Finally, the predictive capability of the present formula has been shown to be better than those of existing literature approaches.

Author keywords: Bridge piers; Local scour; Scour prediction; Flow intensity; Sediment coarseness; Temporal evolution.

Abstract (Italian)

Durante gli eventi alluvionali i ponti fluviali possono essere significativamente danneggiati, o anche distrutti, dai fenomeni di erosione localizzata alla base delle strutture in alveo (pile e spalle), con evidenti conseguenze negative sul sistema viabilistico. I processi erosivi rappresentano una delle cause di maggior rilievo di vulnerabilità dei ponti.

I processi erosive localizzati sono stati oggetto di una vasta ricerca negli ultimi decenni; sfortunatamente, nonostante i notevoli sforzi profusi nello studio, gli strumenti per la previsione della profondità di scavo ancora non consentono di condurre stime affidabili, stante la non capacità delle formule proposte di rappresentare correttamente i dati dei vari autori. In questa tesi sono stati considerati parecchi dati di letteratura (provenienti da 516 prove di laboratorio) relativi all'erosione alle pile circolari in condizioni di acque chiare. La prima importante parte del lavoro ha riguardato un'attenta selezione delle prove che potessero essere in qualche modo inficiate da problematiche occorse durante l'esperimento, risultando in andamenti evidentemente irregolari.

Per l'analisi dei dati sperimentali è stato messo a punto un adeguato inquadramento adimensionale. Riconoscendo che i diversi autori hanno svolto i propri esperimenti a partire da scelte differenti, uno sforzo significativo è stato fatto per rendere i dati confrontabili tra loro. Un aspetto cruciale è stato identificato nella maniera di trattare la velocità del flusso. È stata fatta in primo luogo un'analisi della stima delle condizioni di incipiente movimento, a seguito della quale si è deciso di considerare il criterio proposto da Melville & Coleman (2000) applicandolo a tutti gli esperimenti. In secondo luogo, la velocità del flusso è stata sempre espressa in termini di valore relativo all'asse del canale e mediato sulla verticale, effettuando le opportune conversioni dalla velocità media sulla sezione quando necessario. In questa maniera è stato possibile omogeneizzare i dati in maniera significativa.

È stata analizzata la dipendenza della profondità di scavo (adimensionalizzata sulla dimensione della pila) rispetto alla velocità del flusso, alla dimensione dei sedimenti e al tempo, arrivando a proporre una formula interpolare. L'equazione è composta da un contributo esponenziale per la dimensione dei sedimenti, da un polinomio di terzo grado per l'effetto della velocità del flusso, e da una costante moltiplicativa che tiene conto del tempo. La formula proposta, che si è dimostrata avere un'affidabilità maggiore di quelle delle formule di letteratura attualmente disponibili, è valida in un range i condizioni relativamente ampio ($0.48 \leq U \leq 1.39$; $2 \leq D_{50} \leq 325$).

Author keywords: Pila di ponte; Erosione localizzata; Previsione dell'erosione; Intensità di trasporto; Sedimenti; Evoluzione temporale.

Abstract (Persian)

عمده خسارت های وارده به پلها، در هنگام وقوع سیل اتفاق می افتد. دلایل متعددی برای بروز این خسارات وجود دارد، که آبشستگی بستر رودخانه در ناحیه پی (پایه ها ودیواره ی پل) از عمده ترین آنها به شمار می آید. شدت خسارت های وارده می تواند از آبشستگی جزئی و موضعی تا تخریب کامل اسکلت پل متغییر باشد و در نهایت منجر به ایجاد اختلال در ترافیک منطقه شود.

محققان زیادی در مورد پدیده ی آبشستگی موضعی و خصوصاً آبشستگی پایه پلها تحقیق کرده اند و مقالات متنوعی دراین خصوص به چاپ رسیده است. با وجود مطالعات متعدد در این زمینه، به علت عدم توانایی معادلات ارائه شده برای تخمین مقدار آبشستگی داده های بدست آمده توسط دیگر محققان، کماکان روش جامعی برای طراحی ارائه نشده است. در این پایان نامه اطلاعات زیادی (۵۱۶ آزمایش) از مطالعات وآزمایشات گذشته در مورد آبشستگی در حالت آب زلال پیرامون ستونهای استوانه ای گردآوری شده است. در این میان، آزمایشات با تکامل زمانی نامنظم آبشستگی، که می تواند نشانه ای از وقوع مشکلاتی در اجرا یا اندازه گیری باشد، حذف شده اند.

تحلیل دادهای بدست آمده از منابع متنوع، به کمک انتخاب ترکیب مناسبی از پارامترهای بی بعد صورت گرفته است. با توجه به اختلاف های موجود در نحوه آزمایش دادهای جمع آوری شده از منابع مختلف، همگن سازی آزمایشات از اهمیت خاصی برخوردار است. به علت تأثیر بالای سرعت جریان در پدیده آبشستگی، توجه ویژهای به همگنسازی این پارامتر شده است. در این خصوص، برای تأیین آستانه حمل رسوبات و تعیین روش مناسب برای تخمینن آن، معیارهای موجود در مقالات مختلف مورد تحلیل قرار داده شده اند. در این میان معیار ارائه شده توسط ملویل و کولمن (۲۰۰۰) به عنوان معیار برتر برای تخمین آستانه حمل رسوبات برگزیده و سپس سرعت بحرانی تمام آزمایشات جمع آوری شده، توسط این معیار بدست آورده شد. از سویی دیگر، تمامی مقادیر سرعت جریان اعلام شده توسط مولفان، به منظور یکپارچه سازی هر چه بیشتر داده ها، به سرعت متوسط عمقی در محور کانال تبدیل شدند. در نتیجه با توجه به استراتژی های اتخاذ شده، می توان از آزمایشات جمع آوری شده به عنوان یک پایگاه داده واحد استفاده نمود.

عمق آبشستگی بدون بعد (نسبت بین عمق آبشستگی به قطر ستون) بر اساس وابستگی آن به شدت جریان، زبری رسوبات و زمان بدون بعد مورد بررسی قرار گرفت وسپس معادله ای برای تخمین عمق آب شستگی ارائه شد. این معادله شامل عاملی نمایی برای در نظر گرفتن اثر زبری رسوبات و یک چند جمله ای درجه سه برای در نظر گرفتن اثر شدت جریان می باشد؛ اثر زمانهای مختلف نیز به کمک یک ضریب ثابت به حساب آمده است. مدل ارائه شده برای بازه وسعیی از نسبت شدت جریان (۰٫۴۸ ≤ U ≤ ۱٫۳۹) و زبری رسوبات (۲ ≤ D50 ≤ ۳۲۵) صادق است. در نهایت، با کمک مقایسه برتری مدل ارائه شده نسب به مدلهای موجود در منابع نشان داده شده است.

کلید واژه ها: پایه پل؛ آبشستگی موضعی؛ شدت جریان؛ زبری رسوبات؛ تکامل زمانی.

Acknowledgments

I would like to express my gratitude to my sincere supervisors, Professor Dr. Alessio Radice and Prof. Silvio Franzetti for the constant and useful comments, remarks and engagement through the learning process of this master thesis. I feel motivated and encouraged every time I attend their meeting.

Many friends have helped me stay sane through these difficult years. Their support and care helped me overcome setbacks and stay focused on my graduate study. I greatly value their friendship and I deeply appreciate their belief in me.

Last, but not least, I would like to extend my deepest gratitude to my parents, my sister and my brother without whose love, support and understanding I could never have completed this master degree.

Seyed Kamran Jalali
Politecnico di Milano
July 2014

List of Tables

Table 1.1: Basic bed forms in alluvial channels (classification by increasing flow velocities) ... 25
Table 2.1: Full trend data sources and number for each source..... 38
Table 2.2: Isolated points sources and number for each source. 39
Table 2.3: Sediment properties used in Ettema (1980) experiment..... 42
Table 2.4: Pier size used in Ettema (1980) experiment 42
Table 2.5: Ettema (1980) critical shear velocity definition 43
Table 2.6: Flow, sediment and structure parameters summary 47
Table 2.7: The local scour results summary 48
Table 2.8: VAW pier data- test conditions 51
Table 2.9: VAW Pier Data- summary of test conditions..... 52
Table 2.10: Characteristic controlling variable of Lanca et al. (2013)'s experiment 53
Table 2.11: Summary of Girmaldi (2005) and Simarro et al. (2011) experiment used for validation..... 55
Table 2.12: Sediments characteristics..... 55
Table 2.13: Approach flow characteristics 56
Table 2.14: Chabert, J. and Engeldinger, P. (1956) test characteristic summary 61
Table 2.15: Mignosa, P. (1980) test characteristic summary..... 62
Table 2.16: Franzetti et al (1989) and Azzaroli, D. (1983) tests characteristic summary 64
Table 3.1: Ettema (1980) critical shear velocity definition 67

List of Figures

Figure 1.1: Force acting on a sediment particle (inter-granular forces not shown) 17
Figure 1.2: Diagram of forces acting on a sediment particle in open channel flow (Yang, 1973) 18
Figure 1.3: Experimental data by Shields (1936) 20
Figure 1.4: Shields diagram for incipient motion (Vanoni, 1975) 21
Figure 1.5: Bed-load motion: (a) Sketch of saltation motion (b) definition sketch of bed-load layer 22
Figure 1.6: Suspended-sediment motion by convection and diffusion processes. 24
Figure 1.7: Bed form is movable boundary hydraulics: (a) typical bed forms and (b) bed form motion. 24
Figure 1.8: Total scour and its components 27
Figure 1.9: Schematic representation of scour at a cylindrical pier 27
Figure 1.10: Diagrammatic Flow Pattern at Cylindrical Pier 28
Figure 1.11: (a) Time development of clear-water and live-bed scour (b) scour depth as a function of shear velocity (after Chabert & Engeldinger 1956) 29
Figure 2.1: Cross-section of the working section of 1.52 m wide, flow recirculating, flume by Ettema (1980) 40
Figure 2.2: Cross-section of the working section of the 0.46 m wide flume by Ettema (1980) ... 41
Figure 2.3: Digitization of Ettema (1980) sample 44
Figure 2.4: Schematic drawing of flume used for Sheppard et al.'s (2002) research 45
Figure 2.5: Isometric drawing of the flume 46
Figure 2.6: Definition sketch and measurement points for: (a) pier and (b) abutment. Points defining (●) scour or aggradation depths; (+) scour or aggradation area 50
Figure 2.7: Evolution of dimensionless scour depth at pier nose under steady flow (Chang et al. (2005)) 56
Figure 2.8: Test flume, plan and profile 57
Figure 2.9: Scour data for cylindrical pier 58
Figure 2.10: Uniform sediments size and gradations 59
Figure 2.11: Test flume from Chabert and Engeldinger (1956) 60
Figure 2.12: Scour depth with respect to time trend taken from Franzetti et al.'s (1981) experiment 63
Figure 2.13: Scour depth with respect to time graph taken from Azzaroli, D.'s (1983) experiment 64
Figure 3.1: Comparison of different criteria for computing u_c 70
Figure 3.2: Comparison of different criteria for computing u_c^* 70
Figure 3.3: Comparison of different criteria for deriving shear critical stress with respect to Shields experiments with Re* as x axis 71
Figure 3.4: Comparison of different criteria for deriving shear critical stress with D* as x axis. 71

Figure 3.5: Comparison of measured and calculated values of velocity by means of conversion formula by Paleari (2014) 73
Figure 3.6: Local scour depth variations with respect to flow shallowness 74
Figure 3.7 : An example of test with regular trend 76
Figure 3.8: Disregarded test from Mignosa (1980) and Ettema (1980) due to trend non-regularity 77
Figure 3.9: Selection procedure for dimensionless time, T, equal to 10^5 (a) and 10^6 (b) 78
Figure 3.10: flow regime verification procedure 79
Figure 3.11: The outcomes of regime verification. (a) For T=10^5 (b) For T= 10^6 79
Figure 3.12: presentation of valid tests for T=10^6 on moody diagram 80
Figure 3.13: presentation of valid tests for T=10^5 on moody diagram 80
Figure 3.14: Presentation of valid data for D_{50} with respect to U 81
Figure 3.15: Presentation of valid data for H with respect to U 82
Figure 3.16: Presentation of valid data D_s with respect to T 82
Figure 3.17: Presentation of valid data U with respect to T 83
Figure 3.18: Cumulative distribution function of u^*/u_c^* for valid data 83
Figure 3.19: Cumulative distribution function of dimensionless time for valid data 84
Figure 3.20: Cumulative distribution function of D_s (d_s/b) for valid data 84
Figure 3.21: Presentation of valid data at T=10^5 and T=10^6 in Shield Diagram 85
Figure 3.22: Example of interpolation for finding scour depth (d_s) at requested nondimensional time (T) 86
Figure 3.23: presentation of accepted range and valid tests for assuming that the final scour depth is equal to scour depth at T=10^6 for isolated points data 87
Figure 3.24: D_s with respect to D_{50} divided into groups of U (a) T=10^5 (b) T=10^6 87
Figure 3.25: D_s with respect to U divided into groups of D_{50} (a) T=10^5 (b) T=10^6 88
Figure 3.26: Valid data in D_s-D_{50} space for both T=10^5 and T=10^6 89
Figure 3.27: First attempt for f_2 (D_{50}) at T=10^6 (up) and T=10^5 (down) (0.8<U<1.2) 90
Figure 3.28: First attempt for f_3 (U) at T= 10^6 (up) and T= 10^5 (down) 91
Figure 3.29: Calculated Vs. measured values of D_s at T=10^6 (left) and T=10^5 (right) for the first attempt 92
Figure 3.30: f_2 (D_{50}) obtained from final attempt at T=10^6 (up) and T= 10^5 (down) 93
Figure 3.31: Final attempt for obtaining f_3 (U) with two different equation forms for T=10^6 (up) and T=10^5 (down) 94
Figure 3.32: Comparison of proposed formulas with previous results in literature 95
Figure 3.33: Calculated Vs. measured values of D_s at T= 10^6 (up) and T=10^5 (down) for the final attempt 96
Figure 3.34: Calculated Vs. measured values of D_s at T= 10^6 (up) and T=10^5 (down) using Melville & Chiew (1999) 98
Figure 3.35: Calculated Vs. measured values of D_s at T= 10^6 (up) and T=10^5 (down) using Lanca, et al. (2013) 100

Figure 3.36: Calculated Vs. measured values of D_s at T= 10^6 (up) and T=10^5 (down) using Sheppard et al. (2014) 101
Figure 3.37: Calculated Vs. measured values of D_s at T= 10^6 (up) and T=10^5 (down) using Oliveto and Hager (2002) 103
Figure 3.38: Calculated Vs. measured values of D_s at T= 10^6 (up) and T=10^5 (down) using Oliveto and Hager (2002) and velocity proposed by the authors 104

List of Symbols

ρ: Density of water;

μ: Dynamic viscosity of water;

ν: Kinematic viscosity of water;

γ: Specific weight of water;

g: Acceleration of gravity;

l_c: Width of the channel;

h: Mean approach flow depth;

b: Width of the pier (Diameter of cylindrical pier);

d_s: Local scour depth at time t;

d_{se}: Local scour depth at equilibrium;

d_{50}: Median grain size;

σ: Standard deviation of sediment particle size distribution;

ρ_s: Sediment density;

t: Time;

u: Mean approach flow velocity;

u_c: Mean approach flow velocity at threshold condition for sediment movement;

u^*: Shear velocity;

u_c^*: Critical shear velocity for sediment movement;

R_h: Hydraulic radius of channel;

Re: Reynolds number;

Re_p: Particle Reynolds number;

Fr: Froude number;

D_{50}: Sediment coarseness (b/d_{50});

H: Flow shallowness (h/b);

Δ: Relative submerged weight of sediments;

T: Dimensionless time (t.u/b);

U: Flow intensity (u/u_c); and

D_s: Dimensionless scour depth (d_s/b).

Contents

Abstract (English) 2
Abstract (Italian) 3
Abstract (Persian) 4
Acknowledgments 5
List of Tables 6
List of Figures 7
List of Symbols 10
Introduction 15
1. GENERAL DESCRIPTION & OBJECTIVES 17
1.1. Sediment transport in open channels 17
1.1.1. Introduction 17
1.1.2. Incipient motion of sediments 17
1.1.2.1. Forcing action on sediment particle 17
1.1.2.2. Threshold of sediment movement 18
1.1.2.3. Dimensional analysis 19
1.1.2.4. Shileds diagram 19
1.1.3. Sediment transport mechanism 22
1.1.3.1. Bed-load transport 22
1.1.3.2. Bed-load transport rate 23
1.1.3.3. Suspended-load transport 23
1.1.4. Bed formation 24
1.2. Scour 25
1.2.1. An introduction to scour 25
1.2.2. Contribution to total scour 26
1.2.2.1. Aggradation and Degradation 26
1.2.2.2. General Scour (contraction scour & other general scour) 26
1.2.2.3. Local scour 26
1.2.2.4. Lateral stream migration 26
1.3. Local scour 27

1.3.1. Local scour mechanism 27
1.3.2. Clear-water and Live-bed scour 28
1.3.3. The parameters of local scour at piers 30
1.3.4. Dimensionless analysis of local Scour depth 31
1.3.5. Some existing formula for evaluation of local scour 33
1.4. Objectives 37
2. AVAILABLE DATA AND LITERATURE REVIEW 38
2.1. Introduction 38
2.2. Data Characteristics 39
2.2.1. Full trend scour depth data 39
2.2.1.1. Ettema (1980) 39
2.2.1.2. Sheppard, et al. (2002) 45
2.2.1.3. Oliveto and Hager (2002) 49
2.2.1.4. Lanca, et al. (2013) 52
2.2.1.5. Change et al. (2004) 55
2.2.1.6. Yanmaz and Altinbilek (1991) 57
2.2.1.7. Raikar and Dey (2005) 59
2.2.1.8. Chabert and Engeldinger (1956) 60
2.2.1.9. Mignosa (1980) 61
2.2.1.10. Franzetti et al (1989) 63
2.2.1.11. Azzaroli (1983) 63
2.2.2. Isolated scour depth points 64
3. DATA ANALYSIS 65
3.1. Introduction 65
3.2. Analysis of threshold conditions 66
3.2.1. Introduction 66
3.2.2. Introducing criteria under study 66
3.2.3. Comparisons of different criteria 69
3.3. Velocity Conversion formulas 72
3.4. Data selection 73
3.4.1. Introduction 73

3.4.2. Selection Criteria 74
3.4.3. Flow regime verification 78
3.5. Presentation of valid data 81
3.5.1. Dispersion of valid data 81
3.5.2. Valid data in Shields diagram 84
3.6. Dependency verification 85
3.7. Interpolation with valid data 88
3.7.1. Introduction 88
3.7.2. Initial attempt 88
3.7.3. Further attempts 92
3.7.4. Final attempt 92
3.7.5. Summary of final results 97
3.8. Model comparison with previous studies 97
3.8.1. Melville & Chiew (1999) 97
3.8.2. Lanca et al. (2013) 99
3.8.3. Sheppard et al. (2014) 100
3.8.4. Oliveto and Hager (2002) 102
Conclusions 106
Recommendations for further research 107
References 108
Appendix 1: Summary of full trends and isolated points scour depth data 111
Appendix 2: Interpolation further attempts 125

Introduction

Scour is a natural phenomenon caused by the erosive action of the flowing water on the bed and banks of river and channels. It is the removal of sediments around or near structures located in flowing water. Erosion induces lowering of the riverbed level, with a tendency to expose the foundations of a bridge. Such scour around pier and pile-supported structures and abutments can result in structural collapse and loss of life and property. The construction of bridges in river and channels can cause contraction in the waterway at the bridge cross section and, as a consequence, gives rise to significant scour at that location. As the scour continuously progresses at the site, it undermines the foundations of the structure leading to possible failure.

Many bridges failed around the world because of extreme scour around piers. Failure of bridges due to scour at their foundations, considering both abutments and piers, is a common occurrence. For example, a study of the US Federal Highway Administration in 1973 concluded that of 383 bridge failures, 25% involved pier damage and 72% involved abutment damage.

Prediction of local scour holes at hydraulic structures plays an important role in their design and especially in designing bridge structure. Excessive local scour can progressively make the foundation of the structure weaker and lead to failure of the whole structure. Scour-induced structural failure tends to occur suddenly and without prior warning. Thus, this type of bridge failure threatens serious damage in terms of both economic cost and human life and may severely disrupt traffic flows. Because complete protection against scour is too expensive, generally, the maximum scour depth and the location of the hole have to be predicted to minimize the risk of failure by having a suitable design for facing its series consequences.

The localized scour phenomenon has been the subject of extensive investigations and vast literature exists on the topic. The main aim of this thesis is to investigate and analyze the experimental data that are available in literature on the scour-depth evolution at circular piers. Based on full time series (whenever available) and isolated scour depth points obtained in experiments by several authors and by making them collapse in dimensionless form, an effort has been made to find a predictive equation for scour depth in uniform sediments under clear-water steady flow.

In chapter 1 some general explanation about fundamental subjects relevant to local scour phenomena can be found. This chapter includes some essential information about sediments transport mechanisms, threshold of incipient grain motion, different types of scour, local scour mechanism due to acceleration of flow and resulting vortices. The chapter finally states the general objectives of the work.

The literature experiments, from different authors, that are used in this thesis are presented in chapter 2. The brief review mostly accounts for experimental procedures used, whose knowledge is important understand limitations in experiment unification towards a comprehensive analysis.

In chapter 3, first the key aspects for experiments characterization are identified. A general comparison of different criteria provided by various authors for the purpose of introducing a suitable threshold of sediment movement is presented. This attempt was done based on the fact

that, according to the critical analysis, velocity may be one of the most problematic factors for unifying different experiments as one database. Thus it is necessary to define a unique criterion for computing the velocity for inception of sediment movement for all of the experiments that are going to be used in the analysis. A criterion was finally selected and applied to all the tests under investigation. Afterwards, a strategy which was taken for unifying the velocity measurement among different experiment is explained. The velocity measurement method differs from one experiment to the other one and may be in term of average bulk velocity or depth-averaged velocity. Therefore, for having an integrated database it was necessary to select a suitable velocity measurement method from existing ones and convert velocities which had been measured with a different method. Third, , the imposed restrictions and the motivation of considering them for selecting appropriate tests are discussed. Fourth, The path that was taken for deriving a predictive equation for scour depth is provided: the process of data clustering and curve fitting based on the effective parameters is explained. Finally, the predictive capability of the proposed formula is assessed in comparison with that of some of the existing ones in the literature.

A summary of major outcomes and conclusions completes the work.

A summary of the data that have been used in this study can be found in Appendix 1. In Appendix 2, more details are provided about the regression procedure towards the final predictive equation.

Chapter 1

GENERAL DESCRIPTION & OBJECTIVES

1.1. Sediment transport in open channels

1.1.1. Introduction

Waters flowing in natural streams and rivers have the ability to scour channel beds, to carry particles (heavier than water) and to deposit materials, hence changing the bed topography. This phenomenon is of great economical importance specially to predict the risks of scouring of bridges.

The transported material is called the sediment load. Distinction is made between the bed load and the suspended load. The bed load characterizes grains rolling, sliding or saltation along the bed while suspended load refers to grains maintained in suspension by turbulence.

1.1.2. Incipient motion of sediments

1.1.2.1. Forcing action on sediment particle

For an open channel flow with a movable bed, the forces acting on each sediment particle are (Figure 1.1):

- the gravity force $\rho_s g v_s$
- the buoyancy force $F_b = \rho g v_s$
- the drag force $C_D A_s V^2/2$
- the lift force $C_L \rho A_s V^2/2$
- the reaction forces of the surrounding grain,

Where v_s is the volume of the particle, A_s is a characteristic particle cross-sectional area, C_D and C_L are the drag and lift coefficients, respectively, and V is a characteristic velocity next to the channel bed. The gravity force and the buoyancy force act both in the vertical direction while the drag force acts in the flow direction and the lift force in the direction perpendicular to the flow direction.

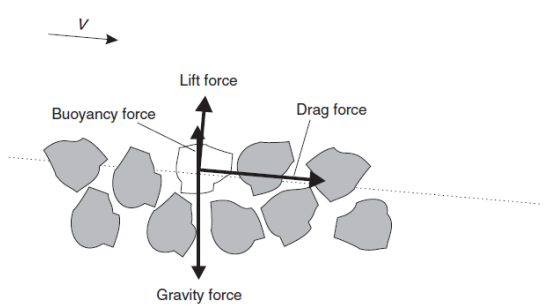

Figure 1.1: Force acting on a sediment particle (inter-granular forces not shown)

1.1.2.2. Threshold of sediment movement

Incipient motion is important in the study of sediment transport, channel degradation, and stable channel design. Due to the stochastic nature of sediment movement along an alluvial bed, it is difficult to define precisely at what flow condition a sediment particle will begin to move. Consequently, it depends more or less on an investigator's definition of incipient motion. They use terms such as “initial motion,” “several grain moving,” “weak movement,” and “critical movement!” In spite of these differences in definition, significant progress has been made on the study of incipient motion, both theoretically and experimentally. Figure 1.2 shows the forces acting on a spherical sediment particle at the bottom of an open channel. For most natural rivers, the channel slopes are small enough that the component of gravitational force in the direction of flow can be neglected compared with other forces acting on a spherical sediment particle. The forces to be considered are the drag force F_D, lift force F_L, submerged weight W_s, and resistance force F_R. A sediment particle is at a state of incipient motion when one of the following conditions is satisfied:

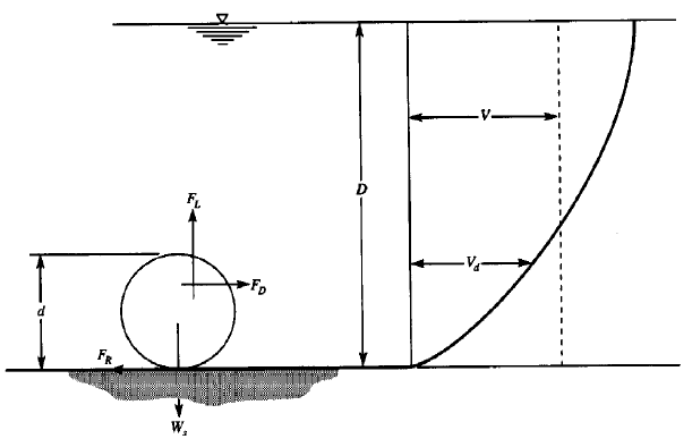

Figure 1.2: Diagram of forces acting on a sediment particle in open channel flow (Yang, 1973)

$F_L = W_s$ (1.1)

$F_D = F_R$ (1.2)

$M_O = M_R$ (1.3)

Where M_O = overturning moment due to F_D and F_L

M_R = resisting moment due to F_L and W_s

1.1.2.3. Dimensional analysis

The relevant parameters for the analysis of sediment transport threshold are the bed shear stress τ_0, the sediment density ρ_s, the fluid density ρ, the grain diameter d_S, the gravity acceleration g and the fluid viscosity μ,

$$f_1(\tau_0, \rho, \rho_s, \mu, g, d_S) = 0 \qquad (1.4)$$

In dimensionless terms, it yields,

$$f_2\left(\frac{\tau_0}{\rho g\, d_S}, \frac{\rho_s}{\rho}, \frac{d_S\sqrt{\rho\tau_0}}{\mu}\right) = 0 \qquad (1.5)$$

The ratio of the bed shear stress to fluid density is homogeneous (in units) with a velocity squared. Introducing the shear velocity u* defined as:

$$u^* = \sqrt{\frac{\tau_0}{\rho}} \qquad (1.6)$$

In this way we can have an equation in the form of:

$$f_3\left(\frac{u^*}{\sqrt{g\, d_S}}; \frac{\rho_s}{\rho}; \rho\, \frac{d_S u^*}{\mu}\right) = 0 \qquad (1.7)$$

The first term is a form of Froude number. The second is the relative density (also called specific gravity). The last term is a Reynolds number defined in terms of the grain size and shear velocity. It is often denoted as Re* and called the shear Reynolds number or particle Reynolds number.

1.1.2.4. Shileds diagram

Most incipient motion criteria are derived from either a shear stress or a velocity approach. One of the most prominent and widely used incipient motion criteria is the Shields diagram (1936) based on shear stress. Shields framework is consistent with dimensional analysis in section 1.1.2.3. The mentioned quantitates can be grouped into two dimensionless quantities, namely,

$$Re^* = d_s\, \frac{(\frac{\tau_c}{\rho_f})^{1/2}}{\nu} = \frac{dU_*}{\nu} \qquad (1.8)$$

and,

$$\tau^* = \frac{\tau_0}{d_s(\rho_s - \rho_f)g} = \frac{\tau_0}{d_s[\left(\frac{\rho_s}{\rho_f}\right) - 1]} = \frac{u_*^2}{g d_s(s-1)} \qquad (1.9)$$

Where:

ρ_s *and* ρ_f=densities of sediment and fluid, respectively

γ= specific weight of water,

ν=fluid kinematic viscosity,

g=gravity,

u_*=shear velocity, and

τ^*= stability parameter or shields parameter

Re^*= Shear Reynolds number

Critical value of the stability parameter may be defined at the inception of bed motion: i.e.

$$\tau^* = (\tau^*)_c \qquad (1.10)$$

Bed load motion occurs for:

$$\tau^* > (\tau^*)_c \qquad (1.11)$$

The relationship between these two parameters is then determined experimentally. Figure 1.3 shows the experimental data which was obtained by Shields during the experiment and Figure 1.4 shows the experimental results obtained by Shields and other investigators at incipient motion. Any point in region above the curve indicates the situation of particle movement. In region below the curve, the flow is unable to move the particles.

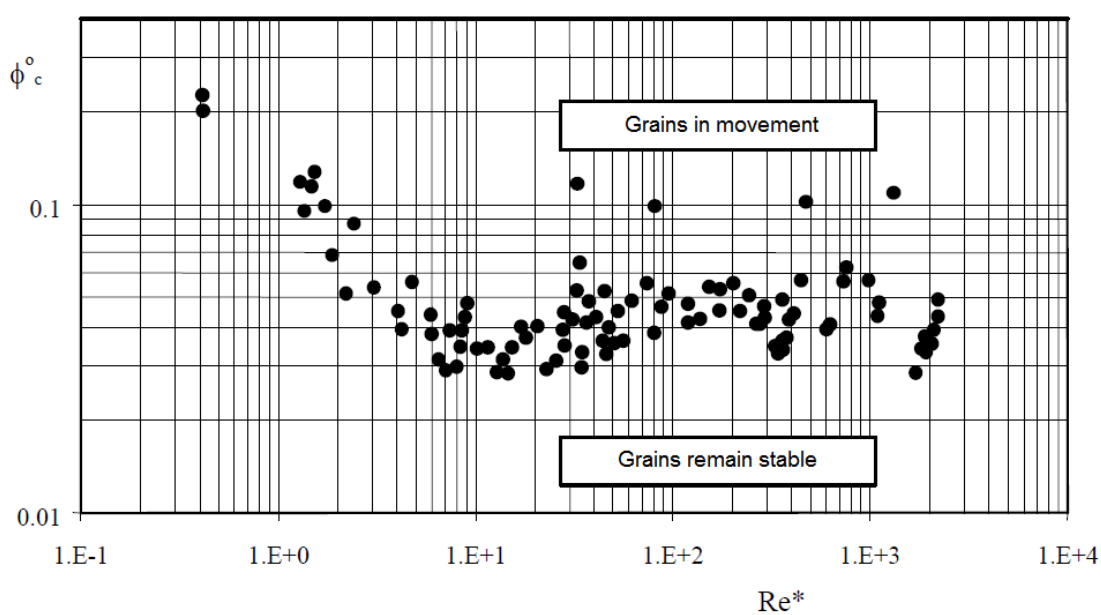

Figure 1.3: Experimental data by Shields (1936)

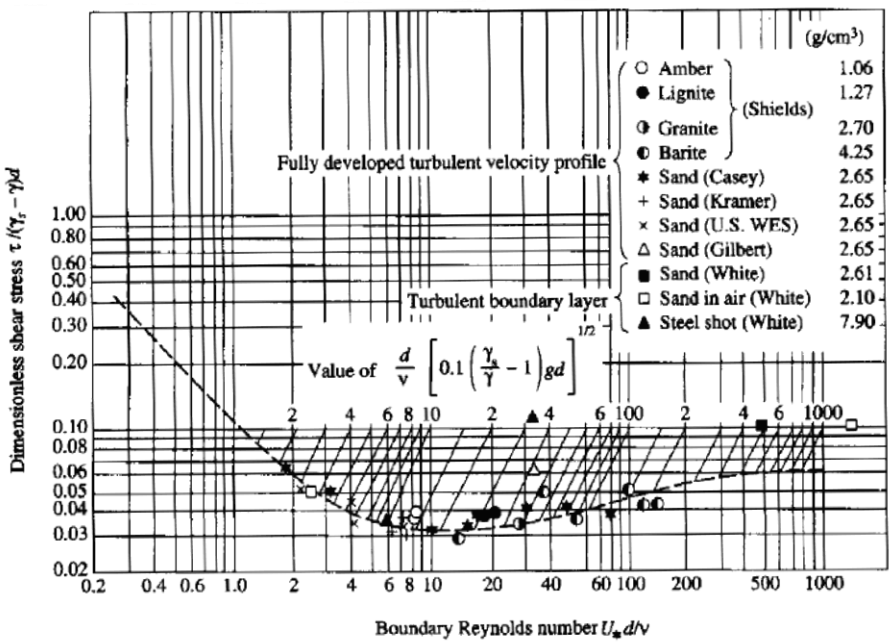

Figure 1.4: Shields diagram for incipient motion (Vanoni, 1975)

Thus the critical shields parameter is:

$$\tau_c^* = \frac{\tau_c}{\rho \Delta g . d_{50}} \qquad (1.12)$$

And the critical grain Reynolds number is:

$$R_{*c} \equiv \sqrt{\frac{\tau_c d_{50}^2}{\rho \nu^2}} \qquad (1.13)$$

Where: $\Delta = \frac{\rho_s}{\rho} - 1$ (1.14)

On the Shields diagram (Fig. 1.4), the Shields parameter and the particle Reynolds number are both related to the shear velocity and the particle size. Some researchers proposed a modified diagram: τ_c^* as a function of a dimensionless particle parameter d_*. In this way, the above equation can be manipulated and alternatively written as:

$$\tau_{*c} = f(d_*) \qquad (1.15)$$

Where d_* is the dimensionless sediment size defined as:

$$d_* = \sqrt[3]{R_{*c}^2/T_{*c}} = \sqrt[3]{g\Delta d_{50}^3/\nu^2} \qquad (1.16)$$

The second equation is usually preferred to original one because the critical shear stress appears only in one dimensionless parameter.

1.1.3. Sediment transport mechanism

There are two types of sediment transport mechanisms. Transported sediment material that is maintained in suspension and sediment material transported by rolling, sliding and saltation motion along the bed.

1.1.3.1. Bed-load transport

When the bed shear stress exceeds a critical value, sediments are transported in the form of bed load and suspended load. For bed-load transport, the basic modes of particle motion are rolling motion, sliding motion and saltation motion. (Figure 1.5)

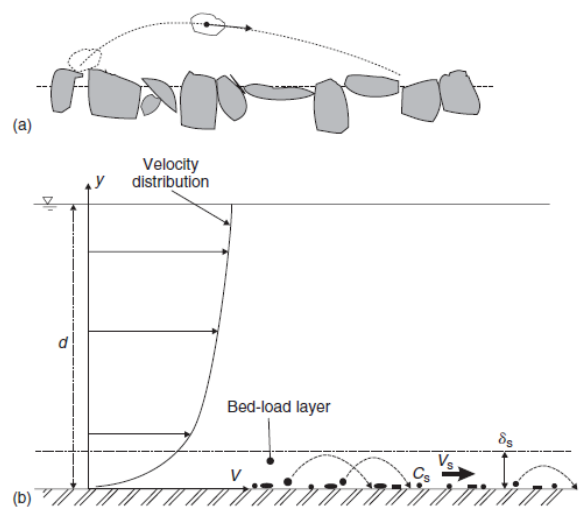

Figure 1.5: Bed-load motion: (a) Sketch of saltation motion (b) definition sketch of bed-load layer

The sediment transport rate may be measured by weight (units: N/s), by mass (units: kg/s) or by volume (units: m^3/s). In practice the sediment transport rate is often expressed by meter width and is measured either by mass or by volume. These are related by:

$$\dot{m}_s = \rho_s q_s \qquad (1.17)$$

Where $\dot{m}_s$ is the mass sediment flow rate per unit width, q_s is the volumetric sediment discharge per unit width and ρ_s is the specific mass of sediment.

1.1.3.2. Bed-load transport rate

The bed-load transport rate per unit width may be defined as:

$$q_s = C_s \delta_s V_s \qquad (1.18)$$

Where V_s is the average sediment velocity in the bed-load layer (Fig.1.5 (b)). Physically the transport rate is related to the characteristics of the bed-load layer; its mean sediment concentration C_s, its thickness s, which is equivalent to the average saltation height measured normal to the bed, and the average speed V_s of sediment moving along the plane bed.

1.1.3.3. Suspended-load transport

The other type of sediment transport mechanism is suspended-load transport. Although this type of sediment transport mechanism is not too relevant with the topic of this study, but it will be briefly discussed in this section for the sake of completeness.

Sediment suspension can be described as the motion of sediment particles during which the particles are surrounded by fluid. The grains are maintained within the mass of fluid by turbulent agitation without (frequent) bed contact. Sediment suspension takes place when the flow turbulence is strong enough to balance the particle weight. The amount of particles transported by suspension is called the suspended load.

The transport of suspended matter occurs by a combination of advective turbulent diffusion and convection. Advective diffusion characterizes the random motion and mixing of particles through the water depth superimposed to the longitudinal flow motion. In a stream with particles heavier than water, the sediment concentration is larger next to the bottom and turbulent diffusion induces an upward migration of the grains to region of lower concentrations. A time-averaged balance between settling and diffusive flux derives from the continuity equation for sediment matter:

$$D_s \frac{dC_s}{dy} = -w_0 C_s \qquad (1.19)$$

Where C_s is the local sediment concentration at a distance y measured normal to the channel bed, D_s is the sediment diffusivity and w_0 is the particle settling velocity. Sediment motion by convection occurs when the turbulent mixing length is large compared to the sediment distribution length scale. Convective transport may be described as the entrainment of sediments by very large scale vortices: e.g. at bed drops, in stilling basins and hydraulic jumps (Fig 1.6).

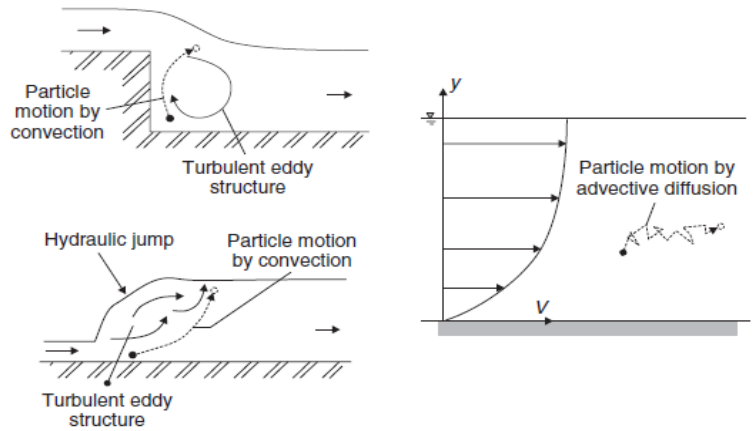

Figure 1.6: Suspended-sediment motion by convection and diffusion processes.

1.1.4. Bed formation

In most practical situations, the sediments behave as a non-cohesive material (e.g. sand and gravel) and the fluid flow can distort the bed into various shapes. The bed form results from the drag force exerted by the bed on the fluid flow as well as the sediment motion induced by the flow onto the sediment grains. This interactive process is complex.

The basic bed forms which may be encountered are the ripples (usually of heights less than 0.1 m), dunes, flat bed, standing waves and antidunes. The typical bed forms are summarized in Figure 1.7 and Table 1.1.

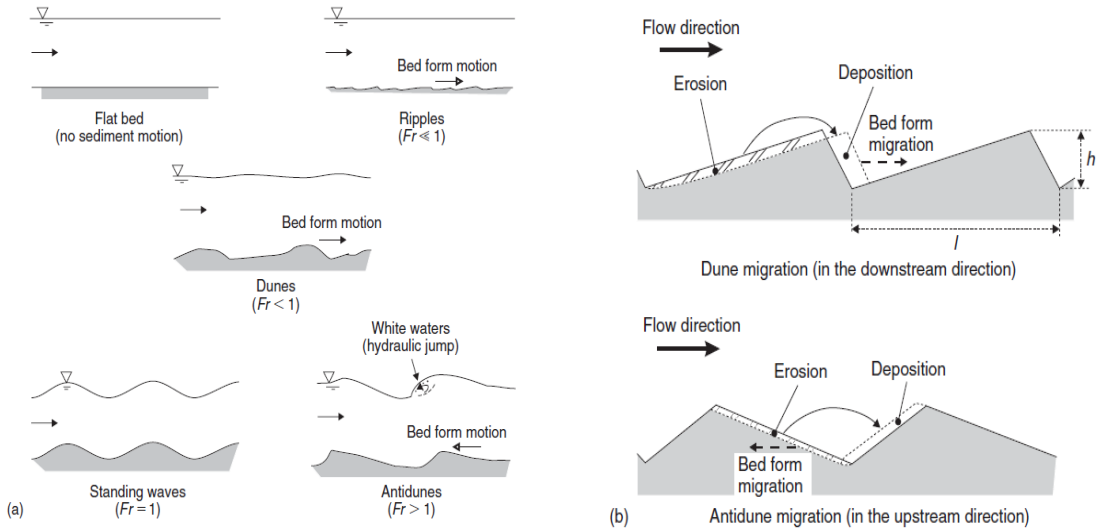

Figure 1.7: Bed form is movable boundary hydraulics: (a) typical bed forms and (b) bed form motion.

Bed form (1)	Flow (2)	Bed form motion (3)	Comments (4)
Flat bed	No Flow (or $Fr \ll 1$)	NO	No sediment motion
Ripples	$Fr \ll 1$	D/S	Three-dimensional forms; observed also with air flows (e.g. sand ripples in a beach caused by wind)
Dunes	$Fr < 1$	D/S	Three-dimensional forms; sand dunes can also be caused by wind
Flat bed	$Fr \leq 1$	NO	Observed also with wind flow
Standing waves	$Fr = 1$	NO	Critical flow conditions; bed standing waves in phase with free-surface standing waves
Antidunes	$Fr > 1$	U/S	Supercritical flow with tumbling flow and hydraulic jump upstream of antidune crests
Chute-pools	$Fr > 1$	U/S	Very active antidunes
Step-pools	$Fr > 1$	–	Cascade of steps and pools; steps are often caused by rock bed

References: Henderson (1966) and Graf (1971).
Notes: D/S = in downstream flow direction; Fr = Froude number; U/S = in upstream flow direction.

Table 1.1: Basic bed forms in alluvial channels (classification by increasing flow velocities)

1.2. Scour

1.2.1. An introduction to scour

Scour is the result of the erosive action of flowing water, excavating and carrying away material from the bed and the bank of streams and from around the piers and abutments of bridges. Different materials scour at different rates. Loose soils are tending to scour more rapidly than cohesive or cemented soils which are more scour-resistant. However ultimate scour in both cases can be as deep as each other. Under constant flow condition, scour will increase with respect to time and reach to a nearly constant maximum depth after a period of time. Under flow conditions typical of actual bridge crossings, several floods may be needed to attain maximum scour. Determining the magnitude of scour is complicated by the cyclic nature of some scour processes.

The equations for estimating scour depth time history or equilibrium scour depth are based on laboratory experiments with limited field verification. Uncertainty in predicting scour still remains in all of the equations that were published in literature. But the attempt of decreasing the amount of uncertainty and remaining in the safe side for the estimation of scour depth during all of the researches can be observed.

One of the most important factors for estimation of scour depth is whether it is clear-water or live-bed scour. Clear-water scour occurs where there is no transport of bed material upstream of crossing bridge and live-bed scour occurs where there is transport of bed material from the upstream reach into the crossing. A more detailed discussion is presented in the following sections.

1.2.2. Contribution to total scour

Total scour at a bridge crossing considers three primary components:

- Long-term degradation of the river bed;
- General scour at bridge: a. Contraction scour b. Other general scour,
- Local scour at the piers and abutments.

Total scour and its components are illustrated in figure 1.8.

1.2.2.1. Aggradation and Degradation

Aggradation and degradation are long-term elevation changes due to the natural or man-induced causes which can be affect the reach of the river on which the bridge is located. Aggradation involves the deposition of material eroded from the channel or watershed upstream of the bridge; whereas, degradation involves the lowering or scouring of the streambed due to a lack in sediment supply from upstream.

1.2.2.2. General Scour (contraction scour & other general scour)

General scour is a lowering of the streambed across the stream or waterway bed at bridge. This lowering may be uniform across the bed or non-uniform, that is, the depth of scour may be deeper in some part of the cross section. General scour may result from contraction of the flow, which results in removal of material from the bed across all or most of the channel width, or from other general scour conditions such as flow around a bend where the scour may be concentrated near the outside of the bend. General scour is different from long-term degradation in that general scour may be cyclic and/or related to the passing of a flood.

1.2.2.3. Local scour

Local scour, which is the target of this study specifically among other types of scour, involves removal of material from around piers, abutments, spurs, and embankments. It is caused by an acceleration of flow and resulting vortices induced by obstruction to the flow. Local scour can be either clear-water or live-bed scour. Local scour may occur even where general and constriction scour are not present.

1.2.2.4. Lateral stream migration

In addition to the types of scour mentioned above, naturally occurring lateral migration of the main channel of a stream within a floodplain may affect the stability of piers in a floodplain, erode abutments or the approach roadway, or change the total scour by changing the flow angle of attack at piers and abutments. Factors that affect lateral stream movement also affect the stability of a bridge foundation. These factors are the geomorphology of the stream, location of the crossing on the stream, flood characteristics, and the characteristics of the bed and bank materials.

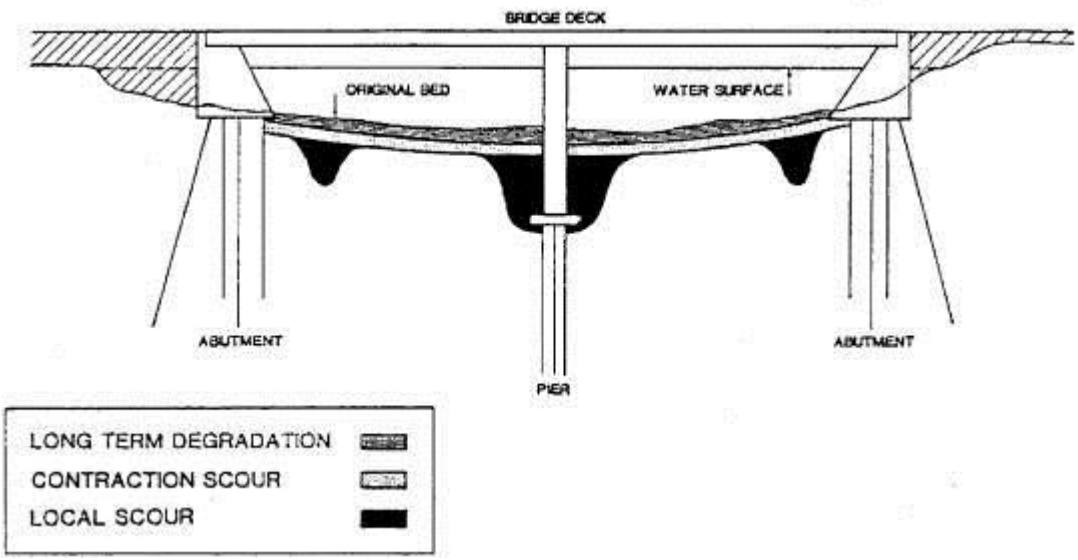

Figure 1.8: Total scour and its components

1.3. Local scour

The following section provides more detailed discussion of the local scour at piers which is the main goal of this research.

1.3.1. Local scour mechanism

The basic mechanism causing local scour at piers or abutments is the formation of vortices (known as the horseshoe vortex) at their base (Figure 1.9). The horseshoe vortex results from the pileup of water on the upstream surface of the obstruction and subsequent acceleration of the flow around the nose of the pier or abutment.

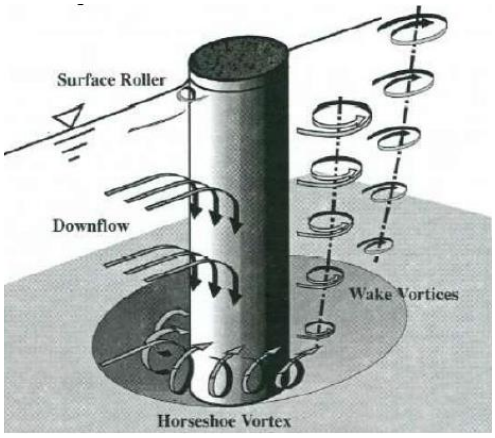

Figure 1.9: Schematic representation of scour at a cylindrical pier

The approach flow velocity goes to zero at the upstream face of the cylinder, in the vertical plane of symmetry, and since the approach flow velocity decreases from the free surface downward to zero at the bed, the stagnation pressure, $\rho u^2/2$, also decreases. This downward pressure gradient drives the downflow (Figure 1.9). The downflow, in the vertical plane of symmetry, has at any elevation a velocity distribution, with zero in contact with the cylinder and again some distance upstream of it. The so-called horseshoe vortex develops as the result of separation of flow at the upstream rim of the scour hole. The horseshoe vortex extends downstream, past of the sides of the pier, for a few pier diameters before losing its identity and becoming part of general turbulence. The horseshoe vortex also pushes the maximum downflow velocity within the scour hole closer to the pier. The action of the vortex removes bed material from around the base of the obstruction. The transport rate of sediment away from the base region is greater than the transport rate into the region, and, consequently, a scour hole develops. As the depth of scour increases, the strength of the horseshoe vortex is reduced, thereby reducing the transport rate from the base region. Eventually, for live-bed local scour, equilibrium is reestablished between bed material inflow and outflow and scouring ceases. For clear-water scour, scouring ceases when the shear stress caused by the horseshoe vortex equals the critical shear stress of the sediment particles at the bottom of the scour hole**.**

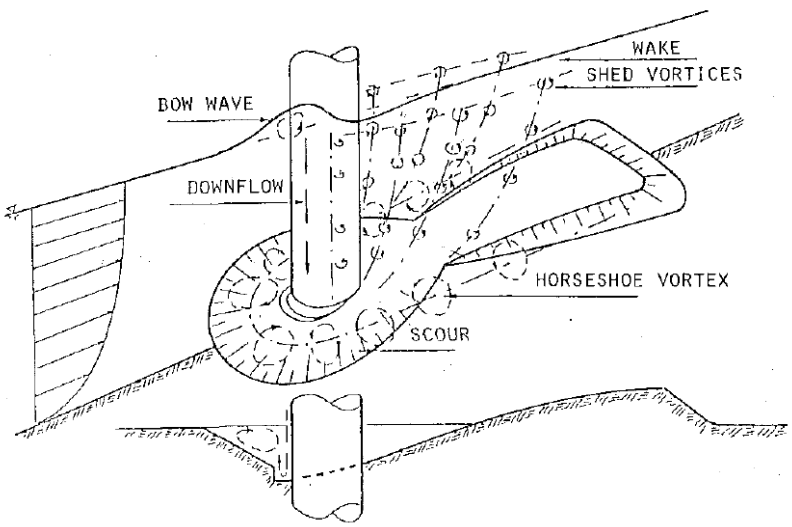

Figure 1.10: Diagrammatic Flow Pattern at Cylindrical Pier

In addition to the horseshoe vortex around the base of a pier, there are vertical vortices downstream of the pier called the wake vortices (Figure 1.10). Both the horseshoe and wake vortices remove material from the pier base region. However, the intensity of wake vortices decrease rapidly as the distance downstream of the pier increases. Therefore, immediately downstream of a long pier there is often deposition of material.

1.3.2. Clear-water and Live-bed scour

Local scour at a pier commences when the shear velocity u* or velocity u exceeds a fraction of the critical or threshold value for movement of the sediment. There are two conditions for contraction and local scour, clear-water and live-bed scour. Clear-water scour occurs when there

is no movement of the bed material in the flow upstream of the crossing or the bed material being transported in the upstream reach is transported in the suspension through the scour hole at the pier or abutment at less than the capacity of the flow. In clear water condition velocity is below the critical velocity and there is no sediment transport and no sediment supply into the scour hole from upstream .At the pier or abutment the acceleration of the flow vortices created by these obstructions cause the bed material around them to move. Live-bed scour occurs when there is transport of bed material around them to move. Live-bed local scour is cyclic in nature; that is, the scour hole that develops during the rising stage of a flood refills during falling stage.

Typical clear-water scour situation (1) coarse-bed material streams, (2) flat gradient streams during low flow, (3) local deposition of larger bed materials that are larger than the biggest fraction being transported by the flow (rock riprap is a special case of this situation), (4) armored streambeds where the only location that tractive forces are adequate to penetrate the armor layer are at piers and/or abutments, and (5) vegetated channel or overbank areas.

During a flood event, bridge over streams with coarse-bed material are often subjected to clear-water scour at low discharge, live-bed scour at the higher discharges and clear-water scour at low discharges on the falling stages. Clear-water scour reaches its maximum over a longer period of time than live-bed scour (Figure 1.11). In fact, local clear-water scour may not reach a maximum until after several floods and reach to its equilibrium asymptotically over a period of days. Live-bed scour develops rapidly and its depth fluctuates in response to the passage of bed features. (Figure 1.11(a)). This is due to the variability of the bed material sediment transport in the approach flow when the bed configuration of the stream is dunes. Shen et al. (1969) suggested that the mean value of the live-bed scour depth was about 10% less than the maximum clear-water scour depth (Figure 1.11(b)).

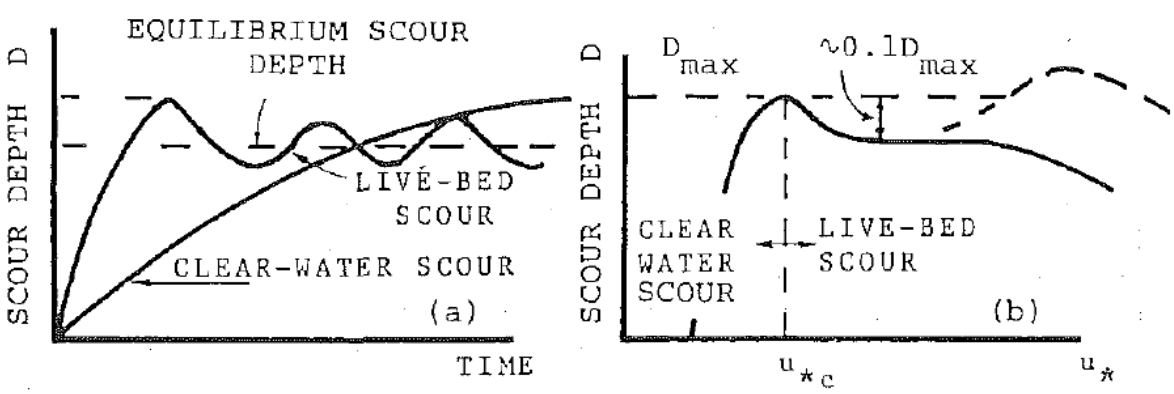

Figure 1.11: (a) Time development of clear-water and live-bed scour (b) scour depth as a function of shear velocity (after Chabert & Engeldinger 1956)

Critical velocity equations with the reference particle size equal to d_{50} can be used to determine the velocity associated with the initiation of motion. They are used as an indicator for clear-water or live-bed scour conditions. If the mean velocity (u) in the upstream reach is equal to or less than the critical velocity (u_c) of the median diameter (d_{50}) of the bed material, then

contraction and local scour will be clear-water scour. If the mean velocity is greater than the critical velocity of the median bed material size, live-bed scour will occur.

1.3.3. The parameters of local scour at piers

Factors which affect the magnitude of local scour depth at piers can be stated as a general function of fluid, flow, pier and sediment properties and time evolution.

- **Fluid:** In mechanics a fluid is defined by its density ρ, kinematic viscosity ν, at temperature *T*.

- **Flow:** The flow of a fluid is determined by its mean depth h, energy slope s_0, and the acceleration due to gravity g which generates the flow. The slope s_0, which produces through the component of gravity the shear stress, τ, to maintain the flow, is more suitably replaced by the shear velocity $u_* = \sqrt{g.h.s_0}$

Flow velocity also affects local scour depth. The greater the velocity, the deeper the scour will be. There is a high probability that scour is affected by whether the flow is subcritical or supercritical. However, most research data are for subcritical flow (i.e., flow with a Froude Number less than 1.0, Fr < 1).

- **Pier:** The action of pier is determined by the effective blockage it presents to the flow. A cylindrical pier is defined by its diameter b. Other shaped piers are specified relative to b in terms of shape factors. Consideration also can be made by introducing some factors for the angle of the approach flow to the pier. As pier width increases, there is an increase in scour depth. There is a limit to the increase in scour depth as width increases.

Pier length has no appreciable effect on local scour depth as long as the pier is aligned with the flow. When the pier is skewed to the flow, the pier length has a significant influence on scour depth. For example, doubling the length of the pier increases scour depth from 30 to 60 percent (depending on the angle of attack).

- **Sediment:** A layer of uniform cohesionless bed material of specific thickness is described by the specific gravity and the sieve diameter of its particles. The degree of uniformity of particle size distribution of a sediment is defined by the value of its standard deviation, σ. The most common and convenient measure of standard deviation used in studies of the distribution of particle size of a sediment is the graphic standard deviation, which is derive by reading two values on the cumulative particle size curve,

$$\sigma = \sigma_g = \left(\frac{d_{84.1}}{d_{15.9}}\right)^{0.5} = \frac{d_{84.1}}{d_{50}} = \frac{d_{50}}{d_{15.9}} \qquad (1.20)$$

The inclusive graphic standard deviation of Folk (1968) gives a better measure of the uniformity of a sediment as it embraces 90 percent of distribution which is used in some of the studies:

$$\sigma_I = \left(\frac{d_{84.1}}{d_{15.9}}\right)^{0.250} . \left(\frac{d_{95}}{d_5}\right)^{0.152} \qquad (1.21)$$

According to Ettema (1980), bed material in the sand-size range has little effect on local scour depth. Likewise, larger size bed material that can be moved by the flow or by the vortices and turbulence created by the pier or abutment will not affect the maximum scour, but only the time it takes to attain it. Very large particles in the bed material, such as coarse gravels, cobbles or boulders, may armor the scour hole. Fine bed material (silts and clays) will have scour depths as deep as sand-bed streams. This is true even if bonded together by cohesion. The effect of cohesion is to influence the time it takes to reach maximum scour. With sand-bed material the time to reach maximum depth of scour is measured in hours and can result from a single flood event. With cohesive bed materials it may take much longer to reach the maximum scour depth, the result of many flood events.

Bed configuration of sand-bed channels affects the magnitude of local scour. In streams with sand-bed material, the shape of the bed (bed configuration) may be ripples, dunes, plane bed and etc. The bed configuration depends on the size distribution of the sand-bed material, hydraulic characteristics, and fluid viscosity. The bed configuration may change from dunes to plane bed during an increase in flow for a single flood event. It may change back with a decrease in flow. The bed configuration may also change with a change in water temperature or suspended sediment concentration of silts and clays. The type of bed configuration and change in bed configuration will affect flow velocity, sediment transport, and scour.

- **Time:** Scour is a dynamic process which seeks to establish a new equilibrium, between the flow of the fluid and the resistance to motion of the bed particles, by the erosion of the flow boundary; the local scour deepens progressively with time.

In summary, the down-flow impingement on the bed, along with the wide range of turbulence structures present in the flow field, entrain and transport material from the scour hole. The details and interaction of the flow field vary with pier characteristics such as shape, angle of attack, and the stage of scour development between initiation and equilibrium, but the essential consideration is that these flow features are responsible for scour.

1.3.4. Dimensionless analysis of local Scour depth

The large number of interacting parameters makes the analysis of local scour at bed sediment around a bridge pier very difficult. This has forced the researchers to use of dimensional analysis. However the dimensional analysis is only a technique for grouping of variables, and yields in itself no information. The relation between the depth of local scour at a bridge pier d_s, and its dependent parameters can be written:

$$\boldsymbol{d_s = f_1(Flood\ Flow(\rho, \mu, h, g, u, l_c), Bed\ Sediment(d_{50}, \sigma, \rho_s), Bridge\ Pier\ Geometry\ (b), Time(t))} \qquad (1.22)$$

Where,

$\rho =$ fluid density;

μ = fluid dynamic viscosity;

h = mean approach flow depth;

g= acceleration of gravity;

u= mean approach flow velocity;

d_{50}= median size;

$\sigma =$ geometric standard deviation of the sediment particle size distribution ;

$\rho_s =$ sediment density;

$b =$ pier width;

$l_c =$ width of the flow; and

$t =$ time.

An expression for the depth of local scour at a cylindrical pier of diameter *b* can be written as a combination of dimensionless parameters:

$$\frac{d_s}{b} = f_2(\frac{\rho u h}{\mu}, \frac{u}{\sqrt{gh}}, \frac{l_c}{h}, \frac{h}{b}, \frac{b}{d_{50}}, \sigma, \frac{\rho_s - \rho}{\rho}, \frac{tu}{b}) \qquad (1.23)$$

Where we can substitute these terms by consider the following definitions:

$\Delta = \frac{\rho_s - \rho}{\rho} =$ relative submerged weigh of sediments

Considering Reynolds number (Re) that is being used as a criterion to distinguish between laminar and turbulent flow and is a measure of the ratio of the inertia force on an element of fluid to the viscous force on an element and is equal to:

$$Re = \frac{\rho u l}{\mu} \qquad (1.24)$$

Where *l* is a characteristic length. Thus, particle Reynolds number can be written as:

$$Re_p = \frac{d_{50}\sqrt{\frac{\rho_s - \rho}{\rho}.\mathrm{gd}_{50}}}{\nu} \qquad (1.25)$$

Froude number (Fr) is also defining as a measure of the ratio of the inertia force on an element of fluid to the weight of the element and it is equal to:

$$Fr = \frac{V}{\sqrt{gh}} \qquad (1.26)$$

As mentioned before, the Shield diagram defines a u_c^* for a given d_{50}. A corresponding u_c can be found for the given flow depth, and thus the Froude number can be written, using the given data as u/u_c.

Thus the equation (1.23) can be rewritten as:

$$\frac{d_s}{b} = f_3(Re, \frac{l_c}{h}, \frac{h}{b}, \frac{u}{u_c}, \frac{b}{d_{50}}, \sigma, \Delta, \frac{tu}{b}) \qquad (1.27)$$

The density ratio is assumed constant, and the Reynolds number influences are assumed negligible for the highly turbulent flows envisaged. On the other hand, the effect of width of the flow, l_c, in wide flows can be neglected and also by considering uniform sediment it is possible to disregard the dependency to σ. Therefore, the other form which can represent the scour depth as the function of dimensionless parameters is:

$$D_s = f(U, H, D_{50}, T) \qquad (1.28)$$

Where: $U = \frac{u}{u_c}, H = \frac{h}{b}, D_{50} = \frac{b}{d_{50}}$ $and\ T = \frac{tu}{b}$

The functional relationships between dimensionless variables have to be obtained from experiments, but when the number of dimensionless numbers is large severe experimental problems occur. In this way the relationship between the four parameters mentioned above can be obtained by less effort and in a more economical manner.

1.3.5. Some existing formula for evaluation of local scour

In literature, it is possible to find several empirical or semi-empirical formulas for the determination of the scour depth at equilibrium condition (final stage) or with respect to time evolution. The differences in theses formulas are mostly due to their various experimental conditions. Moreover, the validity range of existing formulas in literature is not similar for all of them. This is the consequence of the difference in selection of the under consideration range for dependent parameters of these studies. In addition, it is necessary to have constant values of different effective parameters when the dependency of two parameters on each other is under study. In some cases the mentioned required stability condition is failed and put a negative effect on the accuracy of the final proposed formula. This dispersion in resulting formula by different authors shows that scour depth determination is not clearly defined yet.

Each formula is only valid for the limited range of the author's studies and cannot be extended to other conditions such as different pier size, river width and flow velocity outside of the mentioned range by the author.

In literature there are many authors who have expressed the dimensionless Scour depth D_s as a function of multiplication of different factor in which each of them take into account the dependency of specific parameter. One of the most relevant combinations is as below:

$$D_s = K_1(T).K_2(U).K_3(H).K_4(D_{50}) \qquad (1.29)$$

Where $K_1, K_2, K_3 and\ K_4$ define empirically through interpolation of the results usually independently. It should be noted that, other factors rather than those mentioned here also can be considered.

Below, they are few definitions of the mentioned factors define by various authors:

- **Franzetti et al (1994)**

$K_T = 1 - e^{(-0.028T^{\frac{1}{3}})}$

$K_U = 1 - 10(1 - U)^3$ $\quad$ $0.67 \leq U \leq 1$

$K_H = 1 - e^{(1.3.H)}$ $\quad$ $H \geq 2$

$K_{D_{50}} = 3.868.D_{50}^{1.572}.e^{[-2.64(D_{50})^{0.234}}$

- **Chiew (1995)**

$K_U = 3.77\,U - 1.13$ $\quad$ $0.3 \leq U \leq 1$

$K_{D_{50}} = 0.398\ \ln(D_{50}) - 0.034[\ln(D_{50})]^2$ $\quad$ $1 \leq D_{50} \leq 50$

$K_{D_{50}} = 1$ $\quad$ $D_{50} \geq 50$

$K_H = 0.783[(D_0)]^{0.322} - 0.106$ $\quad$ $0 < H < 3$

$K_H = 1$ $\quad$ $H \geq 3$

- **Dey et al. (1999)**

$K_U = [21.28\,U^{3.508} - 1]^{0.5}$ $\quad$ $0.42 \leq U \leq 1$

$K_H = (H)^{0.15}$

- **Melville and Chiew (1999)**

$K_U = U$ $\quad$ $U < 1$

$K_U = 1$ $\quad$ $U > 1$

$K_H = 2.4\,H$ $\quad$ $H < 0.7$

$K_H = 2.H^{0.5}$ $\quad$ $0.7 < H < 5$

$K_H = 4.5\,H$ $\quad$ $H > 5$

$K_{D_{50}} = 0.57 \log(2.24.H)$ $\quad D_{50} < 25$

$K_{D_{50}} = 1$ $\quad D_{50} > 25$

$$\frac{d_s}{d_{se}} = \exp\left[-0.03\left|\frac{u_c}{u} ln\left(\frac{t}{t_e}\right)\right|^{1.6}\right]$$

$t_e(days) = 48.26\frac{b}{u}(U - 0.4)$ $\quad H > 6$

$t_e(days) = 30.89\frac{b}{u}(U - 0.4)H^{0.25}$ $\quad H \leq 6$

- **Oliveto and Hager (2002)**

$K_U = c_0 U^{1.5}$

- **Sheppard (2002)**

$K_U = 1 - 3.31\ (U - 1)^2$

$K_H = \tanh[(H)^{0.4}]$

$$K_{D_{50}} = \frac{3.03}{2.6\ e^{0.43\log(D_{50}-0.707)} + 0.43\ e^{-2.6\log(D_{50})+4.27}}$$

- **Chang et al (2004)**

$K_U = U - 0.4$ $\quad 0.4 \leq U \leq 1$

$K_{D_{50}} = 0.398 \ln(D_{50})$- $0.034[\ln(D_{50})]^2$ $\quad 1 \leq D_{50} < 50$

$K_{D_{50}} = 1$ $\quad D_{50} \geq 50$

$K_H = 0.783[(H)]^{0.322} - 0.106$ $\quad 0 < H < 3$

$K_H = 1$ $\quad H > 3$

K_σ= Obtain by a graph

- **Sheppard et al (2004)**

$K_U = 1 - 1.75[\ln(U)]^2$

$K_H = \tanh[(H)^{0.4}]$

$$K_{D_{50}} = \frac{D_{50}}{0.4D_{50}^{1.2} + 10.6D_{50}^{-0.13}}$$

- **Raikar and Dey (2005)**

$K_{D_{50}} = 0.26\ln(3.88.D_{50})$ $\quad D_{50} \leq 9$

$K_{D_{50}} = 0.08\ln(14070.D_{50})$ $\quad 9 < D_{50} \leq 25$

$K_{D_{50}} = 1$ $\quad D_{50} > 25$

$K_\sigma =$ Obtain from graph

- **Lanca et al. (2013)**

$$K_T = \frac{d_s}{d_{se}} = 1 - e^{-a_1.T^{a_2}}$$

Where:

$a_1 = 1.22(D_{50})^{-0.764}$

$a_2 = 0.09(D_{50})^{0.244}$

$K_{H-D_{50}} = 7.3(D_{50})^{-0.29}H^{0.12}$ $\quad 60 \leq D_{50} \leq 500,\ H \geq 0.5$

$K_H = 1.2H^{0.12}$ $\quad D_{50} > 500,\ H \geq 0.5$

1.4. Objectives

The objectives of this research work can be summarized as below:

- ✓ Collection of clear-water scour data for cylindrical piers from reliable sources in literature;
- ✓ Selection of long-duration, suitable and reliable data from previous research and experiments by imposing appropriate selection criteria;
- ✓ Homogenization of the available data, particularly by an analysis of threshold conditions to choose a suitable criterion to be applied to all the experiments for defining the threshold for inception of bed material motion;
- ✓ Investigation of the effect of nondimensional time, T (t.u/b), sediment coarseness, D_{50}(b/d_{50}), and upstream flow intensity, U (u/u_c), on the scour depth;
- ✓ Regression-based calibration of a predictive formula;
- ✓ Comparison of the final proposed equation with several previous ones available in the literature.

Chapter 2

AVAILABLE DATA AND LITERATURE REVIEW

2.1. Introduction

Relatively large quantities of local scour data have been used for the purpose of the analysis. The sources and quantities of these data are listed in table 2.1 and 2.2. Laboratory data are derived from experiments that were carefully performed and all the dependent parameters are given by the author.

A total number of 516 experiments were used in this study. The data that have been employed can be divided into two general categories:

1. ***Full trend scour depth data (324 experiments)*****;** which are the experiments where the full scour depths evolution from the beginning of the experiments until the experiments stops, with respect to time, were reported by authors. (Table2.1)

2**. *Isolated scour depth points (192 experiments);*** which are the data where only final or maximum scour depth is provided by the authors and the time history of the scour holes evolution were not reported or measured. (Table 2.2)

Main characteristics of data sources are given in the following section.

Full trend scour depth data	
Sources	number of data
Ettema (1980)	105
Sheppard et al. (2002)	14
Oliveto and Hager (2002)	88
Lanca et al. (2013)	46
Chang et al. (2004)	10
Yanmaz and Altinbilek (1991)	18
Raikar and Dey (2005)	16
Chabert and Engeldinger (1952)	12
Mignosa (1979/1980)	13
Franzetti (1989)	1
Azzaroli (1983)	1
Total number of series	**324**

Table 2.1: Full trend data sources and number for each source.

Isolated scour depth points	
Sources	number of data
Yanmaz, Altinbilek (1991)	15
Melville and Chiew (1992)	27
Chiew (1995)	13
Chiew (1984) from NCHRP	4
Graf from Melville and Chiew (1999)	3
Melville and Chiew (1999)	51
Melville and Chiew (1999) from NCHRP	17
Dey et al (1995)	18
Ettema, RAUD	1
Ettema (1980) from NCHRP	2
Ettema, Kirkil and Muste (2006)	6
Sheppard and Miller (2006)	24
Raikar and Dey (2005)	4
Lee and Sturm (2009)	4
Ettema (1980)	3
Total number of points	**192**

Table 2.2: Isolated points sources and number for each source.

2.2. Data Characteristics

In this section a brief summary about the experiments done by the various authors and the aim and an achievement of their study is provided to have a better understanding about the data that are going to be used in this study. For employing different experiment results from various sources it is necessary to understand the assumptions which have been made. In this way, it is possible to use these experiments as a unique database and attempt to make all of them homogenous via analysis. It should be remembered that, all the collected experiments are in clear-water condition according to authors report.

2.2.1. Full trend scour depth data

2.2.1.1. Ettema (1980)

- **Introduction and objectives**

The aim of this project was to investigate experimentally the development of local scour in uniform and non-uniform sediments as well as in beds formed of layers of uniform sediments. It was hoped that each set of experiments would lead to recommendation for design of bridge piers. Three main series of experiments were augmented.

In all the experiments cylindrical piers were used. The approach flow was steady for all experiments.

For the purpose of this study the experiments related to local scour of uniform sediment around a pier were used. The stage of particle motion, expressed in terms of shear velocity parameter u^*/u_c^*, was set on that all the experiments were performed at clear water local scour.

The experimental study was conducted in two parts:

The first part investigated the temporal development of local scour for a range of bed particle sizes and cylindrical pier diameter, at similar values of the shear velocity parameter u^*/u_c^* with different value of 0.95, 0.9, 0.75 or 0.5 at the center line of the approach flow. Two different flumes were used in this study. The greater part of the study was performed in a 1.52 m wide re-circulating flume for which the approach flow depth was kept constant at 0.6 m. Additional experiments were conducted in a 0.46 m wide flume with flow provided by an outlet pipe from the ring-main system of the laboratory with constant approach flow equal to 0.2 m for these experiments.

The second parts was concerned with the influence of the approach flow depth, h (y_0 by Ettema notation), on the development of local scour at a cylindrical pier found in uniform sediment. Shear velocity parameter was held constant at u^*/u_c^*= 0.9, at the center line of the approach flow to the pier. The experiments were carried out in the 1.52 m wide flume. Three piers sizes and three uniform bed sediments were used to investigate the influences of flow depth, as well as that of pier and particle sizes, on the development of local scour.

- **Hydraulic Models**

Most of the experiments on the temporal development of local scour were carried out in a 1.52 m wide, 1.22 m deep, glass-sided flume of approximately 45 m length (Figure 2.1). The flow through the flume was re-circulated by two variable speed axial flow pumps driven by thyristor controlled electric motors. In all experiments the flume slope was adjusted to ensure that the depth of the flow was constant over the full length of the working section.

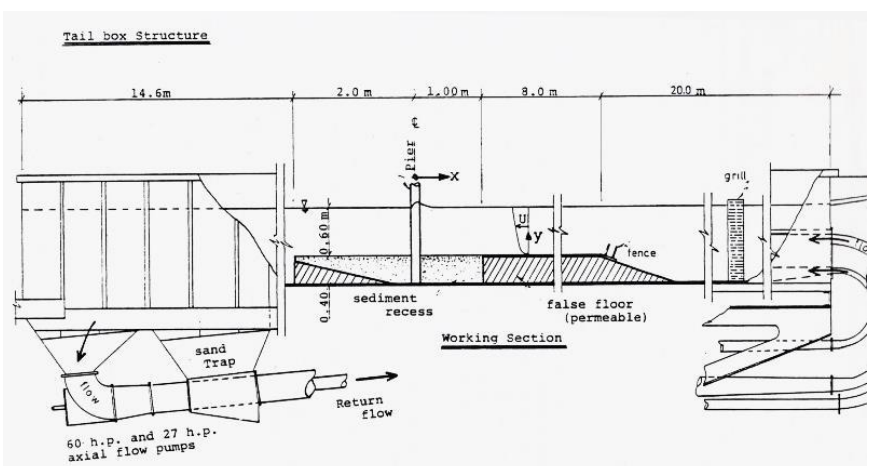

Figure 2.1: Cross-section of the working section of 1.52 m wide, flow recirculating, flume by Ettema (1980)

The working section of the flume commenced at 20 m from the upstream end of the flume. It consisted of an 8 m length false floor, upstream of 1.5 m wide and 3 m long sediment recess, in which the pier was placed.

The approach bed roughness was simulated with the use of roughened sheet metal covers which were fixed to the false floor. A selection of roughened sheets was made to cover the range of sediment sizes used in the study.

An additional series of experiments was performed in a smaller glass-sided flume 0.456 m wide, 0.44 m deep and approximately 19 m in length, served with water circulation system of the laboratory. The water level in the flume was controlled by a tail gate. The roughness of the approach bed was simulated in a similar manner to that described for the approach bed in 1.52 m wide flume (Figure 2.2).

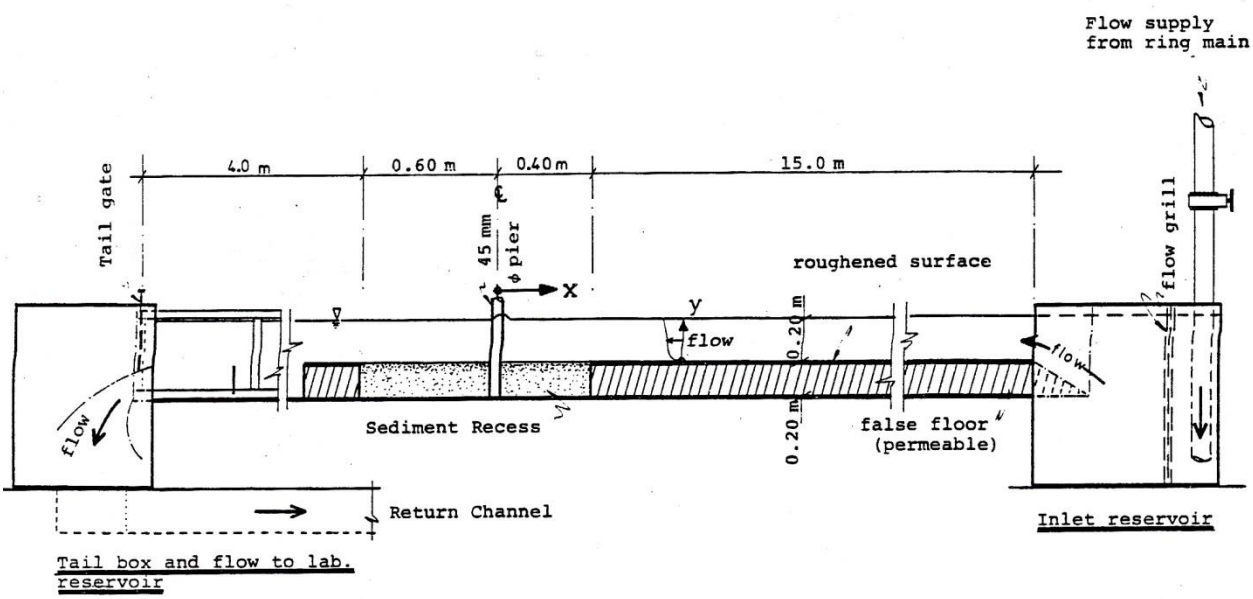

Figure 2.2: Cross-section of the working section of the 0.46 m wide flume by Ettema (1980)

- **The bed sediments**

Sediment properties used in this experiment are listed in Table (2.3) where d_{50} is mean particle size of uniform sediments, σ_g and σ_I are two measurements of standard deviation of particle size distribution of each bed sediments (σ_g<1.5 may be considered as being virtually of a uniform particle size. All of the eight bed sediment that used in this experiments fulfill this limit so they can be considered as uniform sediments.), S_s is specific gravity, u_c^* is critical shear velocity and computed by using shields function. S.F is particle shape factor which has a negligible influence of u_c^*, W_{50} is fall velocity of the mean particle size determined by Rouse (1937) and α is the angle of static particle response.

	Bed Sediment Number							
	1	2	3	4	5	6	7	8
d_{50} (mm), d	0.24	0.38	0.80	0.84	1.90	3.80	5.37	7.80
σ_g	1.18	1.29	1.33	1.17	1.34	1.07	1.24	1.10
σ_I	1.20	1.30	1.39	1.19	1.33	1.08	1.24	1.12
S_s	2.65	2.65	2.65	2.65	2.65	2.65	2.65	2.65
u_{*c} (x 10^2 ms^{-1})	1.30	1.52	2.13	2.18	3.41	5.87	6.93	8.41
S.F.	1.0	1.0	1.0	1.0	1.0	0.82	0.76	0.70
w_{50} (ms^{-1})	0.03	0.06	0.14	0.15	0.27	0.32	0.45	0.49
α	29°	31°	34°	36°	37°	38°	38°	38°

Table 2.3: Sediment properties used in Ettema (1980) experiment

- **Piers and scour depth**

The sizes of the cylindrical piers used in the experiments are given in table (2.4) below:

Flume Width B (mm)	Pier Diameter D (mm)	$\frac{B}{D}$
1524.0	28.5	53.5
	50.8	30.0
	101.6	15.0
	150.0	10.2
	240.0	6.4
457.2	45.0	10.16

Table 2.4: Pier size used in Ettema (1980) experiment

Several techniques were adopted to measure the depth of the local scour. Scour depths could be read to within ±1 mm. It is worthy to mention that the value of B/D is provided as 10.6 instead of 10.16 for the last row of table (2.4) in the authors report.

- **Approach flows and flow measurement**

The approach flow for each experiment was initially set so that the experiments were run for similar values of the shear velocity ratio, u^*/u_c^*, for all the sediment sizes. For each flow and sediment size, the channel slope, S_0, was adjusted so that the flow had a uniform depth over the working section. Required value of the slope, S_0 were estimated from:

$$s_0 = \frac{u_*^2}{gh} \qquad (2.1)$$

The magnitudes of d_{65} and u_c^* for corresponding value of d_{50} is provided by author in table (2.5).

d65(mm)	corresponding d50(mm)	Shields uc*
0.225	0.24	0.013
0.432	0.38	0.0152
1.054	0.8	0.0213
0.862	0.84	0.0218
1.935	1.9	0.0341
3.829	3.8	0.0587
5.497	5.37	0.0693
1.013	7.8	0.0841

Table 2.5: Ettema (1980) critical shear velocity definition

The mean approach flow velocity, u, of the center line velocity profile was determined from equation:

$$u = u * [5.75\ log\left(\frac{h}{d_{65}}\right) + 6] \qquad (2.2)$$

Similarly for critical approach flow velocity:

$$u_c = u_c^* \left[5.75 log\left(\frac{h}{d_{65}}\right) + 6\right] \qquad (2.3)$$

It can be concluded form equation (2.2) and (2.3):

$$\frac{u}{u*} = \frac{u_c}{u_c^*} \rightarrow \frac{u}{u_c} = \frac{u*}{u_c^*} \rightarrow u = \frac{u*}{u_c^*}.u_c \qquad (2.4)$$

The approach flow velocity profiles were measured with two mini-propeller flow meters.

- **Results and procedure**

Following observations were made for each experiment:

- *The temporal development of the scour hole*. The frequency of scour depth measurement decreased as the rate scouring decrease. The experiment was stopped when no change occurred to the maximum depth of scour hole over a minimum period of four hours.
- *The mechanisms of local scour*. A visual record of the important feature distinguishing the development of local scour around a cylindrical pier kept with aid of photographs.
- Water temperature.

- *Scour hole profile*. At the completion of each experiment the profile of the scour hole, in the plane of symmetry of the pier and parallel to the flow direction was recorded with 3 mm diameter pointer gauge.

It is assumed that the following relationship can be stated for the depth of local scour at a pier:

$$\frac{d_s}{b} = f(\frac{h}{b}, \frac{b}{d_{50}}, \frac{t}{t_0}, \frac{u^*}{u_c^*}) \qquad (2.5)$$

The curve formed by the collapse of the data is defined by four straight-line segments which approximate the different local scour development. The principal erosion phase is approximated by two straight-line segments. Each segment is of the form:

$$\frac{d_s}{b} = k_1 \ln(\frac{d_{50}}{b} . \frac{u^* t}{b} . \frac{\nu}{u^* . b})) + lnk_2 \qquad (2.6)$$

Where k_1 and k_2 are constants defined for each phase segments.

- **Deriving data**

Most of the data from the Ettema (1980) reports was obtained by techniques of digitization and converting the graphs to spreadsheets of data. In this manner the quantities related to scour depth with respect to time can be defined. This procedure was done by Matlab function. A sample of the process of digitization is provided below (Figure 2.3).

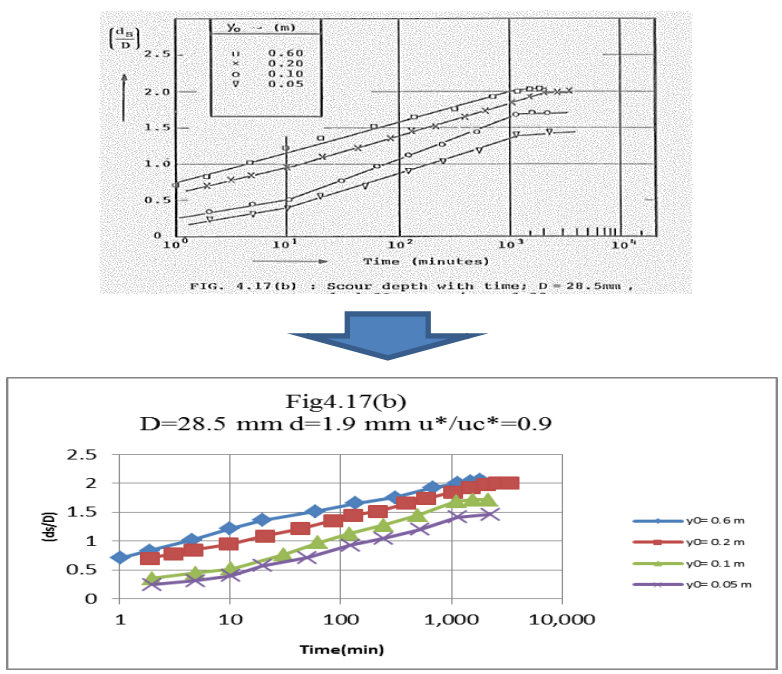

Figure 2.3: Digitization of Ettema (1980) sample

2.2.1.2. Sheppard, et al. (2002)

- **Introduction and objectives**

This bridge scour research program at the University of Florida was directed at increasing the understanding of scour processes and improving the accuracy of design scour depth prediction through large-scale experiments.

All of the experiments were conducted in large, flow-through type flume. Three circular cylinder diameters (0.915 m, 0.305 m and 0.114 m), three different sediment grain sizes (d_{50} equal to 0.22 mm, 0.80 mm and 2.9 mm) and a range of water depths were investigated. This study covers the clear-water scour range of velocities (i.e., 0.45≤u/u_c≤1).

Normalized equilibrium local scour depths was described in terms of three dimensionless parameters, h/b, u/u_c, and b/d_{50} where according to the author notation are:

h= water depth,

b= structure diameter/width,

u= the depth averaged Velocity,

u_c= the depth averaged Critical Velocity,

d_{50}= the median sediment grain diameter.

In this experiments indicated a trend in the data with increasing values of b/d_{50}. Thus, one of the objectives of his research was to obtain local scour data for larger values of b/d_{50}.

The rate at which local scour occurs and the dependence of this rate on the sediment, flow and structure parameters is another object of this experiment.

- **Hydraulic models**

All of the tests were conducted in a large 6.1 m wide, 6.4 m deep, and 38.4 m long flow through type flume. Schematic drawings of the flumes used in this research are shown in figure 2.4 and 2.5.

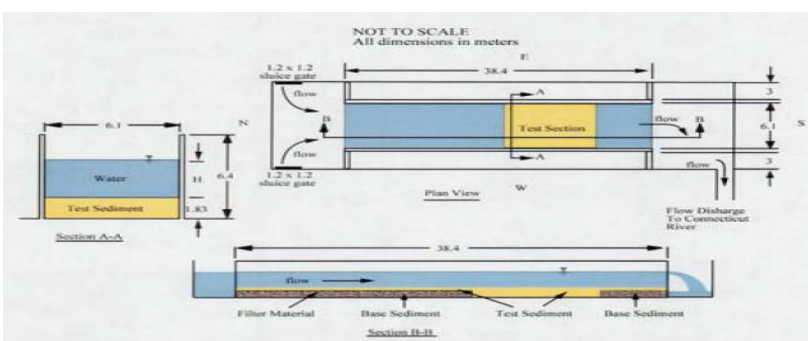

Figure 2.4: Schematic drawing of flume used for Sheppard et al.'s (2002) research

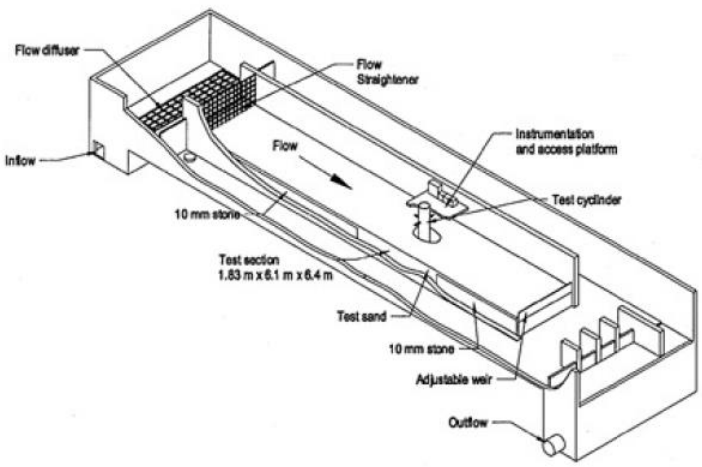

Figure 2.5: Isometric drawing of the flume

The test section was the width of the flume, 9.8 m long and started 24.4 m downstream of the entrance. The sediment in the test area was 1.83 m deep. Water for the flume was supplied from hydroelectric power plant reservoir adjacent to building housing the flume. Water flowed from the reservoir, through the flume, and discharged into river downstream of control structure. The flow discharge and depth-averaged velocity was controlled with a weir located at the downstream end of the flume.

The instrumentation used in this research can be divided into two categories: 1) That which measures the flow parameters, and 2) That which measures scour depth. The flow parameters monitored were flow discharge, velocity at specific locations, water depth, and temperature. The scour hole depth was monitored with internal and (on some occasions) external video cameras and with arrays of acoustic transponders.

- **Bed sediment**

Three different sediment grain sizes with d_{50}=0.22 mm, 0.80 mm and 2.9 mm where used in this experiment and the value of their standard deviation, σ, are 1.51, 1.29 and 1.21 respectively. In table 2.6 the value of d_{50} and σ correspond to each test are listed.

- **Pier and scour depth**

Three circular cylinder piers with 0.915 m, 0.305 m and 0.114 m diameter were used. Quantitative scour depth measurements were obtained by video cameras mounted on a platform that traversed vertically and the length scales were attached to the inside of the cylinders in view of the cameras. Miniature video cameras were also mounted in streamline waterproof housing for viewing scour hole from outside the structure.

Three arrays of acoustic transponders were attached to the cylinder just below the water surface. This system provided scour hole depth measurement at the 12 locations along three radial lines throughout the experiments.

Pier and scour depth measurement summary of all tests are provided in table 2.6.

- **Approach flows and flow measurement**

Flow velocities were measured at two locations, 2 m upstream and 1 m to the side of the center of the test structure with electromagnetic flow meters. The vertical position of the meters was set at 40 % of the water depth from the bed. The velocity at this location was considered approximately equal to the depth-averaged velocity for the fully developed logarithmic velocity profile.

A commercial water level instrument, which used a near bottom mounted pressure transducer measured water depth at a location between the test structure and the weir. The water temperature was measured just downstream of the structure. The value of flow depth and velocity for each test is provided in table 2.6.

Test	Flow		Sediment		Structure
	Depth (m)	Velocity (m/s)	D_{50} (mm)	σ	Diameter (m)
1	1.19	0.29	0.22	1.51	0.114
2	1.19	0.31	0.22	1.51	0.305
3	1.27	0.40	0.80	1.29	0.915
4	0.87	0.39	0.80	1.29	0.915
5	1.27	0.39	0.80	1.29	0.305
6	1.27	0.41	0.80	1.29	0.114
7	1.22	0.76	2.90	1.21	0.915
8	0.56	0.65	2.90	1.21	0.915
9	0.29	0.57	2.90	1.21	0.915
10	0.17	0.50	2.90	1.21	0.915
11	1.90	0.70	2.90	1.21	0.915
12	1.22	0.40	0.22	1.51	0.305
13	0.18	0.30	0.22	1.51	0.305
14	1.81	0.30	0.22	1.51	0.915

Table 2.6: Flow, sediment and structure parameters summary

- **Procedure and results**

The procedure used in performing the local sediment scour experiments is outlined below.

➢ **Pre-experiment**

1. Compact and level the bed in the flume.

2. Fill the flume slowly and allow standing for approximately 12 hours or until all the air trapped in the sediment has escaped. Drain the flume and re-compact the bed.

3. Take pre-experiment photographs.

4. Fill the flume slowly and allow trapped air to escape (approximately six hours).

5. Start and check all instrumentation

- **During experiment**

1. Measure the scour depth as a function of time with acoustic transponders and video cameras.

2. Measure the velocity, water depth, and temperature. Observe water clarity as an indicator of suspended sediment.

- **Post-experiment**

1. Take post-experiment photographs.

2. Observe and note bed condition throughout the flume (presence of bed forms, etc.)

3. Survey the scour hole with a point gauge.

4. Reduce and analyze the data.

A significant amount of local sediment scour data and information were gathered during this research program. A brief summary of the results is given in tables 2.7. Two different scour depths are given in this table, the measured values at the end of the experiment and the estimated equilibrium depth. Most of the experiments conducted as part of this work were long in duration and thus the scour depths were near equilibrium at the end of the test. During some of the test there was an increase in suspended sediment in the water from the reservoir and this proved to impact the equilibrium scour depth.

Test	Test Duration (hr)	Time to 90% d_{se} (equil.) (hr)	Max. Measured Scour Depth (m)	Estimated Equilibrium Scour Depth (m)
1	89	111	0.133	0.17
2	163	408	0.257	0.41
3	360	322	1.112	1.10
4	143	905	0.638	0.99
5	88	128	0.416	0.51
6	41	29	0.185	0.23
7	188	151	1.270	1.41
8	330	186	1.058	1.14
9	448	347	0.896	0.96
10	616	831	0.659	0.72
11	350	720	1.004	1.24
12	256	71	0.377	0.39
13	216	66	0.296	0.31
14	580	913	0.787	0.97

Table 2.7: The local scour results summary

Equilibrium depths were estimated by extrapolating a curve fit to the data. The function used to fit the data was first used by J. Sterling Jones and is:

$$d_s = a\left(1 - \frac{1}{1+abt}\right) + c\left(1 - \frac{1}{1+cdt}\right) \tag{2.7}$$

The resulting Sheppard's equation is:

$$\frac{d_s}{b} = K_s K_{cp} f_1(\frac{h}{b}) f_2(\frac{u}{u_c}) f_3(\frac{b}{d_{50}}) \tag{2.8}$$

Ks= shape factor (1 for circular piles)

K_{cp}= Peak values of normalized Clearwater scour depth= 2.5 in these equations.

For K_{cp}=2.5 we are going to have:

$$\frac{d_s}{b} = k_s 2.5\left\{tanh\left[\left(\frac{h}{b}\right)^{0.4}\right]\right\}\left\{\left[1 - 3.31\left(\frac{u}{u_c} - 1\right)^2\right]\right\} \tag{2.9}$$

$$\left\{\frac{3.03}{2.6exp\left[0.43log_{10}\left(\frac{b}{d_{50}}\right) - 0.707\right] + 0.43exp\left[-2.6log_{10}\left(\frac{b}{d_{50}}\right) + 4.27\right]}\right\}$$

2.2.1.3. Oliveto and Hager (2002)

- **Introduction**

This work presents new research on bridge pier and abutment scour based on a large data set collected at ETH Zurich, Switzerland. In total six different sediments were tested, of which three were uniform. Also a large variety of scour elements were considered, from 1 to 60% of the channel width, and flow depths ranging from 1 to about 40% of the channel width.

- **Hydraulic models**

The experiments were conducted in two rectangular channels, one having a width l_c=1.00 m, the other l_c=0.50 m. The 1 m channel had a total length of 11 m, with a working section of about 5 m, a glass wall on the left side, and a smooth steel wall on the right side. The sediment was placed horizontally, and the free surface measured along the flow. The determining approach flow depth h was taken at (l_c-b)/2 upstream from the scour element face, with b as the pier diameter. All experiments were run essentially under plane bed conditions. The sediment surface was measured with a so-called shoe gauge having a 4 mm by 2 mm wide horizontal plate at its base, whereas the water surface was read with a conventional point gauge, typically to ±0.5–1 mm, depending on the local surface turbulence.

- **The bed sediment**

Six different sediments were used, three of which were uniform with grain sizes 0.55, 3.3, and 4.8 mm, and three mixtures, with d_{50}= 5.3, 1.2, and 3.1 mm, and σ= $(d_{84}/d_{16})^{1/2}$=1.43, 1.80, and 2.15, respectively. The uniform sediment with d_{50}=3.3 mm had a density of ρ_s=1.42 t/m^3, whereas the remainder had ρ_s=2.65 t/m^3. The plastic sediment originated from a circular extruder, the rest was from Swiss rivers with a typical ellipsoidal shape.

- **Pier and scour depth**

The circular cylinders had diameters b=0.011, 0.022, 0.050, 0.064, 0.110, 0.257, 0.400, and 0.500 m. All elements were fabricated in transparent plexi-glass to allow for visual determination of scour depths to 1 mm during the progress of an experiment.

The temporal start of an experiment (t=0) was set at scour inception. Subsequent measurements were taken at times t=1, 3, 6, 10, (15), and 20 min up to several days and even several weeks in selected runs.

The scour surface was measured at the maximum scour depth z along the element side, the maximum lateral and upstream scour extensions, and the aggradation maximum downstream of the element. Figure 2.6 shows a definition sketch with typical points of interest measured for all experiments.

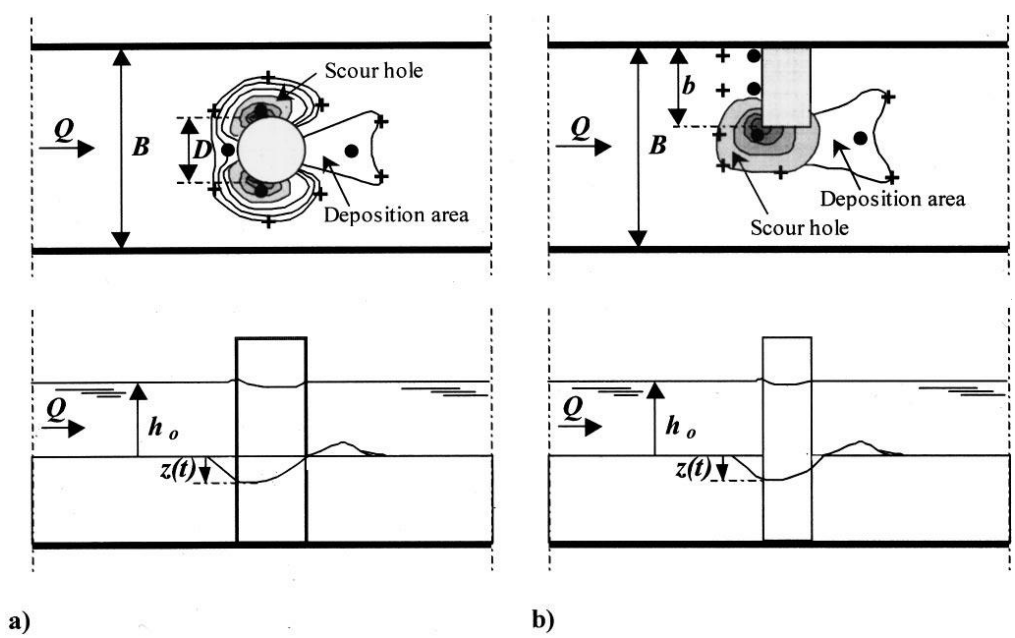

Figure 2.6: Definition sketch and measurement points for: (a) pier and (b) abutment. Points defining (●) scour or aggradation depths; (+) scour or aggradation area

- **Approach flow and flow measurement**

The channel had a closed-loop water system, with a pump at the upstream channel side, of maximum discharge Q = 0.130 m^3/s with an accuracy of about 1%. A submerged sill at the end of the working section inhibited sediment movement out of the working section.

The flow depths measured at a certain time t always included the section 1 m downstream from the flow straightener, the section upstream from the pier and at a downstream section located between 3.3 and 3.8 m. Flow depths ranging from 1 to about 40% of the channel width.

In table 2.8, densimetric particle Froude number $F_d = u/(g' d_{50})^{1/2}$ with $g' = \{(\rho_s - \rho)/\rho\}g$, threshold Froude number F_t, and approach Reynolds number $R_0 = 4hu/\nu$, with u=upstream velocity and ν=kinematic viscosity is provided. The value for approach flow velocity is given as cross-sectional velocity (average bulk velocity) and in terms of Froude and Reynolds numbers in the table.

- **Results**

In total 200 scour experiments were conducted over almost 2 years. Summary of test condition is provided in the table 2.9 and include the mean grain size d_{50} , its standard deviations, and relative density $\rho' = (\rho_s - \rho)/\rho$, test duration in days, pier width b, the ranges of average approach flow depth h.

Series	F_d	F_t	$R_0.10^3$
(-)	(-)	(-)	(-)
24	1.48–3.34	0.71–1.30	19–290
10	1.38–2.79	0.54–0.99	82–506
13	2.00–3.52	0.55–0.96	38–298
19	1.47–3.68	0.55–1.31	75–536
11	1.71–2.39	0.44–0.69	50–257
4	2.24–3.86	0.59–1.14	108–393

Table 2.8: VAW pier data- test conditions

Series	d50 (mm)	σ	ρ'	t experiment (days)	b (m)	h (m)
24	3.3	1	0.42	0.11–46.88	0.02–0.26	0.02–0.30
10	4.8	1.25	2.65	0.46–1.87	0.06–0.50	0.05–0.20
13	0.55	1.37	2.65	0.14–21.06	0.06–0.26	0.05- 0.30
19	5.3	1.43	2.65	0.02–4.74	0.06–0.26	0.05–0.20
11	1.2	1.8	2.65	0.88–2.95	0.06–0.40	0.05–0.20
4	3.1	2.15	2.65	0.13–14.30	0.11–0.50	0.05–0.20

Table 2.9: VAW Pier Data- summary of test conditions

2.2.1.4. Lanca, et al. (2013)

- **Introduction**

long-duration clear-water scour data were collected at single cylindrical piers with the objective of investigating the effect of sediment coarseness, b/d_{50} (b = pier diameter; d_{50} = median grain size) on the equilibrium scour depth and improving the scour depth time evolution modeling by making use of the exponential function suggested in the literature. Experiments were carried out for the flow intensity close to the threshold condition of initiation of sediment motion, imposing wide changes of sediment coarseness and flow shallowness, h/b (h = approach flow depth).

- **Hydraulic models**

Two flumes were used in the experimental study. One, located at the University of Beira Interior, is 28.00 m long, 2.00 m wide and 1.00 m deep. Discharge was measured by an electromagnetic flow meter with an accuracy of 0.5% of full scale. The central reach of the flume, starting at 14.00 m from the entrance, includes a 3.00-m-long, 2.00-m-wide, and 0.60-m-deep recess box in the channel bed.

The second flume, located at the University of Porto, is 33.15 m long, 1.00 m wide, and 1.0 m deep; it's central reach starts at 16.00 m from the entrance. The recess box is 3.20 m long, 1.0 m wide and 0.35 m deep. The area located around the pier was covered with a thin metallic plate to avoid uncontrolled scour at the beginning of each experiment. The flumes were filled gradually, imposing a high water depth and low flow velocity. The discharge corresponding to the chosen approach flow velocity was then adjusted to pass through the flumes. The flow depth was regulated by adjusting the downstream tailgates. Once the discharge and flow depth were established, the metallic plates were removed and the experiments started. The characteristic of each experiment is provided in table 2.9.

- **The bed sediment**

A uniform quartz sand (ρ_s=2650 kg/m^3; d_{50} =0.86 mm; σ_D =1.36) was used to fill each of the recess boxes of the two channels.

- **Pier and scour depth**

Single vertical cylindrical piers were simulated by PVC pipes with b=50, 75, 110, 160, 200, 250, 315, 350, 400 mm, placed at ~1.0 m from the upstream boundary of the bed recess box. The maximum pier diameter was 200 mm, so as to minimize contraction effects.

The depth of scour hole was measured, to an accuracy of±1 mm, with adapted point gauges, approximately every 5 minutes during the first hour. Afterwards, the interval between measurements increased and, after the first day, only a few measurements were carried out each day. When the scour rate was less than approximately 2 mm (≈$2d_{50}$) in 24 hours and at least 7 days had passed, the experiments were stopped. The sand bed approach reach located upstream of the piers stayed undisturbed through the entire duration of the experiments; this long-term stability ensured that the scour depth was not supplemented by upstream bed degradation.

- **Approach flow and flow measurement**

A reasonably high relative flow depth (0.050 m ≤ h ≤ 0.400 m; 58 < h/d_{50} < 465) was always guaranteed. The average flow intensity, u/u_c, varied in the range 0.93 ≤ u/u_c≤ 1.04, with u_c being calculated using the predictor of Neil (1967). The aspect ratio l_c/h was guaranteed to be greater than 5.0, to avoid significant wall effects on the flow field. All of the velocities are given in terms of average bulk velocity. The corresponding velocity for each test is represented in table 2.10.

Test	lc (m)	h (mm)	b (mm)	u (m/s)	td Hour	dse mm
1	2	55	110	0.28	170	180.1
2	2	80	160	0.29	168	226.2
3	2	100	200	0.29	170	263.1
4	2	125	250	0.3	168	282.1
5	2	158	315	0.29	223	348.1
6	2	175	350	0.33	306	337.3
7	2	200	400	0.31	288	409.2
8	2	50	50	0.27	168	115.6
9	2	75	75	0.28	168	163.9
10	2	110	110	0.29	168	198.9
11	1	160	160	0.3	285	231.1
12	1	200	200	0.31	261	296.5
13	2	250	250	0.32	263	365
14	2	315	315	0.33	186	388.3
15	2	350	350	0.33	291	408.7
16	2	400	400	0.33	224	448.4
17	2	75	50	0.28	168	118.9
18	2	113	75	0.3	168	175.8
19	1	165	110	0.3	241	224.6
20	2	225	160	0.33	267	305.7
21	2	300	200	0.33	262	360.6
22	2	375	250	0.33	221	373.8
23	2	100	50	0.29	170	127.1
24	2	150	75	0.3	169	162.7
25	2	220	110	0.33	216	208.9
26	2	300	160	0.33	330	267.1
27	2	400	200	0.33	219	329.4
28	2	125	50	0.3	168	111
29	1	188	75	0.31	191	146.7
30	2	275	110	0.33	184	234.3
31	2	375	160	0.33	313	278.8
32	1	150	50	0.3	173	109.7
33	2	225	75	0.33	197	170.6
34	2	330	110	0.33	169	222.6
35	2	200	50	0.31	170	133.7
36	2	300	75	0.33	314	197.6
37	2	250	50	0.33	237	116.6
38	2	375	75	0.33	315	184.3

Table 2.10: Characteristic controlling variable of Lanca et al. (2013)'s experiment

- **Results**

It was postulated here that finite equilibrium scour depth must exist (Table 2.10). It was recognized that the probability of occurrence of a sufficiently strong turbulent event capable of entraining sediment grains from the scour hole will never be null though this probability decreases as scour develops, tending asymptotically to zero. Also it was assumed that the time needed to achieve finite equilibrium scour may be rather large, conceptually infinite. For this reason, scour depth records were fitted by using regression as follow:

$$d_s = p_1\left(1 - \frac{1}{1 + p_1 p_2 t}\right) + p_3\left(1 - \frac{1}{1 + p_3 p_4 t}\right) + p_5\left(1 - \frac{1}{1 + p_5 p_6 t}\right) \tag{2.10}$$

Where $p_1$to p_6 are constants. For t=∞ it is assumed that $d_s = d_{se} = p_1 + p_3 + p_5$. For practical applications, the following upper-bound predictor was suggested:

$$\frac{d_{se}}{b} = K_h K_{d_{50}} \tag{2.11}$$

K_h and $K_{d_{50}}$ are defined as below:

$$K_h = \begin{cases} 2.3\left(\frac{h}{b}\right)^{1/3} & 0.5 \le \frac{h}{b} \le 1.45 \\ 2.6 & \frac{h}{b} > 1.45 \end{cases} \tag{2.12}$$

$$K_{d50} = \begin{cases} 1\,, & 60 < \frac{b}{d_{50}} \le 100 \\ 5.8\left(\frac{b}{d_{50}}\right)^{-0.38}, & 100 < \frac{b}{d_{50}} \le 500 \\ 0.55, & 500 < \frac{b}{d_{50}} \end{cases} \tag{2.13}$$

Where b is pier diameter, h is approach flow average depth, d_{se} is equilibrium scour depth, K_h is flow shallowness factor and K_{d50} is sediment coarseness factor. Total numbers of 38 series were obtained from this experiment. The full scour depth is represented for these series by the author.

Simarro, G. et al. (2011) have published five long-duration experiments on scouring at cylindrical piers. The data from these experiments were used for validation of the suggested scour time evolution model. Three experiments from Grimaldi, C. (2005) were also included in the analysis (Table 2.11).

AUTOR	t real time	ds (measured scour)	σ	h (flow depth)	b (pier width)	d50	u (data)	ρ	lc channel Width
	[hr]	[m]	[-]	[m]	[m]	[m]	[m/s]	[kg/m^3]	[m]
GRIMALDI 1 14,0 days	96.00	0.121	1.46	0.15	0.0750	0.00128	0.400	2550	0.80
GRIMALDI 2 6,2 days	147.94	0.179	1.46	0.25	0.0900	0.00086	0.340	2550	2
GRIMALDI 3 6,2 days	146.08	0.225	1.46	0.25	0.1200	0.00086	0.340	2550	2
SIMARRO 1 34,9 days	837.55	0.167	1.40	0.16	0.0750	0.00086	0.270	2650	0.82
SIMARRO 2 45,6 days	1094.50	0.196	1.40	0.16	0.0800	0.00086	0.300	2650	0.82
SIMARRO 3 29,7 days	713.57	0.130	1.46	0.16	0.0800	0.00128	0.340	2650	0.82
SIMARRO 4 24,9 days	596.48	0.135	1.46	0.15	0.0750	0.00128	0.340	2650	0.82
SIMARRO 5 29,0 days	695.67	0.127	1.46	0.13	0.0630	0.00128	0.340	2650	0.82

Table 2.11: Summary of Girmaldi (2005) and Simarro et al. (2011) experiment used for validation

2.2.1.5. Change et al. (2004)

- **Introduction**

The main objective of this study was to investigate and analyze the experimental data on the scour-depth evolution at circular piers. A method was proposed based on the mixing layer concept for calculation of equilibrium scour depth in nonuniform sediment. Based on analysis of scour-rate data obtained in experiments, a model for simulating the scour-depth evolution under steady flow in nonuniform sediment is presented herein. In addition, a scheme for computing the scour-depth evolution under unsteady flow is also proposed.

- **Hydraulic models**

The experiments were conducted in a 36m long, 1 m wide, and 1.1 m deep flume with glass sidewalls at the Hydrotech Research Institute of National Taiwan University, Taipei, Taiwan. A false floor was set in the flume with a recess of 2.8 m long and 0.3 m deep where sediment was placed.

- **The bed sediment**

Uniform sediments having sizes of 1.0 and 0.71 mm, and nonuniform sediments having the same median sizes with σ of 2.0 and 3.0, respectively, were used for experiments. All of these sediments had a specific gravity of 2.65. The sediment size distribution curves were designed to be log-normal for nonuniform sediment (Table 2.12).

test	σ	d50(mm)
S1	1.20	1.00
S2	1.20	1.00
S3	2.00	1.00
S4	3.00	1.00
S5	1.20	0.71
S6	1.20	0.71
S7	2.00	0.71
S8	2.00	0.71
S9	3.00	0.71
S10	3.00	0.71

Table 2.12: Sediments characteristics

- **Pier and scour depth**

A hollow cylindrical pier made of transparent plexiglass with a diameter of 0.1 m was located at the center of the recess. The temporal variation of the bed surface profile around the pier was recorded using two 3 cm long charge coupled device cameras with 2 mm diameter lenses, placed in the hollow Plexiglas pier.

- **Approach flow and flow measurement**

The velocity for each test was given in terms of average depth velocity. Clear-water scour conditions were imposed in the experiments, in which no sediment was picked up upstream of the scour hole. The summary of approach flow velocities and flow depths are presented in table 2.13.

test	u(m/s)	h(m)
S1	0.390	0.2
S2	0.280	0.2
S3	0.280	0.2
S4	0.280	0.2
S5	0.355	0.3
S6	0.227	0.15
S7	0.355	0.3
S8	0.227	0.15
S9	0.355	0.3
S10	0.227	0.15

Table 2.13: Approach flow characteristics

- **Results**

Since the maximum scour depth mostly occurred at the pier nose from observations, experiments in the present study were focused at the pier nose. The measured scour depths at the pier nose plotted against time are presented in figure 2.7.

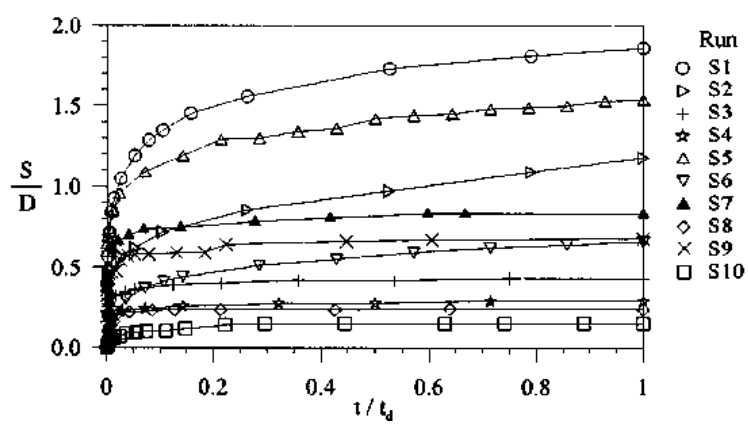

Figure 2.7: Evolution of dimensionless scour depth at pier nose under steady flow (Chang et al. (2005))

2.2.1.6. Yanmaz and Altinbilek (1991)

- **Introduction**

The objective of this study is to develop a semi empirical method to determine the time variation of clear water local scour depth around single cylindrical and square bridge piers. The method to be presented is based on the application of the sediment continuity equation to the scour hole around bridge piers.

- **Hydraulic models**

Experiments to study the development of scour hole around bridge pier models were conducted in a glass flume at the Hydromechanics Laboratory of Middle East Technical University, Ankara, Turkey. The glass flume is an L-shaped horizontal rectangular open channel 90 cm deep, 67 cm wide with a concrete bottom. Side walls (except the test section for visual observations) of the flume are made of steel (Figure 2.8).

- **The bed sediment**

Two different uniform bed materials (quartz sand) were used with the specific weights of 26.4 kN/m^3 and 26.3 kN/m^3, the mean particle sizes of 1.07 mm and 0.84 mm with σ= 1.13 and 1.28, respectively. Bed materials were placed as a 15-cm thick layer in the flume bed with a bed slope of 0.001.

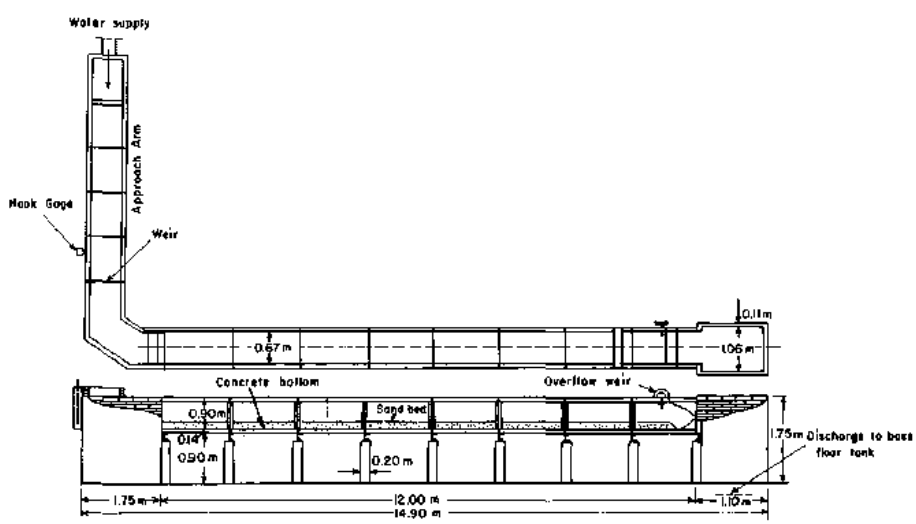

Figure 2.8: Test flume, plan and profile

- **Pier and scour depth**

Cylindrical piers with diameters of 6.7 cm, 5.7 cm, and 4.7 cm were tested. In the experiments, the maximum scour depths around the bridge piers d_s, were measured against time

t, relative to the initial bed level using a vertical scale attached to the interior wall of hollow Plexiglas pier with a stick having a small inclined mirror at its end.

- **Approach flow and flow measurement**

The flow rate in the flume is adjusted by a valve on the pipe. Then the corresponding head on the sharp-crested weir is measured. The upstream flow depth was varied between 4.5 cm to 16.5 cm.

During the experiments, the upstream valve was slowly adjusted without causing any disturbance to the bed material until the desired discharge was given to the flume and the velocities are stated as average bulk velocity. Only clear water conditions with a flatbed were studied. No sediment inflow was allowed into the scour hole from upstream.

- **Results**

The time variation of local scour depth around bridge piers is investigated. Total of 38 cylindrical pier tests were done in this study. The maximum duration of an experiment, was about six hours during which the final equilibrium scour depths were not achieved although the rate of scour did decelerate to smaller values for all experiments. It was observed that the maximum scour depths occurred at the midpoint of the upstream face of cylindrical and square piers.

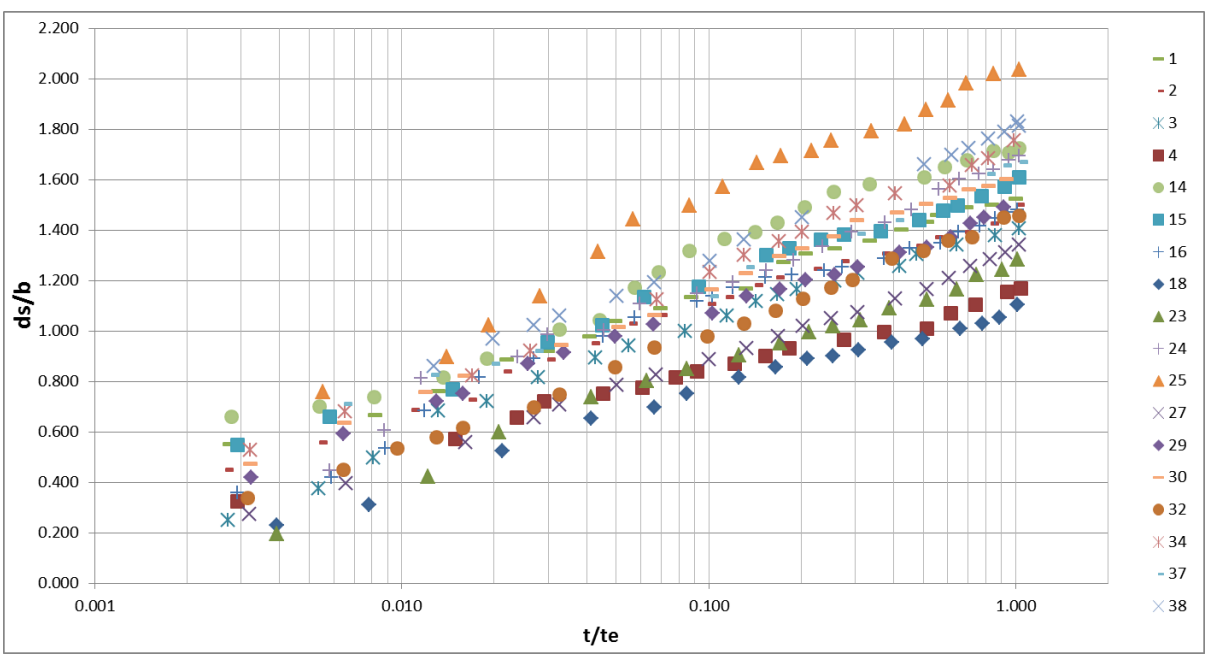

Figure 2.9: Scour data for cylindrical pier

2.2.1.7. Raikar and Dey (2005)

- **Introduction**

This study aims to investigate scour depth at circular and square piers in uniform and non-uniform gravels (fine and medium sizes, 4.10 ≤ d_{50} ≤ 14.25 mm) under clear-water scour at limiting stability of gravels. The findings of the experiments were used to describe the effects of gravel size and gradation on scour depth, including time variation of scour depth.

- **Hydraulic models**

Experiments were conducted in a flume that has length, width, and depth of 12, 0.6, and 0.7 m, respectively. Two types of pier models were used, namely circular and square, having different widths *b*, where only circular pier were taken into consideration for the purpose of the analysis.

- **The bed sediment**

The sizes and gradations of uniform gravels (fine and medium, 4.10 mm ≤ d_{50} ≤ 14.25 mm) used in the experiments are furnished in the Table (2.10). The particle size distribution is less than 1.4 for uniform gravels.

d50(mm)	σ
4.10	1.13
5.53	1.10
7.15	1.08
10.25	1.16
14.25	1.09

Figure 2.10: Uniform sediments size and gradations

- **Pier and scour depth**

Circular pier size with 32, 38, 60 and 77 cm were used in this experiment. The instantaneous scour depth at a pier was measured observing the position of the base of the scour hole by sliding a periscope up and down the pier. After the run was stopped, the maximum equilibrium scour depth d_s was then carefully measured by a vernier point gage.

- **Approach flow and flow measurement**

All experiments were run at constant upstream flow depth of 0.25 m, maintaining a clear-water scour condition by adjusting the upstream flow condition for a period of 18–36 h until the scour equilibrium was reached. The method for measuring the upstream flow measurement is not reported by the author.

- **Results**

16 series of time variation of local scour depth around cylindrical piers were provided by the author for the purpose of this study analysis and the remaining four test results were used as isolated data (Total of 20 tests).

2.2.1.8. Chabert and Engeldinger (1956)

- **Introduction**

In this study, additional experimental result of Chabert, J. and Engeldinger, P. (1956) was used that relate to circular piers in a sandy bed.

- **Hydraulic models**

A rectangular channel with variable inclination was used in this study. The total length was equal to 21 m and the width of the channel remains constant in all of the tests and it was equal to 0.8 m. The schematic view of the channel is illustrated in figure 2.11.

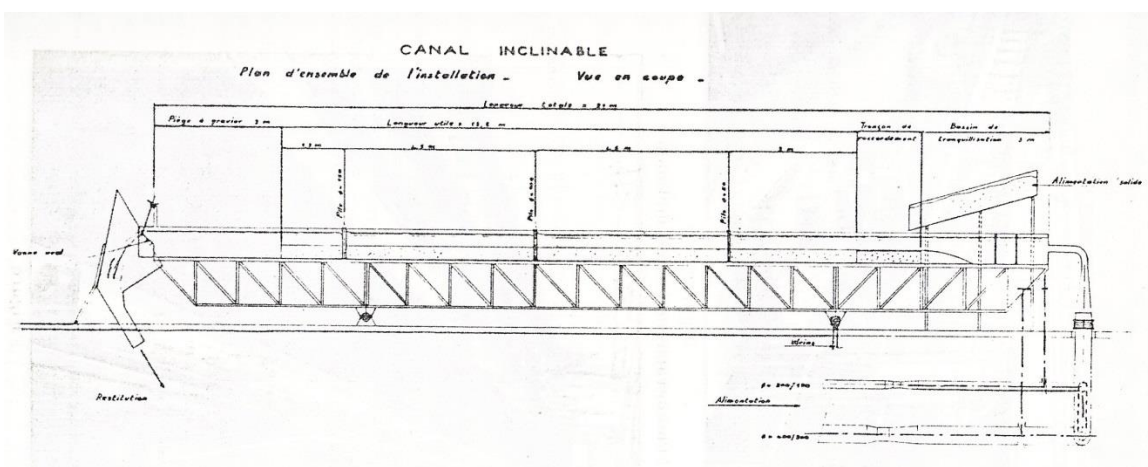

Figure 2.11: Test flume from Chabert and Engeldinger (1956)

- **The bed sediment**

Two different sediments were used with median size d_{50} equal to 1.5 and 0.52 mm with constant sediment standard deviation equal to 1.39 and with density equal to 2680 $^{kg}/_{m^3}$.

- **Pier and scour depth**

In these tests, three different circular piers with diameter equal to 0.05, 0.075, 0.1 m were used. The scour depth evolution was measured by point gauge around circular piers.

- **Approach flow and flow measurement**

Flow depth varies between 0.1 m to 0.35 m. The approach flow velocity was reported in terms of average bulk velocity for all the experiments.

- **Results**

Total number of 12 series was obtained from Chabert, J. and Engeldinger, P. (1956). Table 2.14 gives the values of the fundamental physical, geometrical and kinematic quantities of these tests.

	t test duration	ds measured scour	σ	h flow depth	b pier width	d50	u Velocity	ρ	lc channel Width
	[hr]	[m]	[-]	[m]	[m]	[m]	[m/s]	[kg/m^3]	[m]
1	233.83	0.114	1.39	0.35	0.05	0.0015	0.325	2680	0.8
2	139.13	0.112	1.39	0.1	0.05	0.0015	0.375	2680	0.8
3	210.75	0.124	1.39	0.2	0.05	0.0015	0.350	2680	0.8
4	227.25	0.191	1.39	0.2	0.1	0.0015	0.350	2680	0.8
5	116.13	0.114	1.39	0.35	0.05	0.0015	0.375	2680	0.8
6	113.81	0.194	1.39	0.35	0.1	0.0015	0.375	2680	0.8
7	156.28	0.080	1.39	0.2	0.05	0.00052	0.245	2680	0.8
8	156.28	0.113	1.39	0.2	0.075	0.00052	0.245	2680	0.8
9	72.73	0.110	1.39	0.2	0.05	0.00052	0.325	2680	0.8
10	119.25	0.103	1.39	0.35	0.05	0.00052	0.305	2680	0.8
11	73.85	0.136	1.39	0.2	0.1	0.00052	0.325	2680	0.8
12	143.11	0.103	1.39	0.2	0.05	0.00052	0.325	2680	0.8

Table 2.14: Chabert, J. and Engeldinger, P. (1956) test characteristic summary

2.2.1.9. Mignosa (1980)

- **Introduction**

In addition to data mentioned above, 13 series were employed from experiment done by Mignosa, P (1980).

- **Hydraulic models**

A rectangular channel was used in this experiment. The channel length and width were equal to 5 m and 0.495 m respectively and the slope of the channel was zero.

- **The bed sediment**

In this study, synthetic sediment with only one size is used with d_{50} equal to 2.5 mm, σ equal to 1.39 and density equal to 1180 $^{kg}/_{m^3}$.

- **Pier and scour depth**

Two pier sizes equal to 0.0267 m and 0.048 m were used. The scour depth around piers was measured by point gauge.

- **Approach flow and flow measurement**

In this study, a recirculating system with the capability of flow discharge up to 30 lit/s was used. Approach flow depth varies between 0.125 to 0.127 meter and all of the velocity quantities are given as average bulk velocity by the author.

- **Results**

The final results and the duration of each experiment are summarized in table 2.15.

#	t test duration	ds measured scour	σ	h flow depth	b pier width	d50	u Velocity
	[hr]	[m]	[-]	[m]	[m]	[m]	[m/s]
1	216.00	0.0555	1.39	0.126	0.0267	0.0025	0.136
2	216.00	0.0795	1.39	0.126	0.0480	0.0025	0.136
3	213.50	0.0545	1.39	0.125	0.0267	0.0025	0.141
4	71.00	0.0525	1.39	0.126	0.0267	0.0025	0.139
5	71.00	0.0720	1.39	0.126	0.0480	0.0025	0.139
6	190.50	0.0642	1.39	0.125	0.0267	0.0025	0.150
7	190.50	0.0855	1.39	0.125	0.0480	0.0025	0.150
8	166.50	0.0940	1.39	0.127	0.0480	0.0025	0.161
9	213.50	0.0638	1.39	0.125	0.0480	0.0025	0.141
10	95.50	0.0458	1.39	0.127	0.0480	0.0025	0.170
11	95.50	0.0980	1.39	0.127	0.0480	0.0025	0.170
12	237.50	0.0422	1.39	0.127	0.0480	0.0025	0.183
13	237.50	0.0960	1.39	0.126	0.0480	0.0025	0.185

Table 2.15: Mignosa, P. (1980) test characteristic summary

2.2.1.10. Franzetti et al (1989)

One series from Franzetti et al (1989) was obtained for using in analyses.

- **Hydraulic models**

A rectangular channel with 7 m length and 0.495 m width was used in this study.

- **The bed sediment**

The bed sediment was made by synthetic material with specific weight equal to 11571 N/m^3 and d_{50}= 2.5 mm.

- **Pier and scour depth**

A smooth metallic circular pier was used with b=4.8 cm. The reading of the maximum scour depth at upstream of the pier and also the scour evolution was carried out by using a hydrometer.

- **Approach flow and flow measurement**

A recirculating system was used in this study. The upstream fellow velocity was measured in terms of average bulk velocity.

- **Results**

The final result of this experiment is shown in figure 2.12.

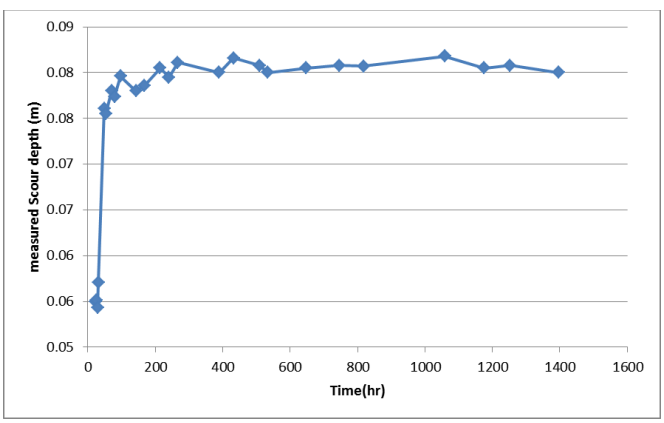

Figure 2.12: Scour depth with respect to time trend taken from Franzetti et al.'s (1981) experiment

2.2.1.11. Azzaroli (1983)

Moreover one more series from Azzaroli, D. (1983) is used in this study; characteristics of the work were obtained through personal communication. In table 2.16 the parameters of this test

are provided. The velocity is given in terms of average bulk velocity. The scour depth time evolution is indicated in figure 2.13.

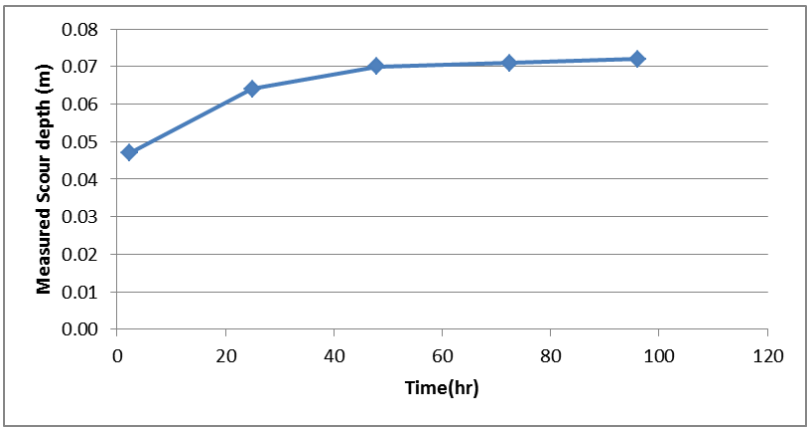

Figure 2.13: Scour depth with respect to time graph taken from Azzaroli, D.'s (1983) experiment

code	t real time	ds measured scour	σ	h flow depth	b pier width	d50	u velocity	ρ	lc channel Width
	[hr]	[m]	[-]	[m]	[m]	mm	[m/s]	[kg/m^3]	[m]
Azzaroli, D. (1983)	96.17	0.0720	1.32	0.098	0.0300	0.98000	0.285	2635	0.500

Table 2.16: Franzetti et al (1989) and Azzaroli, D. (1983) tests characteristic summary

2.2.2. Isolated scour depth points

In this study use has been made also of 192 isolated points that were previously collected by Paleari (2014). These data refer to different experiments by various authors. The Table 2.2 provides a brief summary of the available isolated points. A precise check has been made to verify the validity of collected data. The full properties of these experiments are available in Appendix 1.

CHAPTER 3

DATA ANALYSIS

3.1. Introduction

After the procedure of data collection from different experiments by various authors that has been discussed in the previous chapter, here the process of selecting suitable data and the following analysis are described.

As mentioned before, for analyzing the database, according to the fact that these data are collected from different experiments, it is crucial to unify them by considering similar criteria for computing the key parameters.

One of the most important parameter that characterizes the evolution of scour depth is flow velocity, as it appears in two out of four effective dimensionless parameters (T and U). Velocity is typically made dimensionless by the critical velocity for inception of sediment motion. Thus, the first part of this chapter presents an analysis oriented to choosing an appropriate criterion (to be selected among those available in the literature) to estimate the value of u_c^*, which is the threshold shear velocity for initiation of sediment motion.

As mentioned before, there are several methods for expressing the upstream flow velocity. It can be measured in terms of cross-sectional bulk average or as a depth-averaged velocity according to the researcher's choice. Thus, a formula tuned by Paleari (2014) was used for converting average bulk velocity to central velocity for data analysis. This formula was used to unify the method of velocity measurement among all the collected data, according to the idea that, since the pier is located at the center of the flume in all of the experiments, the central depth-averaged velocity is a better indicator of velocity in this region compared to average bulk one.

Moreover, the procedure of selection of suitable data and criteria which are considered for this task are discussed. Then the final valid data and their characteristics are illustrated.

Furthermore, the dependency of the scour depth on the relevant nondimensional parameters is evaluated and a method for reaching a final predictive equation is presented.

At the end, the final interpolation results are summarized and taken into comparison with some of the available predictive equation in the literature. A brief conclusion brings this chapter to the end.

3.2. Analysis of threshold conditions

3.2.1. Introduction

As mentioned before, particle at the riverbed would start to move when the destabilizing forcing moment become larger than the stabilizing moment of the weight force. Shields (1936) by introducing stability parameter τ_* show that, if its value reaches to a specific value τ_c^* the initiation of bed load transport occurs. It is also worthy to note that, for sediment particles in water, the Shields diagram exhibits different trends corresponding to different turbulent flow regimes. Shields diagram is represented as a series of dispersed experimental point for defining τ_c^* with respect to Re^* and τ^*. Thus there is no function for finding the value of u_c^* for a given sediment median size, specific water and sediment density. This problem lead to the fact that there is no possibility for finding a unique value of u_c^*.

3.2.2. Introducing criteria under study

Various authors define different criteria for computing u_c, u_c^* and τ_c^*. In this section the proposed formula for these parameters is provided and a comparison for finding a suitable final formula for computing stability parameters is given.

- **Chiew(1995)**

By using the Manning-Strickler equation for two dimensional flows to evaluate the critical mean velocity u_c from critical shear velocity u_c^* and assume bed Roughness equal to d_{50}, a following equation is proposed:

$$\frac{u_c}{u_c^*} = 7.66\left(\frac{h}{d_{50}}\right)^{1/6} \qquad (3.1)$$

Thus,

$$u_c = u_c^* \, 7.66\left(\frac{h}{d_{50}}\right)^{1/6} \qquad (3.2)$$

Chiew also assume following relationship for critical mean velocity u_c^* by considering a constant value of 0.056 for τ_c^*,

$$u_c^* = \sqrt{0.056(S_s - 1)g d_{50}} \qquad (3.3)$$

Where S_s is specific gravity of sediment, h is undisturbed approach flow depth in meter, and d_{50} is median grain size of sediment also in meter.

- **Melville and Coleman (2000)**

Melville and Coleman provide different formula for u_c^* for different range of d_{50} as below:

$$u_c^* = 0.0115 + 0.0125 d_{50}^{1.4} \qquad 0.1\,mm < d_{50} < 1\,mm \qquad (3.4)$$

$$u_c^* = 0.0305 d_{50}^{0.5} - 0.0065 d_{50}^{-1} \qquad 1\,mm < d_{50} < 100\,mm \qquad (3.5)$$

Based on u_c^* we have:

$$u_c = 5.75u_c^*.log\left[5.53\left(\frac{h}{d_{65}}\right)\right] \quad (3.6)$$

- **Ettema (1980)**

Ettema represents a table which correlate specific value of d_{65} and corresponding d_{50} values to u_c^* which are obtained by experiment:

d65(mm)	corresponding d50(mm)	Shields uc*
0.225	0.24	0.013
0.432	0.38	0.0152
1.054	0.8	0.0213
0.862	0.84	0.0218
1.935	1.9	0.0341
3.829	3.8	0.0587
5.497	5.37	0.0693
1.013	7.8	0.0841

Table 3.1: Ettema (1980) critical shear velocity definition

Considering logarithmic velocity profile, the mean critical approach flow velocity, u_c, of the center line velocity profile can be evaluated from equation:

$$u_c = u_c^*\left[5.75log\left(\frac{h}{d_{50}}\right) + 6\right] \quad (3.7)$$

- **Brownlie (1981) (from report by Parker (2004))**

Brownlie (1981) fitted a curve to the experimental points of Shields and obtained the following relationship:

$$\tau_c^* = 0.22.Re_p^{-0.6} + 0.06.10^{-7.7Re_p^{-0.6}} \quad (3.8)$$

Where Re_p is particle Reynolds number and can be calculated as:

$$Re_p = \frac{d_{50}\sqrt{\Delta.g.d_{50}}}{\nu} \quad (3.9)$$

Brownlie formula result a constant value of τ_c^* equal to 0.06 for high value of Reynolds number.

- **Parker et al. (2003)**

Based on Neil (1968) and by curve fitting to experimental line of shields same as the technique used by Brownlie (1981):

$$\tau_c^* = 0.5.(0.22.Re_p^{-0.6} + 0.06.10^{-7.7Re_p^{-0.6}}) \quad (3.10)$$

The difference from Brownlie formula is that in the limit of sufficiently large Re_p (fully rough flow), τ_c^* becomes equal to 0.03.

- **Sheppard et al (2013)**

$$u_c^* = \sqrt{\left[16{,}2.d_{50}\left(\frac{9{,}09.10^{-6}}{d_{50}} - d_{50}.(38{,}76 + 9{,}6.\ln(d_{50}))\right) - 0{,}005\right]} \quad (3.11)$$

The value of u_c is given with respect to different ranges of Reynolds number:

$$u_c = 2{,}5.u_c^*.ln\left[73{,}5.h/(d_{50}(Re.(2{,}85 - 0{,}58.\ln(Re^*) + 0{,}002.Re^*) + \frac{111}{Re^*} - 6)\right] \quad 5 \leq Re^* \leq 70 \quad (3.12)$$

$$u_c = 2{,}5.u_c^*.\ln\left(2{,}21.\left(\frac{h}{d_{50}}\right)\right) \quad Re^* > 70 \quad (3.13)$$

Where $Re^* = \frac{u^* d_{50}}{\nu}$ (3.14)

For the range of $Re^* > 70$ Sheppard assume that there is no dependency to Reynolds value for the computation of critical velocity u_c.

- **Oliveto and Hager (2002)**

By subdividing the domain of interest into three portions, depending on the dimensionless grain size, D^*, where is equal to:

$$D^* = \left(\frac{g.\Delta}{\nu^2}\right)^{\frac{1}{3}}.d_{50} \quad (3.15)$$

The value of critical velocity for uniform granulometry and σ≤ 1.3 is defined in for different regime as,

Viscous regime:

$$u_c = \sigma^{\frac{1}{3}}.(g.\Delta.d_{50})^{\frac{1}{2}}.2{,}33.D^{*^{-0.25}}.\left(\frac{R_h}{d_{50}}\right)^{\frac{1}{6}} \quad for\ D^* \leq 10 \quad (3.16)$$

Transition regime:

$$u_c = \sigma^{\frac{1}{3}}.(g.\Delta.d_{50})^{\frac{1}{2}}.1{,}08.D^{*^{\frac{1}{12}}}.\left(\frac{R_h}{d_{50}}\right)^{\frac{1}{6}} \quad for\ 10 < D^* \leq 150 \quad (3.17)$$

Fully turbulent regime:

$$u_c = \sigma^{\frac{1}{3}}.(g.\Delta.d_{50})^{\frac{1}{2}}.1{,}65\left(\frac{R_h}{d_{50}}\right)^{\frac{1}{6}} \qquad for\ D^* \geq 150 \tag{3.18}$$

- **Neil(1967) (reported by Simarro (2007))**

This formula is obtained from experiment done by Neil (1967):

$$u_c^2 = 2{,}5.\left(\frac{h}{d_{50}}\right)^{0,2}.(\Delta.g.d_{50}) \tag{3.19}$$

This experiment is restricted to the following conditions:

1. Straight steady uniform 2-dimensional (wide-channel) flow over a flat bed with fully-developed velocity profile (boundary layer thickness= depth);
2. Uniform material of regular shape exceeding 3 mm in grain-size (for normal density of 2.65 gm/cm^3);
3. Ratio flow depth/grain-size between 2 and 100.

- **Grande (1970) (reported by Simarro (2005))**

According to the Grande the u_c is equal to:

$$u_c = \left[0{,}5.log\left(\frac{h}{d_{50}}\right) + 1{,}63\right].(g.\Delta.d_{50})^{\frac{1}{2}} \tag{3.20}$$

3.2.3. Comparisons of different criteria

In the figure 3.1 the different criteria for computing critical velocity with respect to median size of the sediments d_{50} are illustrated. Parker (2003) and Brownlie (1981) do not provide any relationship for computing u_c. Chiew (1995) and Melville and Coleman (2000) are more similar for all sediment ranges and on the other hand Oliveto and Hager (2002) formula have a close estimation to Grande (1970).

The Ettema (1980) cannot be extended to higher value of d_{50} due to the fact that the value of critical shear velocity is presented in a table rather than as a function.

Neil (1967) formula evaluation is more conservative than the others and shows a relatively lower value of critical velocity than the other criteria.

The Sheppard (2013) equation is only plotted for the value of Re^* between 5 and 70 according to the author. For the lower value of Re^* a trend change and increase in u_c can be seen and for high value of Re^* a sudden decrease occur which cause a big different of critical velocity with respect to other formulas.

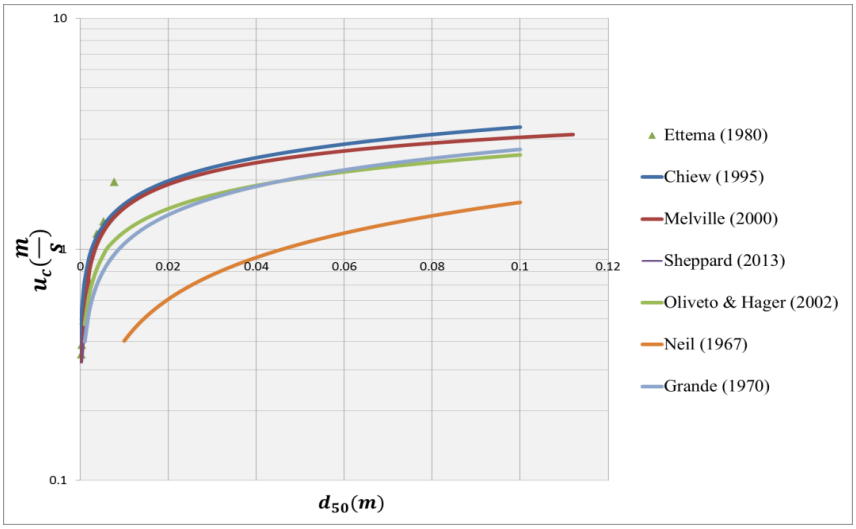

Figure 3.1: Comparison of different criteria for computing u_c

In figure 3.2 also different formula for calculation of critical shear velocity, u_c^*, is provided. Same as previous graph the Sheppard (2013) formula is just plotted for the mentioned range of Re^* between 5 to 70.

Due to the fact that there is no formula for computing u_c^* for Parker (2003), Bowline (1981), Oliveto and Hager (2002) and Neil (1967), they are not presented in this graph. For the Ettema (1980) also the experimental data is plotted.

In this case Parker (2003) represents a lower bond in compare to the other formulas. Chiew (1995), Melville and Coleman (2000) and Brownlie (1981) result approximately equal for same grain median size and also Ettema (1980) and Sheppard (2013) in their valid range.

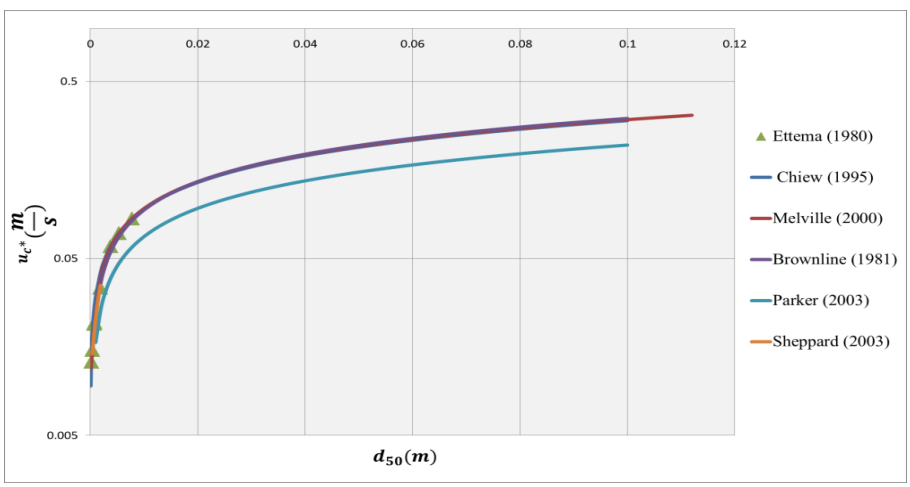

Figure 3.2: Comparison of different criteria for computing u_c^*

Figure 3.3 and 3.4 shows models proposed by different authors for computing critical shear stress and also the scatter data points that were derived by shields experiment.

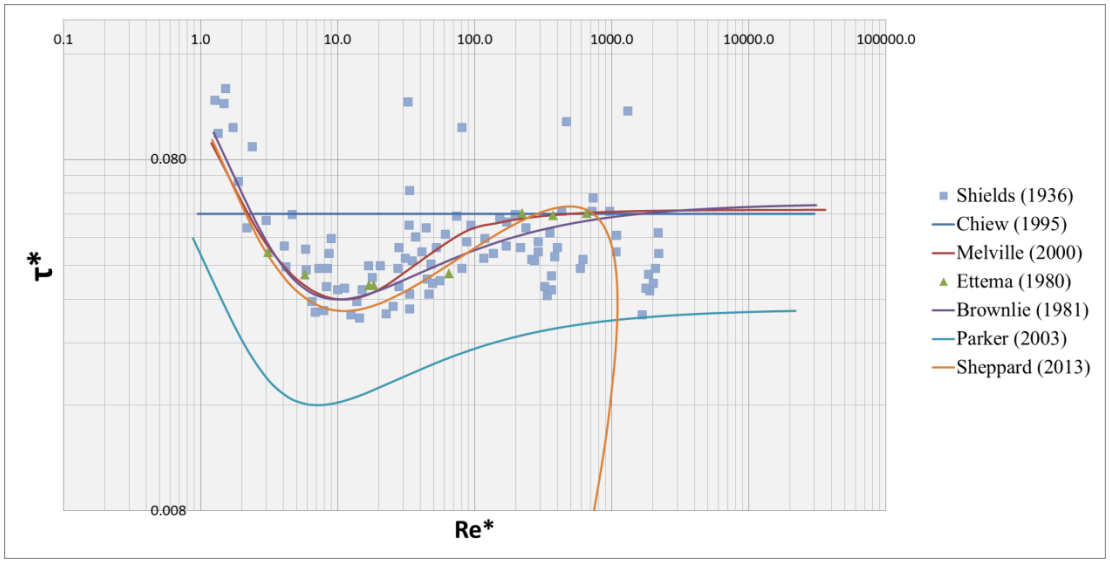

Figure 3.3: Comparison of different criteria for deriving shear critical stress with respect to Shields experiments with Re* as x axis

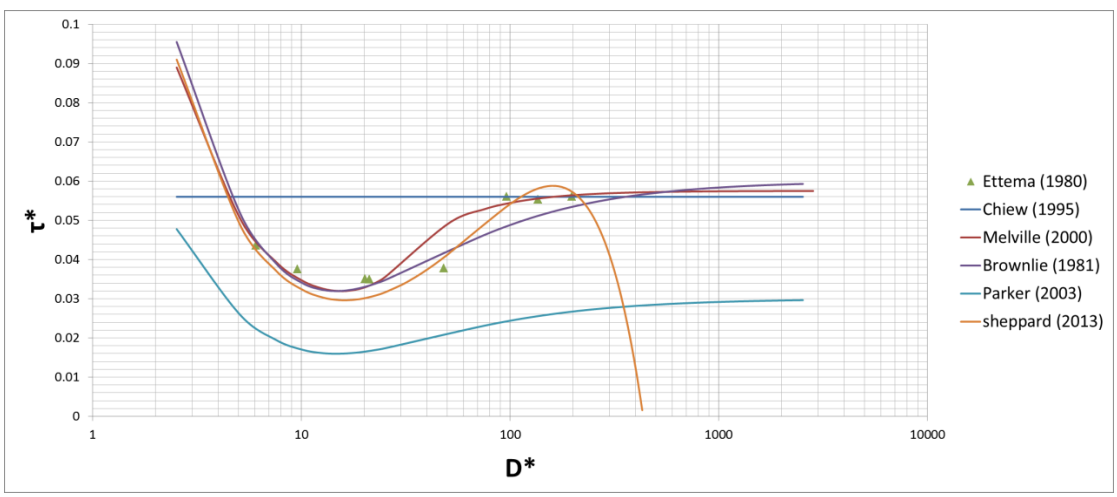

Figure 3.4: Comparison of different criteria for deriving shear critical stress with D* as x axis

The following notes can be inferred from graphic comparison of these different criteria:

- *Ettema(1980)* cannot be used as a general criteria for threshold of sediment motion cause there is no general formula rather than just a number of disperse data for u_c^* and as a result for τ_c^*. However, these points are consistence with curves.

- *Chiew (1995)* indicate a constant value of 0.056 for τ_c^* and does not have any dependency to grain size and it is not consistent with shields graph for low and mid values of Re^*. Thus this formula should not be used for Re^* approximately less than 200.
- *Sheppard (2013)* shows a fairly good trend with respect to Shields experimental data up to shear Reynolds number equal to approximately 800. But the curve is no longer valid for greater values of Re^*. On the other hand, there is a sudden intense decrease in the value of critical shear stress in the approximate range of Re^* from 1 to 80. Sheppard also shows an underestimation of τ_c^* with respect to shields experimental data.
- *Brownlie (1981)* and *Melville & Coleman (2000)* have a similar trend with Sheppard (2013) without any sudden decrease in critical shear stress value. For great values of Re^* they tend to have a similar approximation for τ_c^* as Chiew (1995).
- *Parker (2003)* shows also a similar trend as *Brownlie (1981)* and *Melville & Coleman* (2000) trends but an approximately 50% underestimating the value of τ_c^* in compare to *Melville & Coleman (2000)* formula.

According to the notes mention above, it is obvious that the most suitable criteria for finding the value of sediment incipient motion can be *Brownlie (1981) and Melville & Coleman (2000).* At mid-range *Melville* shows an upper bond of shields experiments data with respect to *Brownlie* and this is the reason in which *Melville & Coleman* criteria have been selected for further analysis of the data.

Thus in order to make all the experiments which are going to be used in the analyses uniform, *Melville & Coleman (2000)* criterion was used for computing the threshold of sediment motion for all the tests. Therefore, a new value of flow intensity was calculated for each experiment based on this criterion and *U* (u/u_c) value provided by the author was discarded.

3.3. Velocity Conversion formulas

As mentioned before in chapter 2, the analysis database consists of various sources and as a consequence there may be different methods for presenting a single parameter and it is mandatory to transform these different methods to a unique one.

In the database they are some experiment results in which the velocity is provided in terms of depth-averaged velocity and on the other hand, some experiments provide the average bulk velocity. Thanks to previous study by Paleari (2014), a formula was proposed that is able to convert the average bulk velocity to depth-averaged velocity as follow and with an acceptable approximation (Figure 3.5):

$$\frac{u_c}{u_m} = -16.48 \log\left(\frac{l_c}{D}\right) + (a.\frac{\varepsilon}{D} + b)/(c.\frac{\varepsilon}{D} + d) \quad (3.21)$$

Where u_c is the depth-averaged velocity at central axis of the channel, u_m is the average bulk velocity, l_c is the width of the channel, ε is the bed roughness that assumed to be equal to d_{50}, D is hydraulic diameter and is equal to $4R_h$ where R_h is hydraulic radius of channel. *a*, *b*, *c* and *d* are constant values obtained by interpolation:

a= 0.582423, b= 0.001007, c= 0.019616, d= 5.07218E-05

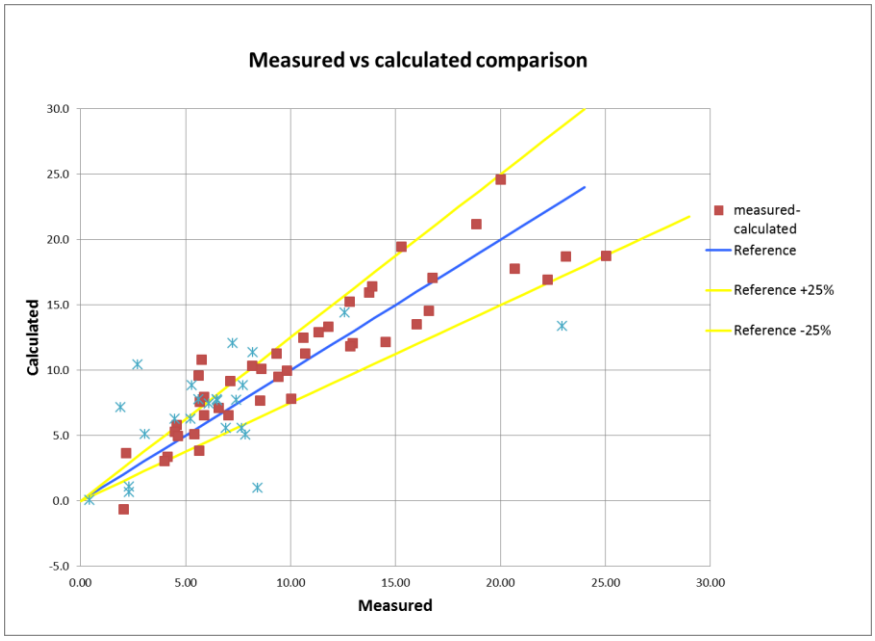

Figure 3.5: Comparison of measured and calculated values of velocity by means of conversion formula by Paleari (2014)

For taking advantage of this formula, it is necessary to have a fully turbulent flow according to the author, unless the formula results are not reliable.

As mentioned before, due to the fact that the pier is located at the center of the flume in all of the experiments, the central depth-averaged velocity is a better indicator of velocity in this region compare to average bulk velocity. Thus, all the velocities that were given as average bulk velocity by the authors and their flow's regime were fully turbulent, were converted to depth-averaged velocity at central axis of the channel.

3.4. Data selection

3.4.1. Introduction

For the purpose of selecting suitable experiments among the existing database various criteria were taken into consideration that they are going to be discussed in this section. The general goal for imposing these conditions is to disregard the experiments that were done in special conditions that can affect the final interpolation for having a scour depth time evolution model.

As previously discussed, it is necessary to have constant values of different effective parameters when the dependency of two parameters on each other is under study. In database there would be some experiments that their results are not reliable because of failure in satisfying this stability condition during the experiments. Therefore, these experiments should be neglected to increase the acuuracy of the analyses.

3.4.2. Selection Criteria

The criteria used for the selection of the suitable isolated points and series are described below:

- **H=(h/b) >2**

As mentioned before, in this analysis the dependency on flow shallowness (H) was disregarded. In order to satisfy the need to simulate a condition in which the estimation of scour depth only depends on the pier size (b) rather than the flow depth (h), this limitation was imposed. In this way the condition would be restricted to narrow piers case as shown in figure 3.6.

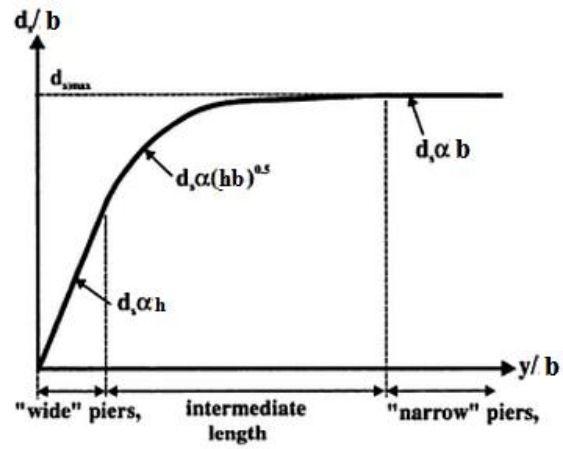

Figure 3.6: Local scour depth variations with respect to flow shallowness

- **L_c =(l_c/h)> 2**

In order to avoid the wall effect the ratio of width of the flow with respect to flow depth is considered to be greater than 2. Lateral walls may increase the complexity of flow movements around the pier and change the trend of scour depth evolution.

Thus together with choice of $L_c > 2$ and H > 2 it can be concluded that the ratio between pier width and width of flow (b/l_c) would restricted to be greater than 0.25. In this way the contraction effects for narrow flows will be controlled. From the continuity principle, a decrease in flow area results in an increase in average velocity and bed shear stress and as a consequence, more bed material is going to remove from riverbed. Thus in narrow channel the local scour will increase in compare to wide channel due to contraction effect and this condition should be avoided.

- **σ<1.4**

Standard deviation of sediment particle size distribution is considered to be less than 1.4 to have an approximately uniform sediment distribution. For nonuniform sediments, armouring

occurs on the channel bed. Armour layer formation within the scour hole reduces the local scour depth.

- $\boldsymbol{d_{50} > 0.5\ mm}$

For clear water scour, the sediment median size of the acceptable experiments is considered to be greater than 0.5 mm to avoid the effects of ripples. The formation of ripples with fine sands limits the scour depth observed in laboratory experiments under clear-water conditions, because of sub-threshold condition that would be formed by ripples.

- **T=t.u/b**

Time plays an important role in scour and under clear-water conditions scour evolves very slowly and scour depth tend to reach to its equilibrium condition after long duration. For interpreting the effect of dependent parameters on each other, it was decided to investigate these dependencies at constant dimensionless times. The investigated dimensionless durations of the experiment are considered to be equal to 10^6 and 10^5. Dimensionless time equal to 10^6 and 10^5 are arbitrary choices. These dimensionless times are acceptably large enough to neglect the effects of initial conditions (for example the effect of starting procedure of an experiment) and as a result the measured values of scour depth tend to have less dispersion compare to the measurements in initial stage of an experiment. These criteria are summarized below:

For series:

$T \geq 10^6$ for T= 10^6

$T \geq 10^5$ for T=10^5

For isolated points:

$5 \times 10^5 \leq T \leq 5 \times 10^6$ for T= 10^6

$7.35 \times 10^4 \leq T \leq 1.42 \times 10^5$ for T=10^5

Measurements of scour depth at initial phases due to high rate of evolution of scour holes may have high level of uncertainty and by increasing time duration these errors will become less and it is possible to do the interpolation process with more reliability. This is the reason behind the choice of suitable interval for isolated points which is greater for T equal to 10^6 and shorter for 10^5. In this way we have same amount of error as a consequence of extrapolation in both cases.

- **Trend Regularity check**

The regularity of each valid experiment (111 and 143 series for T equal 10^6 and 10^5 respectively) satisfying the mentioned criteria was then checked by taking advantage of experimental function provided by Franzetti et al (1982). This function was obtained by applying

least square method to the experimental values of a series of tests and it is an exponential function of dimensionless time as follow:

$$d_s = d_{se}(1 - e^{-0.028\sqrt[3]{\tau}}) \qquad (3.22)$$

Where d_s is the scour depth, d_{se} is ultimate or equilibrium scour depth and τ is dimensionless time.

By fitting this curve to result of each test, using measured scour depths points with dimensionless time greater than 10^5 and using d_{se} as calibrating parameter and extending the obtaining curve to points with lower value of dimensionless time, the regularity of each test was checked by comparing each test trend with fitted curve in a visual manner. An example of regular trend is shown in Figure 3.7. As a result, five tests from *Mignosa (1980)* experiments and one test from *Ettema (1980)* were disregarded due to non-regularity of their trends compared to the fitted curve. These trends are shown in figure 3.8.

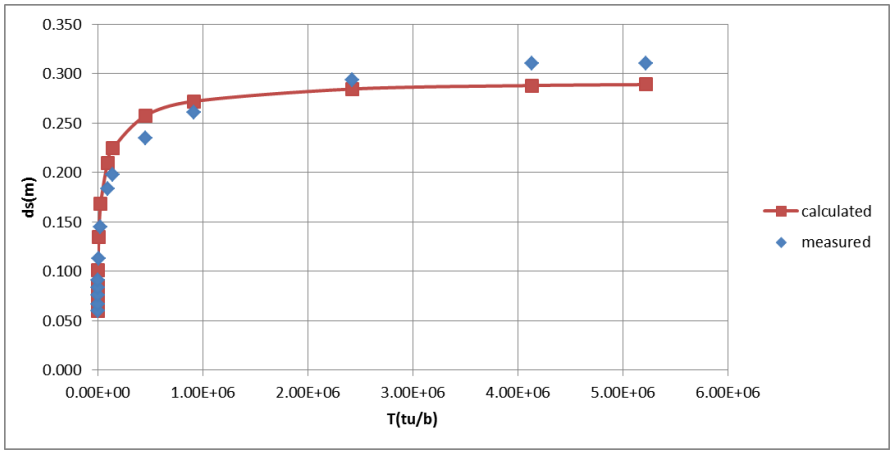

Figure 3.7 : An example of test with regular trend

Non-regularity in the trend of a test may be a result of error in measurements during the experiment, instability of parameters that should be constant during an experiment such as velocity or conducting and experiment in live-bed condition and having an oscillation along the scour depth evolution trend with respect to time and etc.

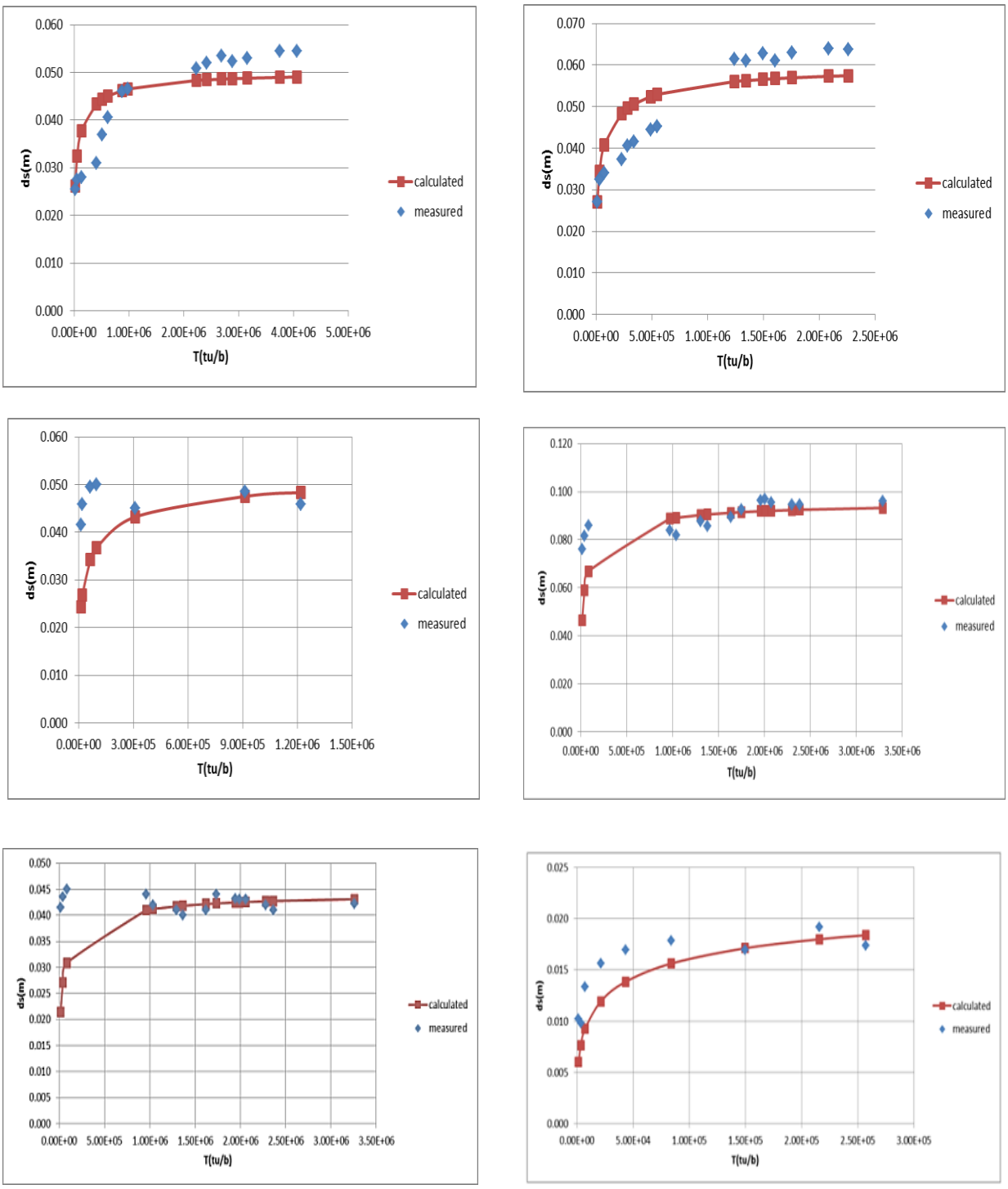

Figure 3.8: Disregarded test from Mignosa (1980) and Ettema (1980) due to trend non-regularity

The number of experimental results that remains after imposing the mentioned criteria and data selection procedure for dimensionless time, T, equal to 10^5 and 10^6 are represented in the following charts (Figure 3.9).

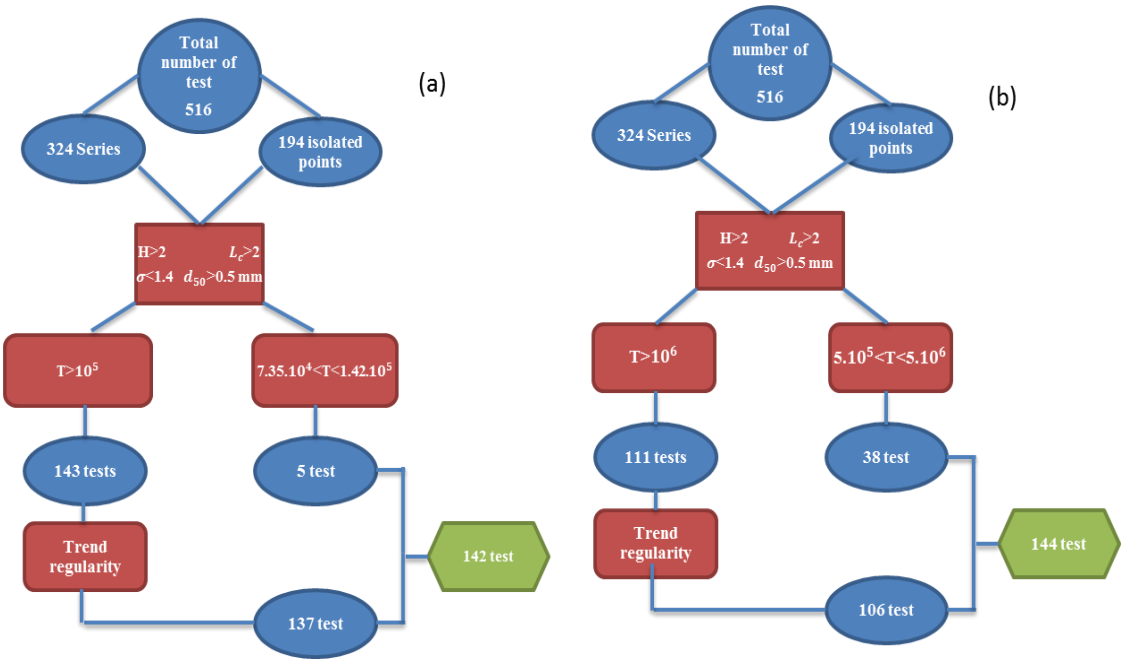

Figure 3.9: Selection procedure for dimensionless time, T, equal to 10^5 (a) and 10^6 (b)

3.4.3. Flow regime verification

For having an integrated database, it is necessary to compute central velocity (depth-averaged velocity) for tests that the value of velocity is given in terms of average bulk velocity. As mentioned in section 3.3, for this conversion and using the existing formula by Paleari (2014), it is mandatory to have a fully turbulent regime.

Friction factor was estimated for each of the tests by Colebrook-White formula (Colebrook 1939) as follow:

$$\frac{1}{\sqrt{f}} = -2.0\, log_{10}\left(\frac{k_s}{3.71 D_H} + \frac{2.51}{Re\sqrt{f}}\right) \qquad (3.23)$$

Where k_s is the equivalent sand roughness height that can assume to be equal to d_{50} and D_H is the hydraulic diameter. Equation (3.23) is a non-linear equation and it is necessary to do a nonlinear analysis for solving it. This task was carried out by Excel solver and the value of friction factor for each test was computed.

For distinguishing whether the test are in fully turbulent condition or is in transitional condition, the Reynolds values were compared to Reynolds value of case Re*=70 according to conversion equation author. The verification procedure of the valid tests is shown in figure 3.9.

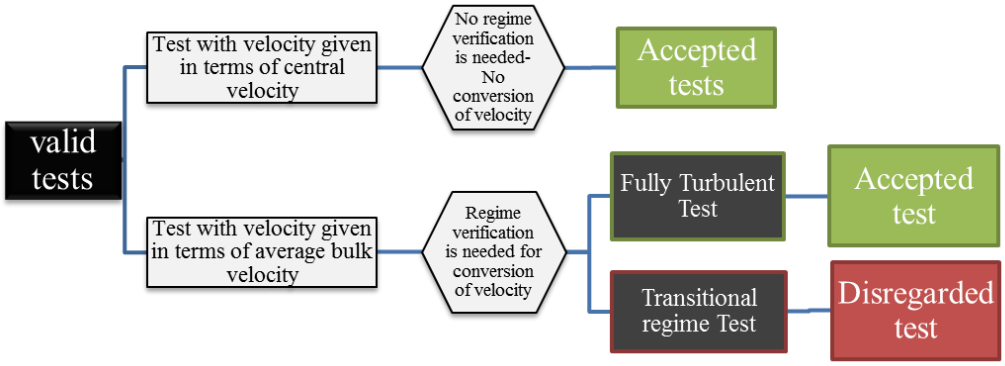

Figure 3.10: flow regime verification procedure

According to the above chart, the final tests number which is suitable for analysis purposes is equal to 86 tests for $T=10^5$ and 78 tests for $T=10^6$ which are indicated by green color in figure 3.11. These tests consist of the tests that their value is already given in terms of depth-averaged velocity or, they are tests with given value of average bulk velocity but they were conducted in fully turbulent condition and it is possible to convert their velocity to depth-averaged velocity.

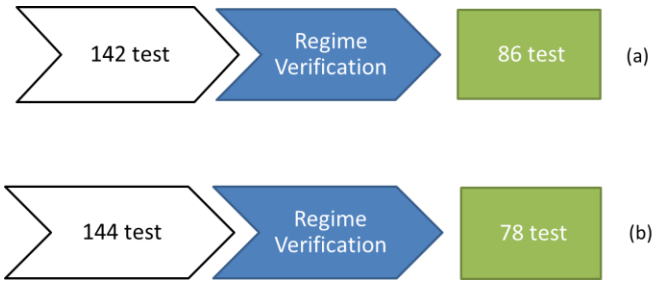

Figure 3.11: The outcomes of regime verification. (a) For $T=10^5$ (b) For $T= 10^6$

By inserting all of the initial valid tests (142 tests) for $T=10^6$ and (144 tests) for $T=10^5$ in Moody diagram (Figure 3.12 and 3.13), it can be seen, due to the fact that these tests are in the lower part of the diagram, their friction factors are not significantly different in compare to fully turbulent case. Therefore it is concluded that, all of these valid tests may be considered in analysis and the conversion can be imposed for unifying their velocities although some of them are not fully turbulent.

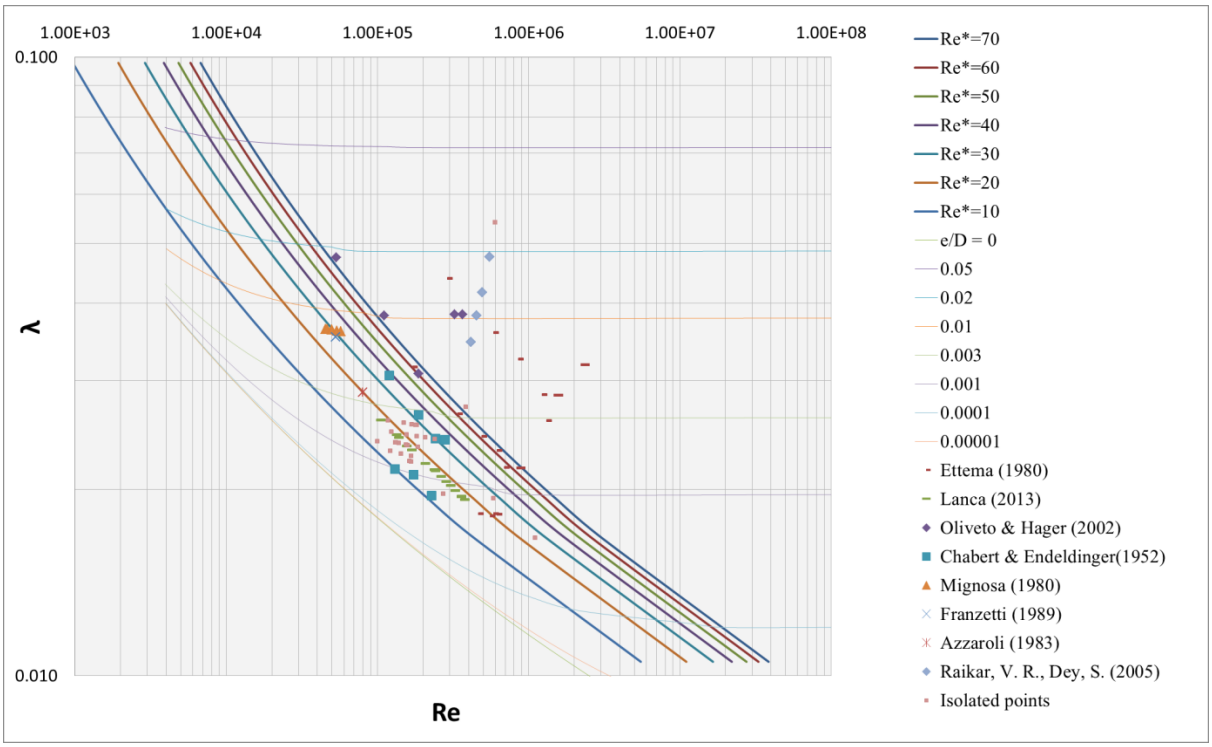

Figure 3.12: presentation of valid tests for $T=10^6$ on moody diagram

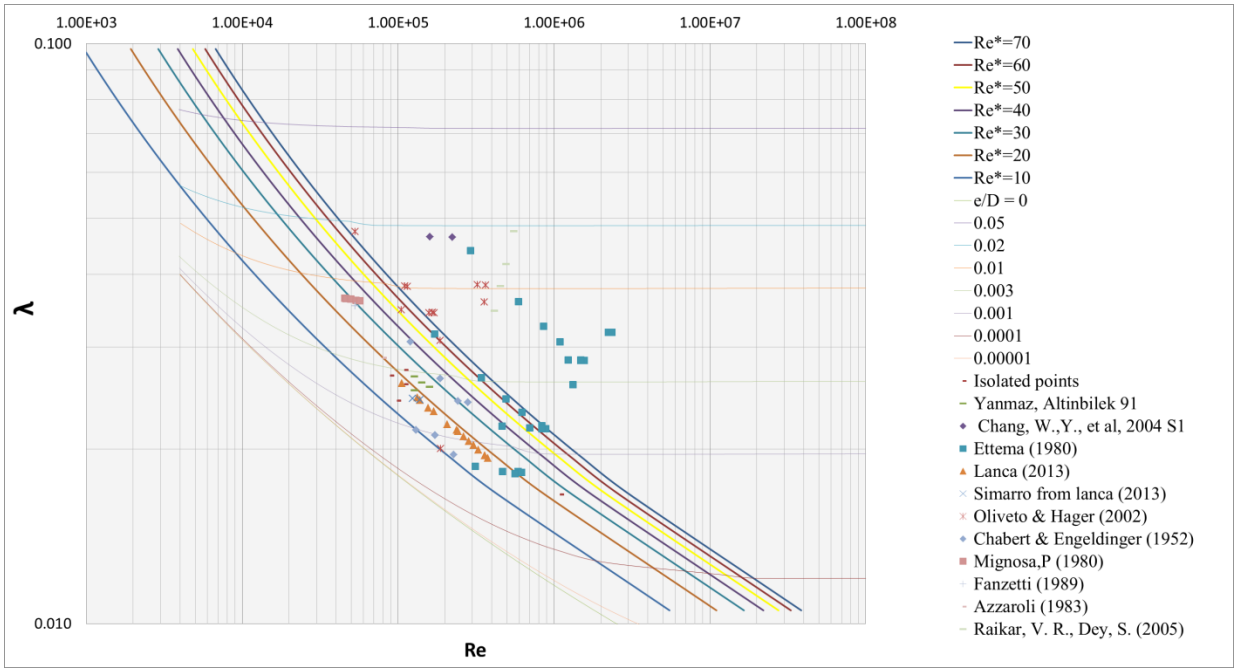

Figure 3.13: presentation of valid tests for $T=10^5$ on moody diagram

3.5. Presentation of valid data

3.5.1. Dispersion of valid data

For final analysis it was decided to use only data that satisfy the regime verification (86 tests for T=10^5 and 78 tests for T=10^6) due to the fact that a sufficient number of tests remain after imposing all the selection criteria. In the following graphs U, D_{50}, H, D_s, and T are plotted with respect to each other for better understanding the final valid data. These graphs are presented for both datasets used (for analysis at dimensionless time equal to 10^5 and 10^6). The total number of valid data include isolated points and series is equal to 86 and 78 for T=$10^5$and T= 10^6 respectively as mentioned before.

Most of the tests under consideration have D_{50} (the ratio between width of the pier, b, and sediment median size, d_{50}) less than 100. For T=10^5 about 75% of data have D_{50} less than 50 and for T=10^6 same condition exist (Figure 3.14).

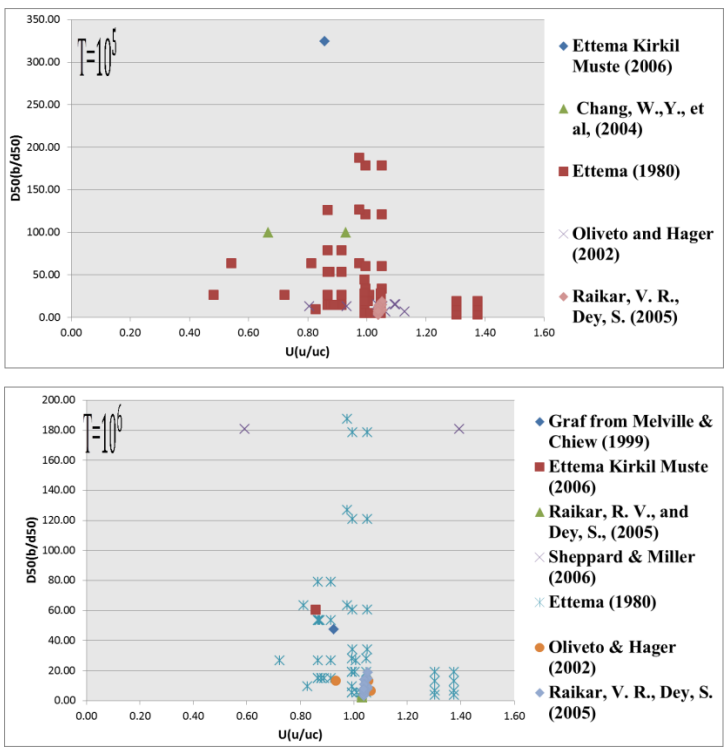

Figure 3.14: Presentation of valid data for D_{50} with respect to U

All of the test respect the criteria imposed for the ratio of the depth to pier width (H>2).The maximum value of H for both case is equal to 21.53 and is derived from Ettema (1980)'s experiment (Figure 3.15).

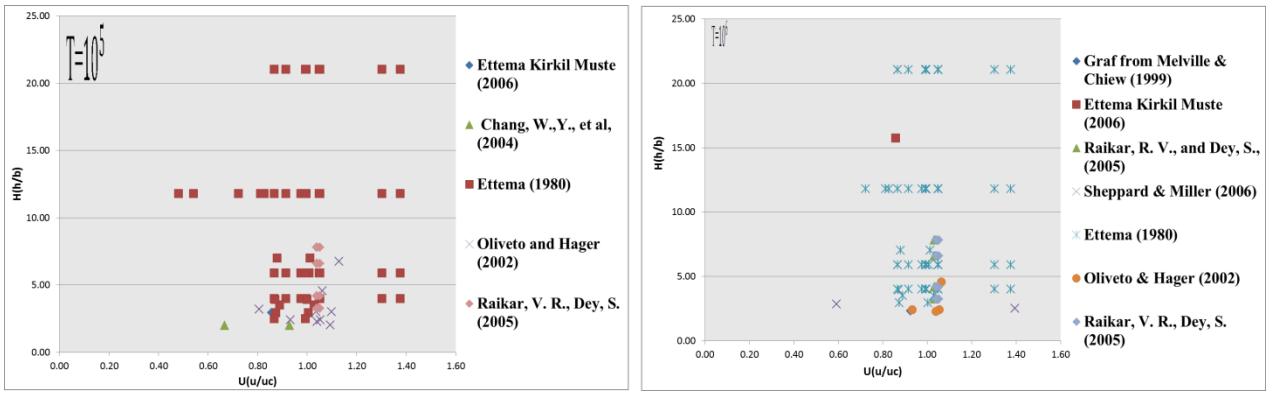

Figure 3.15: Presentation of valid data for H with respect to U

The value of D_s, which is the ratio between scour depth and pier diameter, is within the range of 0.333 and 2.537 for T=$10^5$and between 0.79 and 2.537 for T=10^6 (Figure 3.16).

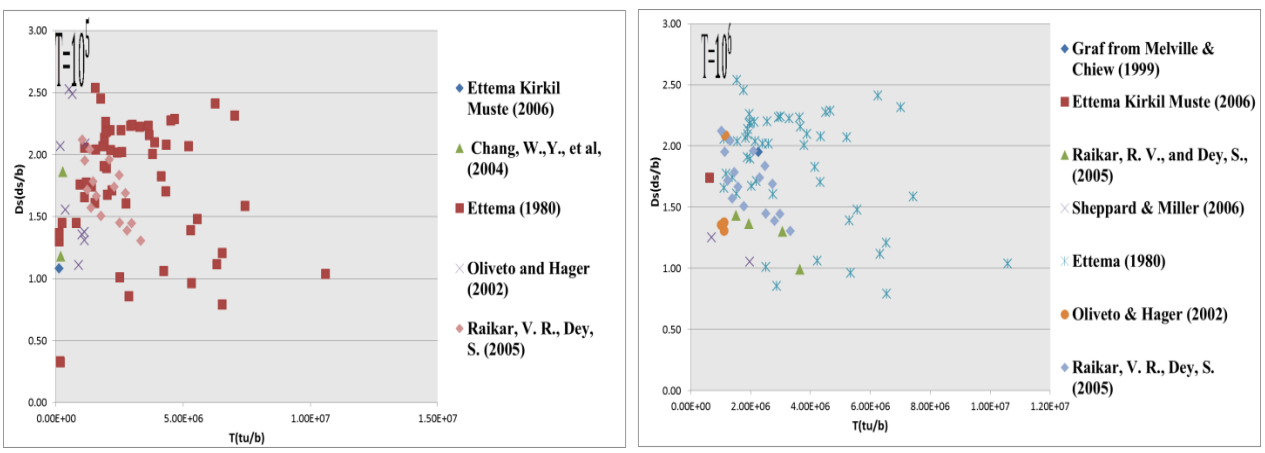

Figure 3.16: Presentation of valid data D_s with respect to T

The nondimensional time of all the accepted tests, respect the previously mentioned selection criteria. All of the accepted tests have T less than 7.424×10^6 except one test from Ettema (1980) with T greater than 10^7.

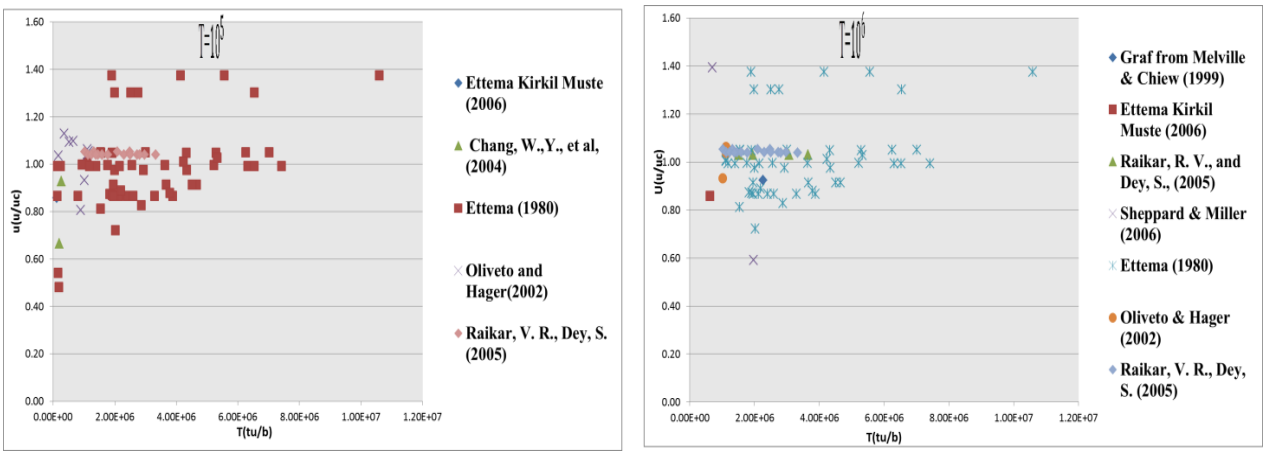

Figure 3.17: Presentation of valid data U with respect to T

All the above plots show that the selected control parameters (H, U, D_{50} and T) are not correlated with each other. This fact is the fundamental requirement of dimensional analysis. In dimensional analysis it is necessary to define a requested parameter as a function of independent parameters.

By considering Melville & Coleman (2000) formulation for computing critical shear velocity, u_c^*, in both T=$10^6$and T=10^5about 75% of accepted series are having u^*/u_c^* less than one and secure clear-water condition.

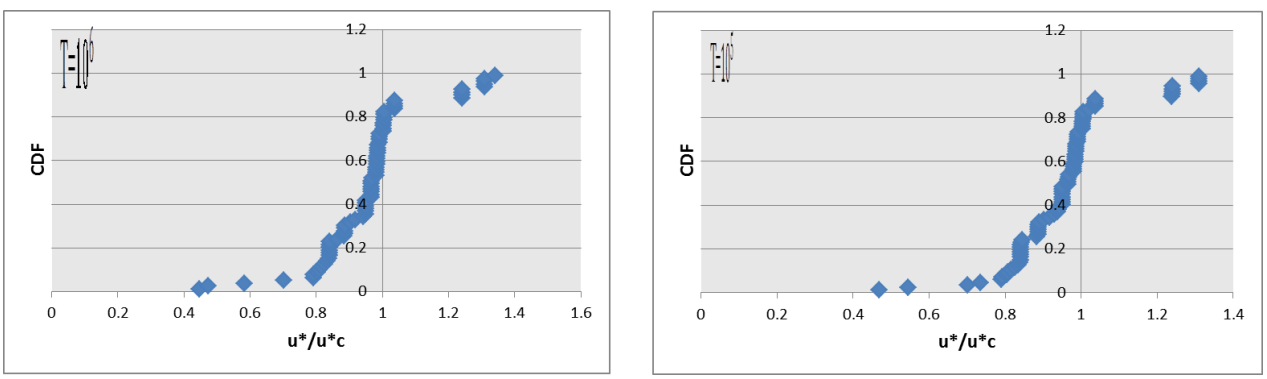

Figure 3.18: Cumulative distribution function of u^*/u_c^* for valid data

As it is indicated in figure 3.18, they are some experiments that their computed ratio of u^*/u_c^*, using Melville & Coleman (2000) equation, are greater than one. As mentioned before, the computed values of u_c^* depends strongly on the evaluation criterion which is going to be used for computation and there is no exact solution for computing a threshold for sediment motion. On the other hand, according to the authors of the tests with u^*/u_c^* greater than one, all of the mentioned tests are conducted in clear-water condition. Moreover, as it is going to be illustrated in next section, all these tests are still located within the region provided by Shields experiments for the threshold of movement. Also the trend regularity check of these experiments approves

clear-water condition in these tests. Thus it is possible to also employ these experiments in analyses.

A cumulative distribution of nondimensional time and scour depth are also presented in following figures (3.19 and 3.20).

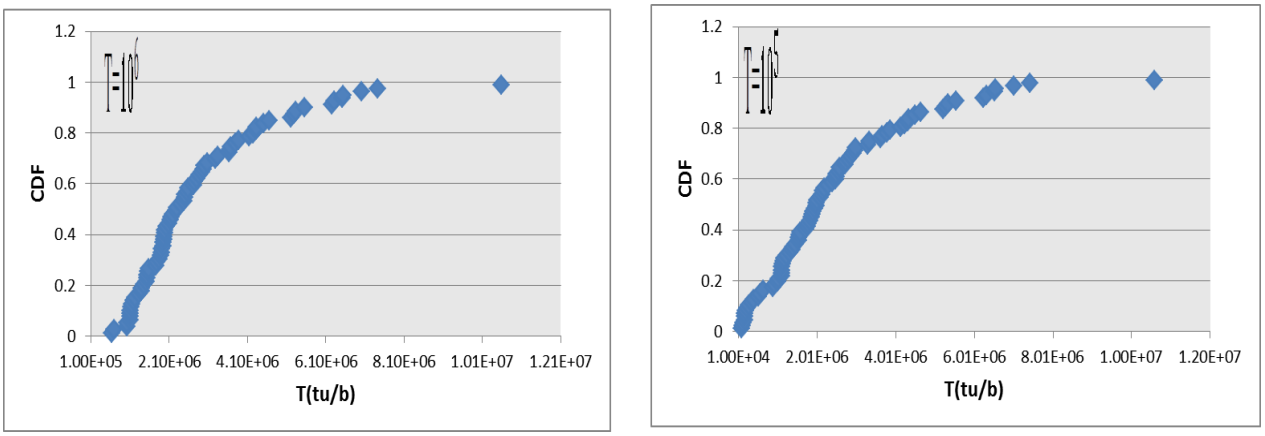

Figure 3.19: Cumulative distribution function of dimensionless time for valid data

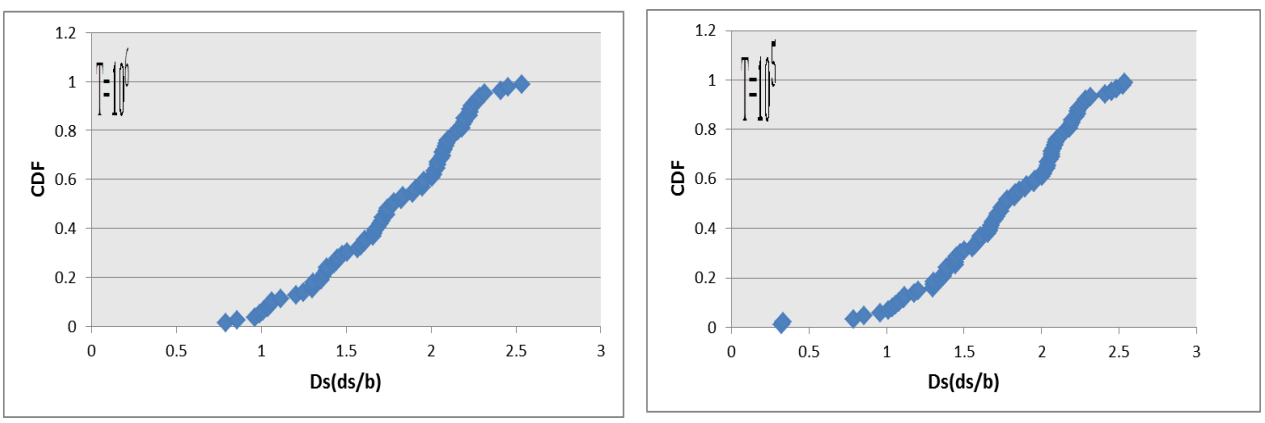

Figure 3.20: Cumulative distribution function of D_s (d_s/b) for valid data

3.5.2. Valid data in Shields diagram

In the figure (3.21), valid data can be found together with experimental data by Shields (1936). The red points represent shields experimental results and yellow and blue points are valid data for analysis at $T=10^6$and $T=10^5$ respectively. It can be seen that all of these data are below or within the Shields region, thus a clear-water condition is predicted for these experiments. The black curve represents Melville & Coleman (2000) criteria for sediment incipient motion.

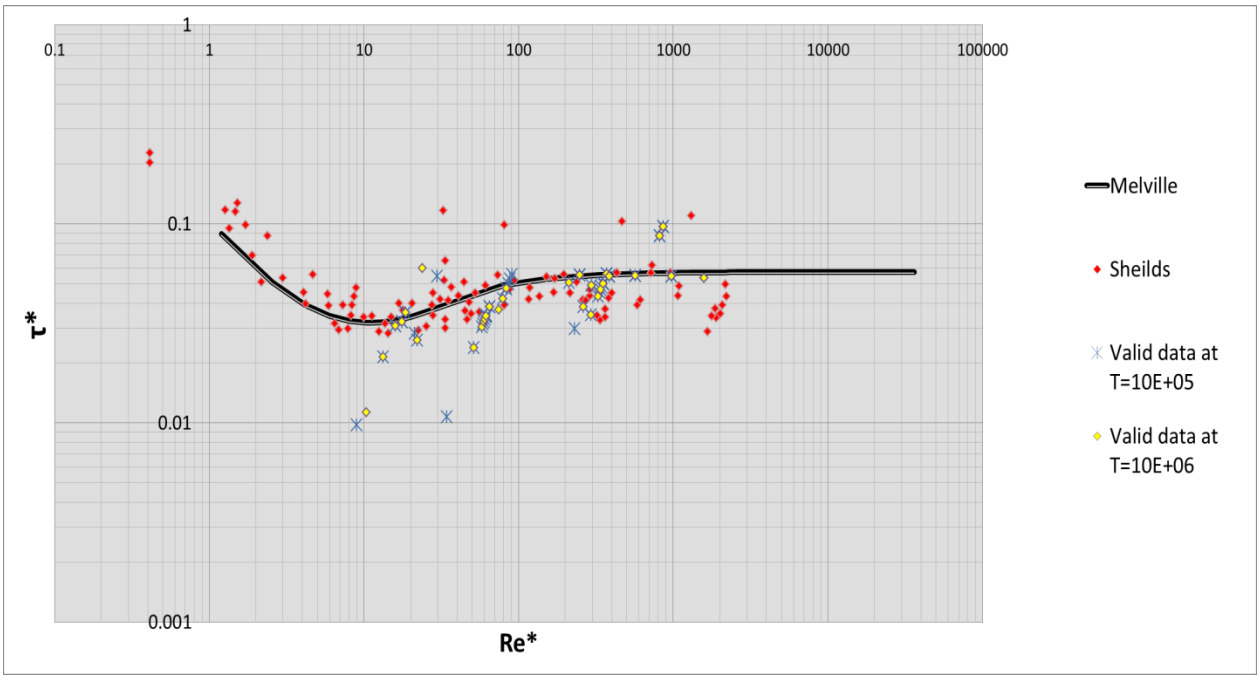

Figure 3.21: Presentation of valid data at T=10^5 and T=10^6 in Shield Diagram

3.6. Dependency verification

According to section 1.3.4 the form which can represent the scour depth as the function of dimensionless parameters is:

$$D_s = f(U, H, D_{50}, T) \qquad (3.24)$$

Where: $U = \frac{u}{u_c}, H = \frac{h}{b}, D_{50} = \frac{b}{d_{50}}$ $and\ T = \frac{tu}{b}$

Thus, the dimensionless Scour depth, D_s, may be defined as a function of multiplication of control parameters:

$$D_s = f_1(T).f_2(D_{50}).f_3(U).f_4(H) \qquad (3.25)$$

The functional relationships between dimensionless variables have to be obtained from experimental results and by means of interpolation. In this section, the effort has been made to verify the existence of possible dependency between dimensionless parameter. The procedure of finding a suitable equation for each of the dimensionless variables will be discussed in detail in the next section on the base of the initial idea which is obtained in this section.

Thanks to the choices made in section 3.4.2 for selection of valid data, by considering H>2 there is no need to take into account the effect of $f_4(H)$ and it is possible to neglect this function from the scour depth predictive formula. Moreover, due to the fact that, the scour depth was decided to be evaluated in only two constant nondimensional times equal to 10^5 and 10^6, the

$f_1(T)$ function will be substituted by a multiplicative constant. This value is representing the result of $f_1(T)$ at dimensionless time equal to 10^5 or 10^6.

For calibrating a function for $f_2(U)$ and $f_2(D_{50})$ at two different dimensionless time equal to T=$10^5$and T=10^6, it is necessary to control the possible dependency of these parameter to each other and check the trend of these parameter with respect to dimensionless scour depth, D_s.

For this purpose, values of D_{50} and U of the valid tests were plotted with respect to D_s at dimensionless times, T, equal to 10^5 and 10^6 separately. The values of D_s at these nondimensional times were obtained by fitting a logarithmic function to scour depth evolution curve and interpolating the corresponding value of scour depth for the entire full trend valid tests. As mentioned before, the amount of dispersion of data in a regular trend is higher in initial phase of scour depth evolution and also there is a higher probability of experimental error in this phase. Therefore, for finding the values of scour depth at requested dimensionless times (10^5 or 10^6), only points with higher value of dimensionless time and a few numbers of points with lower value were employed for interpolating within a full trend. An example of finding the value of scour depth at T equal to 10^6 for Franzetti (1989) test is shown in figure (3.21).

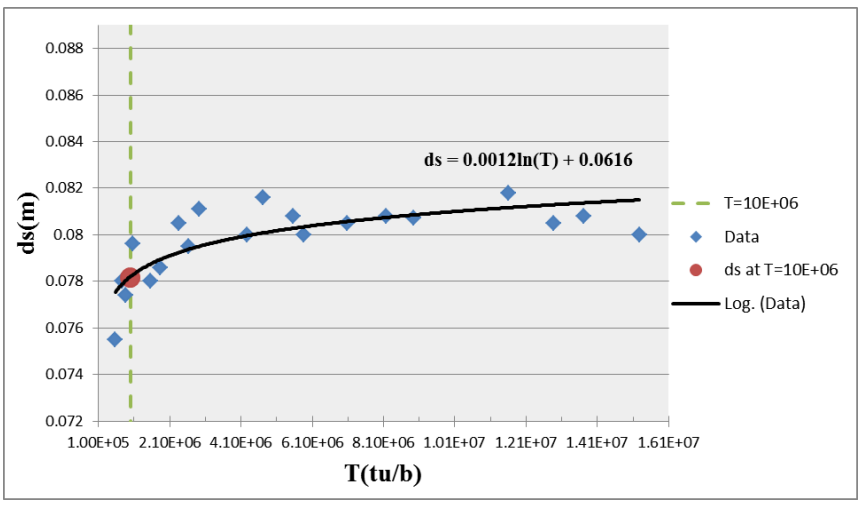

Figure 3.22: Example of interpolation for finding scour depth (d_s) at requested nondimensional time (T)

For the accepted isolated points, which satisfied the previously defined nondimensional time criteria, the value of D_s at the end of the experiment is assumed to be equal to its value at T=10^5 or T=10^6 with a reasonable approximation. As an example the accepted isolated points for T=10^6 is provided in figure (3.23). The upper and lower bounds of the accepted interval are equal to 5×10^6 and 5×10^5 respectively for this case.

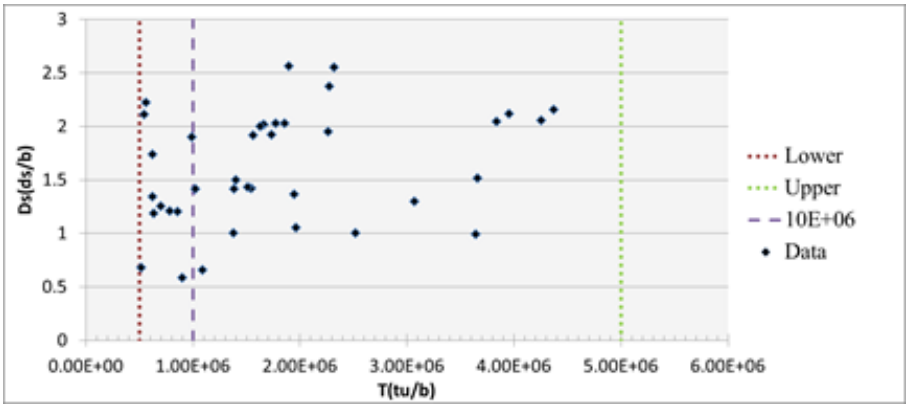

Figure 3.23: presentation of accepted range and valid tests for assuming that the final scour depth is equal to scour depth at $T=10^6$ for isolated points data

For plotting D_s with respect to U and D_{50} and checking the dependency of these data, the valid data were divided into groups with similar size. For plotting D_s with respect to D_{50}, the valid data were divided into intervals of U as represented in figure 3.24. For plotting D_s with respect to U also four intervals were defined for D_{50} that these groups are having same size in logarithmic scale (Figure 3.25).

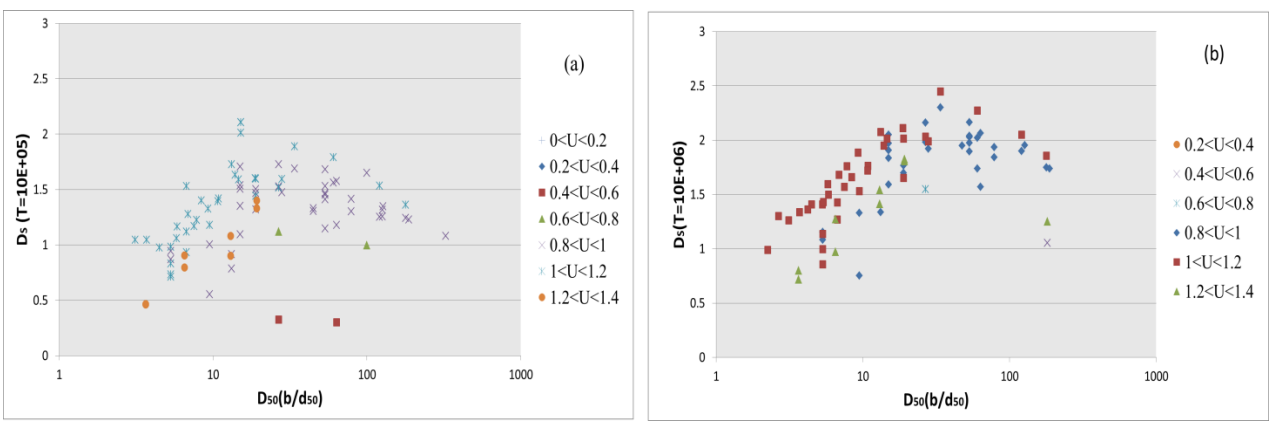

Figure 3.24: D_s with respect to D_{50} divided into groups of U (a) $T=10^5$ (b) $T=10^6$

It is possible to investigate an increasing logarithmic trend for D_s with respect to D_{50} up to an approximate value of 30 for both graphs with different value of nondimensional time (Figure 3.24). Then a reverse situation occurs and the value of D_s decrease by increasing D_{50}. It is worthy to mention that, for both cases the trend seems to be similar and even the maximum value of D_s occurs in approximately same value of D_{50}.

Figure 3.25 presents the values of U and their corresponding D_s for entire valid data. It can be seen that there is an increasing trend up to U equal to one and then the value of D_s decrease by increasing U to values greater than one. The mentioned trend becomes less noticeable for lower values of D_{50} which are illustrated by blue points in figure 3.25. Generally there is a less

remarkable dependency between D_s and U compare to D_{50}. The dispersion of the valid data and the irregularity of the defined classification increase in case of T equal to 10^5 , compare to the case with T equal to 10^6. This phenomenon is due to higher value of scour depth rate in lower times according to logarithmic scour depth evolution with respect to time and as a consequence higher probability of experimental error in early stages.

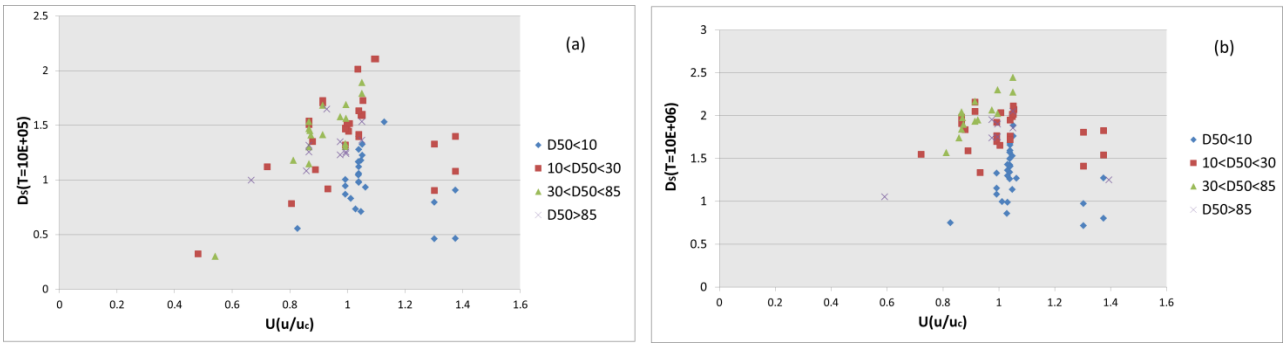

Figure 3.25: D_s with respect to U divided into groups of D_{50} (a) T=10^5 (b) T=10^6

3.7. Interpolation with valid data

3.7.1. Introduction

After obtaining a general view for defining a suitable function for each of the dependent nondimensional parameter, the process of determining a final function for nondimensional scour depth was done by clustering the final valid data. The clustering procedure was done in a stepwise manner by considering D_s equal to multiplication of $f_1(T)$, $f_2(D_{50})$ and f_3(U) as below:

$$D_s = f_1(T).f_2(D_{50}).\ f_3(U) \qquad (3.26)$$

The effect of $f_4(H)$ was neglected as mentioned before. It is clear that the effect of pier size is taken into account in function f_1 (tu/b) and f_2 (b/d_{50}).

3.7.2. Initial attempt

Initial attempt for finding a suitable function for $f_2(D_{50})$ was made by considering only valid data with U (u/u_c) between 0.8 and 1.2. Thus more unified data would remain for regression. After imposing the mentioned filtering for data selection, 67 and 74 data remain for regression at T equal to 10^6 and 10^5 respectively.

- **D_s Vs. D_{50}**

As a first choice for interpolation of function $f_2(D_{50})$, by considering the logarithmic dependency as mentioned in previous section, an exponential function was employed with the following format:

$$f_2(D_{50}) = a.{D_{50}}^{b}.\exp\left(c.{D_{50}}^{d}\right) \qquad (3.27)$$

Where a, b, c and d are constants and are derived by least square method. The equation that produced the best least squares fit to the data was used to obtain the final equation for nondimensional scour depth (D_s).

As it is represented in figure 3.26 and already mentioned in previous section, the trend of data seems to be similar and there is just an upward shift of data by moving from the case with T equal to 10^5 to 10^6. Thus it was decided to use two functions with same shape and with only different in their vertical position.

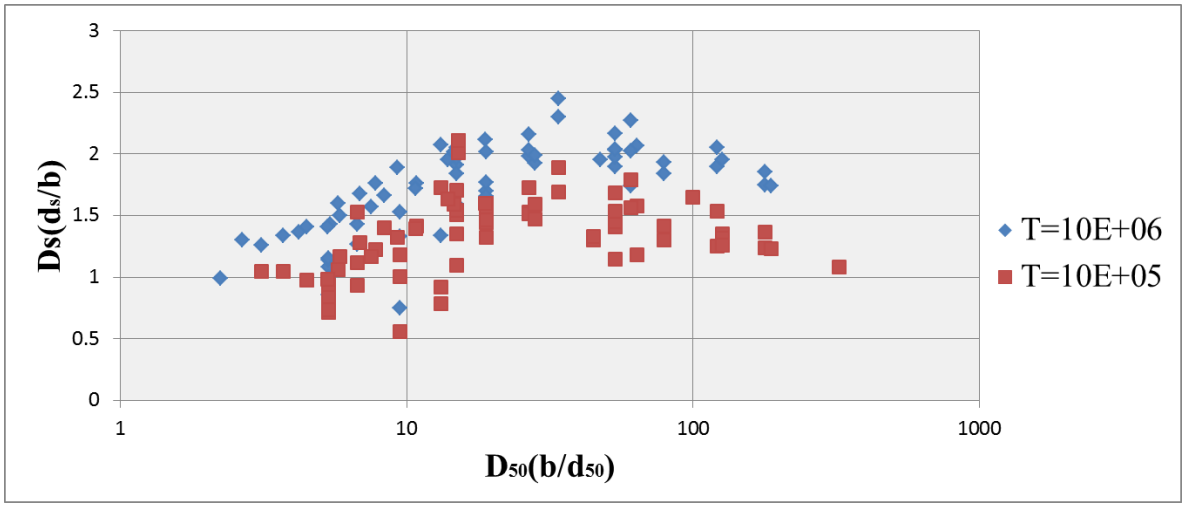

Figure 3.26: Valid data in D_s-D_{50} space for both T=10^5 and T=10^6

The first attempt yielded the following equation for $f_2(D_{50})$:

$$f_2(D_{50}, \mathrm{T} = 10^6) = 4.168.{D_{50}}^{1.6}.\exp\left(-2.6.{D_{50}}^{0.25}\right) \qquad \text{For T=}10^6 \qquad (3.28)$$
$$f_2(D_{50}, \mathrm{T} = 10^5) = 3.207.{D_{50}}^{1.6}.\exp\left(-2.6.{D_{50}}^{0.25}\right) \qquad \text{For T=}10^5 \qquad (3.29)$$

As it can be seen, the only difference in equation 3.28 and 3.29 is the value of constant a, which is a constant that define the vertical position of the curve. Thus it has a lower value at T equal to 10^5. The sum of the squares of the errors made in the result of every calculated points are equal to 5.66 and 5.48 for T equal to 10^5 and 10^6 and it shows that the fitted curve shape induce approximately same error in both case. Thus it can be concluded that the constant a can represent the value of $f_1(T)$ at the corresponding T as below:

$$f_1(\mathrm{T} = 10^6) = 4.168 \qquad (3.30)$$
$$f_1(\mathrm{T} = 10^5) = 3.207 \qquad (3.31)$$

And general formula for $f_2(D_{50})$ is:

$$f_2(D_{50}) = {D_{50}}^{1.6}.\exp\left(-2.6.{D_{50}}^{0.25}\right) \qquad (3.32)$$

Figure 3.27 shows the difference between the calculated D_s for different value of D_{50} and the corresponding measured values obtained by experiment in the literature for both cases.

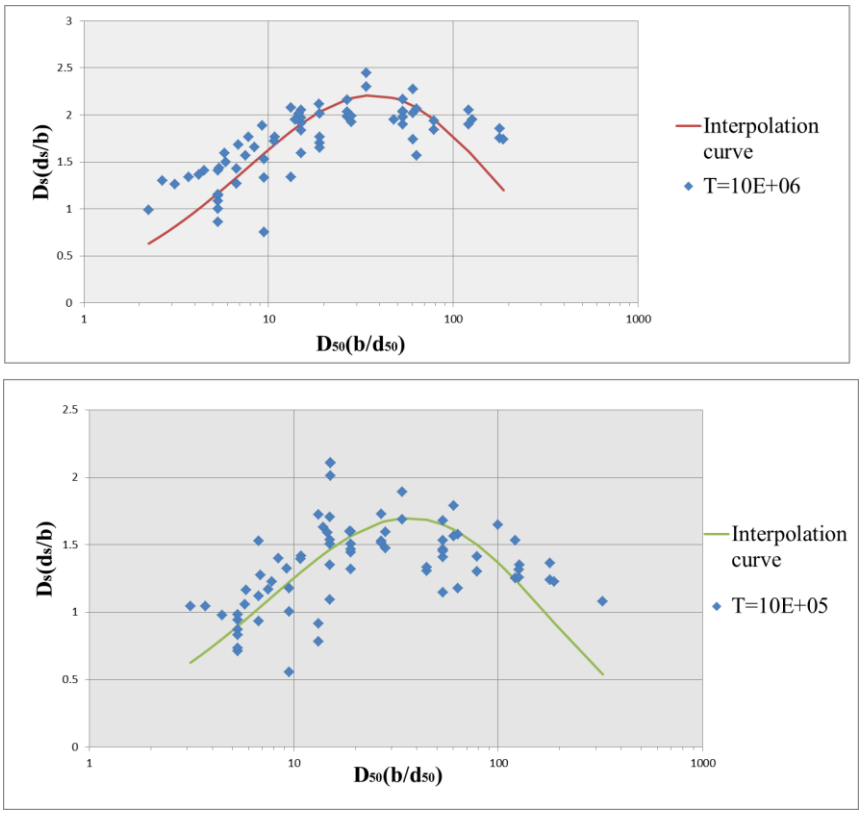

Figure 3.27: First attempt for $f_2(D_{50})$ at $T=10^6$ (up) and $T=10^5$ (down) (0.8<U<1.2)

- **D_s Vs. U**

In the next step after finding a suitable function for $f_2(D_{50})$, a function was chosen for fitting a reasonable curve for $f_3(U)$.

Before choosing an interpolation function and doing the regression, the measured value of D_s was divided by the calculated value of D_s (i.e. $f_2(D_{50}).\ f_1(T)$) which was obtained from the previous step. This operation would cluster the valid data and helps the process of interpolation.

The first choice for interpolation of the function $f_3(U)$ was a 3rd order polynomial with the following format:

$$f_3(U) = a.U^3 + b.U^2 + c.U + d \qquad (3.33)$$

Where *a*, *b*, *c* and *d* are constants to be obtained by curve fitting. Similar to previous step, the value of these constant are define in a way that the obtaining equation has the best least square fit. The resulting equation is as below:

$$f_3(U) = 115.23\, U^3 - 328.6\, U^2 + 312.3\, U - 97.90 \qquad (3.34)$$

Same equations were chosen for both cases with T equal to 10^5 and 10^6 obtaining low and approximately equal amount of errors (sum of the square errors equal to 2.75 and 2.74). Figure 3.28 represent the calculated values of $D_s/[\, f_2(D_{50}).\ f_1(T)]$ for different value of U and their corresponding measured values obtained by experiment.

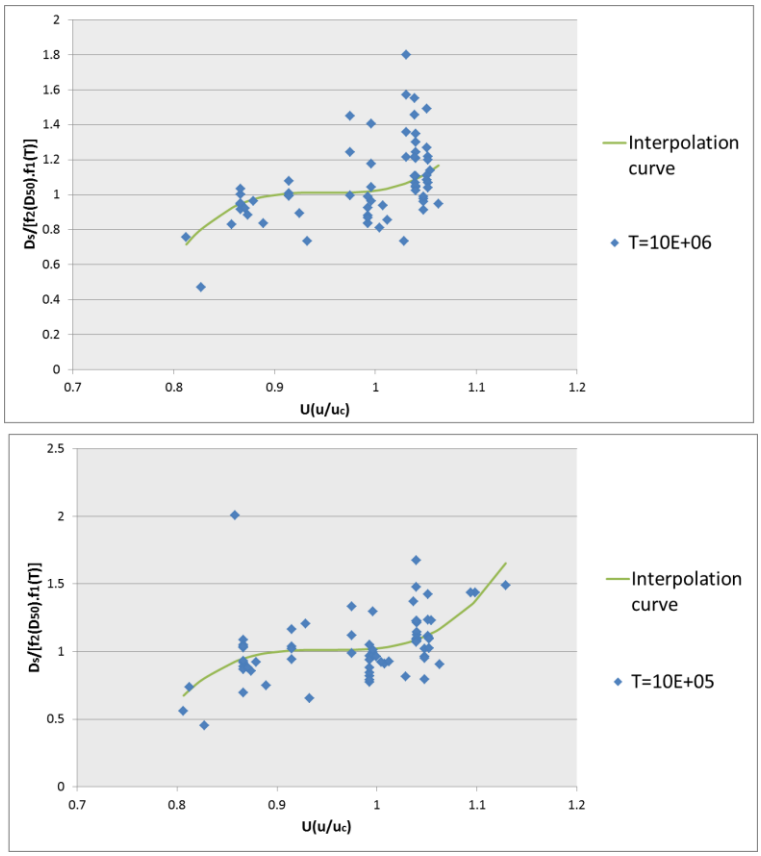

Figure 3.28: First attempt for f_3 (U) at T= 10^6 (up) and T= 10^5 (down)

- **Measured Vs. Calculated**

The final calculated results in the first attempt that obtained by multiplication of $f_1(T)$, $f_2(D_{50})$ and $f_3(U)$, as previously explained in equation (3.26), are plotted with respect to their measured values in figure (3.29). The red and blue lines represent 15 % error of calculated value with respect to its measured one. The green line shows the condition in which the calculated value is exactly equal to measured value and therefore the error is equal to zero .

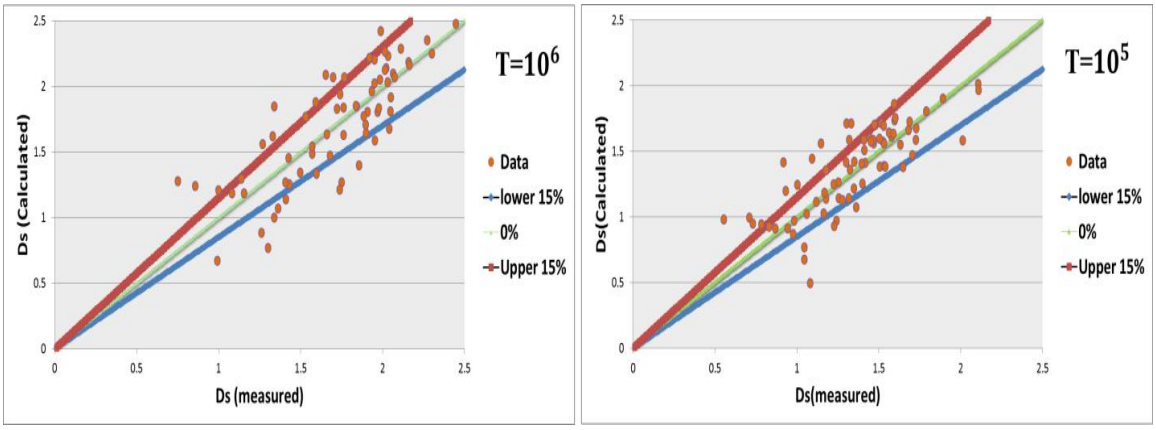

Figure 3.29: Calculated Vs. measured values of D_s at T=10^6 (left) and T=10^5 (right) for the first attempt

The obtained equations are only valid for the condition with U greater than 0.8 and less than 1.2. The predicted equation may improve by repeating the mentioned steps and clustering the valid data and having more compact population of points.

3.7.3. Further attempts

Further attempts were made to improve the final predictive equation as below:

1. Another attempt with the same nondimensional velocity restriction (0.8<U<1.2) was made for obtaining more reliable functions for $f_2(D_{50})$, $f_3(U)$ and more precise value for $f_1(\mathrm{T} = 10^6)$ and $f_1(\mathrm{T} = 10^5)$. Same format of equations were used for interpolation of $f_2(D_{50})$ and $f_3(U)$ as previous attempt. Same method of data clustering was also used. The only difference was in interpolation of D_s with respect to D_{50}. The $f_3(U)$ function, which obtained in the initial attempt, was employed as normalizing function in the first step for finding $f_2(D_{50})$ and therefore the curve fitting was done for valid points in U with respect to D_s / $f_3(U)$ plot.
2. Then the nondimensional velocity restriction was disregarded and the total number of valid data increased to 78 and 86 for interpolation at T equal to 10^6 and 10^5 respectively. In this attempt also same format of equations were used as previous cases. Due to an increase in the number of valid data for interpolation, the amount of errors also become greater as it was predicted.

The obtained formulas and the measured vs. calculated diagram in each of the above attempts are provided in appendix 2.

3.7.4. Final attempt

The final attempt was made after the second step mentioned in section 3.7.3 by considering the entire valid data and without imposing any restriction for the value of nondimensional velocity, U. This attempt yields to the final predictive equation for nondimensional scour depth and is an improvement of the previous attempt.

- $\boldsymbol{D_s}$ **Vs.** $\boldsymbol{D_{50}}$

In this part also same form of the equations as previous attempts were used for regression of valid data at both nondimensional time case; 10^6 and 10^5. For clustering of the valid data, the measured values of D_s were divided by their corresponding values of $f_3(U)$ which were obtained from previous attempt. The final attempt yields in to the following equation for $f_2(D_{50})$:

$$f_2(D_{50}, \mathrm{T} = 10^6) = 20.855\, {D_{50}}^{-0.42}.\exp\left(-5{D_{50}}^{-0.45}\right) \qquad \text{For T=}10^6 \qquad (3.35)$$

$$f_2(D_{50}, \mathrm{T} = 10^5) = 15.646\, {D_{50}}^{-0.42}.\exp\left(-5{D_{50}}^{-0.45}\right) \qquad \text{For T=}10^5 \qquad (3.36)$$

Thus as mentioned before the constant a can be represent the value of $f_1(T)$ at the corresponding T as below:

$$f_1(\mathrm{T} = 10^6) = 20.855 \qquad (3.37)$$

$$f_1(\mathrm{T} = 10^5) = 15.646 \qquad (3.38)$$

And general formula for $f_2(D_{50})$ is:

$$f_2(D_{50}) = {D_{50}}^{-0.42}.\exp\left(-5{D_{50}}^{-0.45}\right) \qquad (3.39)$$

The sum of the squares of the errors made in the result of every calculated points are equal to 3.683 and 2.767 for T equal to 10^6 and 10^5 and it shows a better regression in compare to previous attempts. The final plots are presented in figure 3.30.

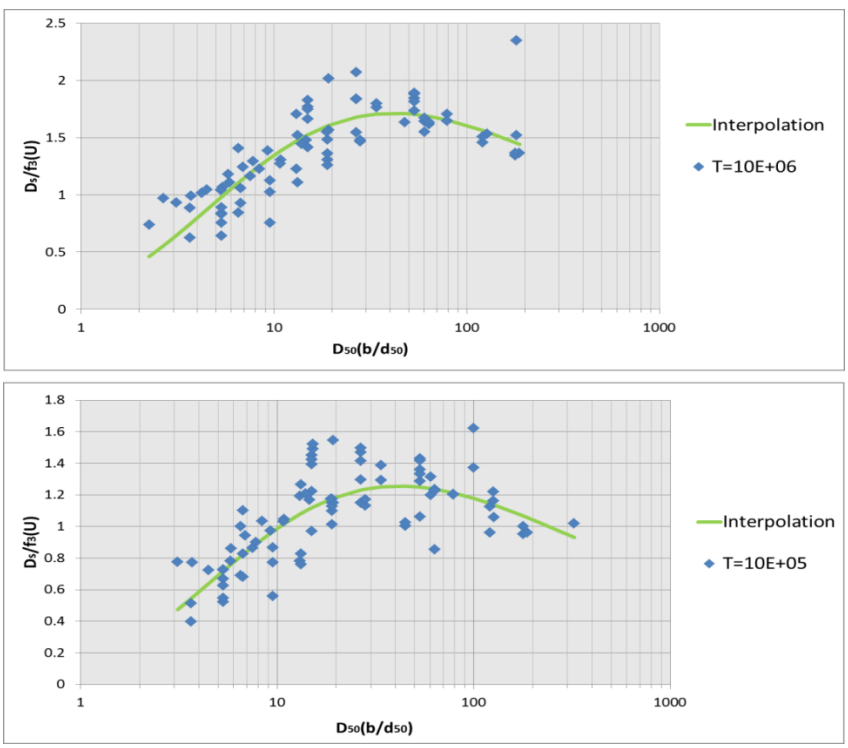

Figure 3.30: f_2 (D_{50}) obtained from final attempt at T=10^6 (up) and T= 10^5 (down)

- $\boldsymbol{D_s}$ **Vs.** $\boldsymbol{U}$

In final attempt for finding a suitable function for $f_3(U)$ same procedure of clustering was done. Two different forms of equation were chosen to see which one yields to better regression:

1. According to previous study by Franzetti et al. (1994) an equation with the following form was selected:

$$f_3(U) = a - b(c - U)^d \qquad (3.40)$$

   Where *a*, *b*, *c* and *d* are constants and obtain by valid interpolation and least square method.
2. a 3rd order polynomial as previous attempts:

$$f_3(U) = a.U^3 + b.U^2 + c.U + d \qquad (3.41)$$

The final regression results with each mentioned equation form are as below:

$$f_3(U) = 1.23 - 10(1.0513 - U)^4 \qquad (3.42)$$

$$f_3(U) = -5.349\,U^3 + 11.790\,U^2 - 6.261\,U + 1.132 \qquad (3.43)$$

The obtain curves for each nondimensional case are provided in figure 3.31.

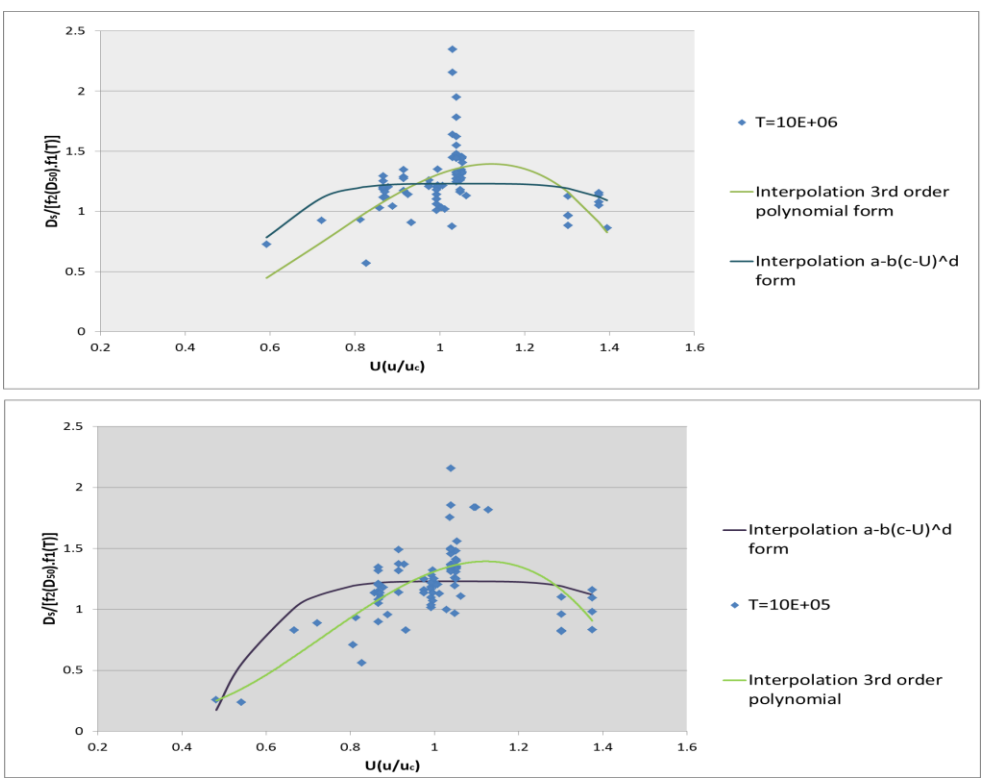

Figure 3.31: Final attempt for obtaining f_3 (U) with two different equation forms for T=10^6 (up) and T=10^5 (down)

The first form yields to total squares of the errors equal to 5.16 and 5.97 for the case with T equal to 10^6 and 10^5 respectively. On the other side, the second form (3rd order polynomial) yields to errors (4.272 and 3.967) which are less compare to resulting errors using first form equation for regression. Moreover the 3rd order polynomial equation shows a better modeling for the region with U greater than 1.3, where valid data illustrate a decrease in value of D_s by increasing U. Besides, the latter form provides a more desirable regression in region with smaller U.

In Figure 3.32 the proposed formula are shown along with two other formulas which are available in literature, one provided by Franzetti et al. (1994) and another by Sheppard et al. (2004).

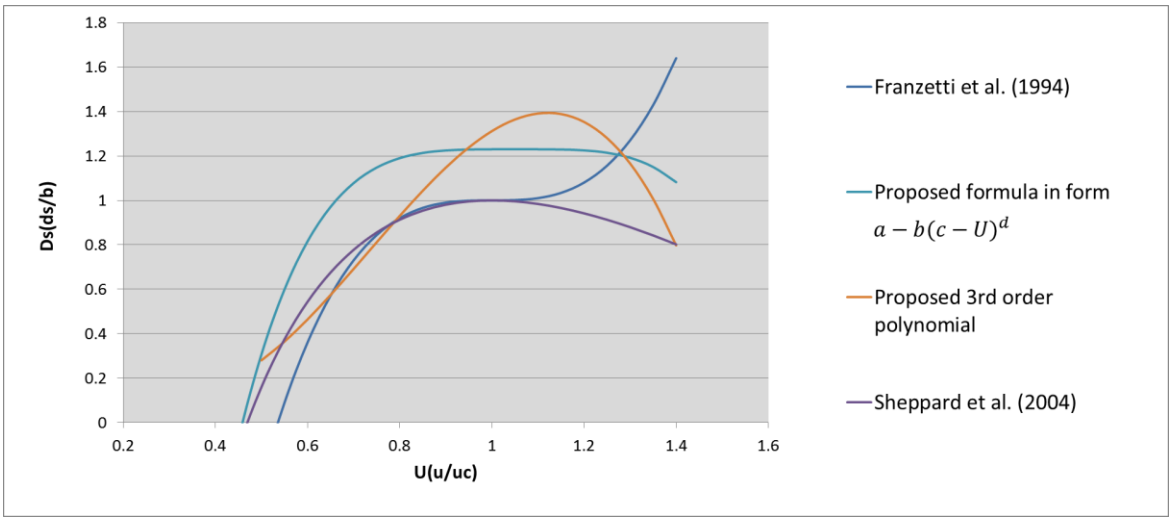

Figure 3.32: Comparison of proposed formulas with previous results in literature

Thus the second equation which is a 3rd order polynomial was chosen as the final equation for $f_3(U)$. It is essential to mention that, the provided formula is only valid in the range of available data for regression, i.e. for values of U between 0.48 and 1.39. Below this region the proposed equation shows an increase in value of D_s which is not logical according to available experimental results in literature.

- **Measured Vs. Calculated**

The calculated value of Ds for the final attempt would be obtained by multiplication of $f_1(T)$, $f_2(D_{50})$ and $f_3(U)$ as previously explained. Once again the measured values of D_s were plotted versus their corresponding calculated values. The red and blue lines represent 15 % error of calculated value with respect to its measured one by experiment. The green line shows the condition in which the error is equal to zero (Figure 3.33).

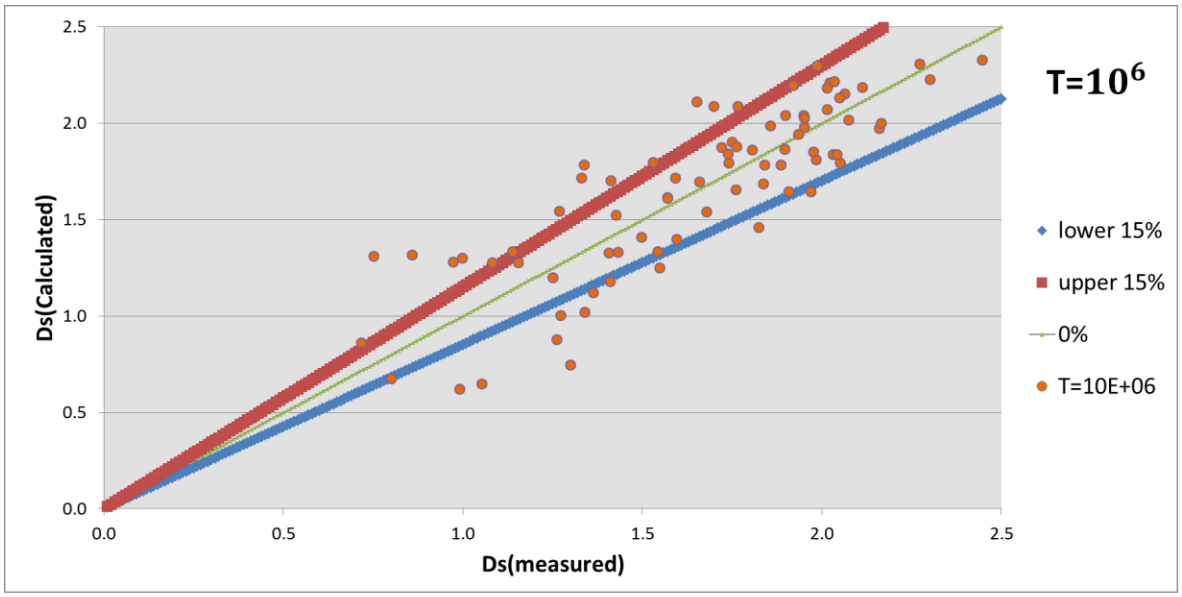

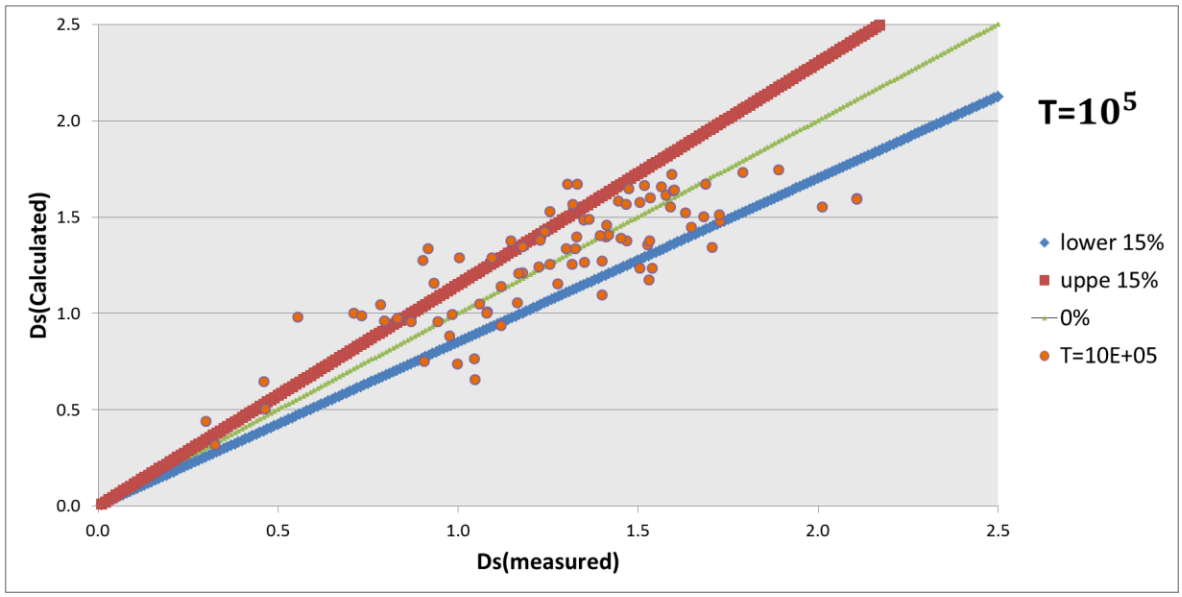

Figure 3.33: Calculated Vs. measured values of D_s at T= 10^6 (up) and T=10^5 (down) for the final attempt

The comparison of measured and calculated values shows a reasonable approximation for prediction of D_s in both cases (T equal to 10^5 and 10^6). The above graphs indicate that about 65% of the calculated values of D_s have less than 15% error in both cases. This value would increase up to 85 %, if the acceptable error rises from 15% to 25%.

3.7.5. Summary of final results

The final results obtained from the last interpolation attempt are summarized below:

$$D_s = f_1(T).f_2(D_{50}).\ f_3(U) \tag{3.44}$$

Where:

$$f_1(\mathrm{T} = 10^6) = 20.855 \tag{3.45}$$
$$f_1(\mathrm{T} = 10^5) = 15.646 \tag{3.46}$$

$$f_2(D_{50}) = {D_{50}}^{-0.42}.\exp\left(-5{D_{50}}^{-0.45}\right) \qquad 2 \leq D_{50} \leq 325 \tag{3.47}$$

$$f_3(U) = -5.349\,U^3 + 11.790\,U^2 - 6.261\,U + 1.132 \qquad 0.48 \leq \mathrm{U} \leq 1.39 \tag{3.48}$$

It is worthy to mention that, valid range for each formula is according to the interval of available data and should be respected; otherwise unreliable values of D_s would be obtained.

Finding a suitable function for $f_1(\mathrm{T})$ needs more known values of this function at different dimensionless times and also choosing a reasonable function that has the ability to model its trend correctly. In this stage it is not logical to do the regression due to lack of available values for $f_1(\mathrm{T})$ in different T (only at 10^5 and 10^6).

3.8. Model comparison with previous studies

According to section 1.3.5 there are several formulas for computing equilibrium local scour depth or its time evolution in literature. In this section the values of dimensionless scour depth, D_s, for valid data were computed by means of models provided by Melville & Chiew (1999), Lanca et al. (2013), Sheppard et al (2014) and Oliveto and Hager (2002). Thus it is possible to find out the ability of the proposed formula for computing D_s with acceptable precision compare to previous models.

3.8.1. Melville & Chiew (1999)

In this model different factors were provided for each of the dependent parameters for estimation of scour depth as below:

Flow intensity:

$$K_U = U \text{ for } \mathrm{U} < 1 \text{ and } K_U = 1 \text{ for } \mathrm{U} > 1 \tag{3.49}$$

Flow depth-pier width:

$$K_H = 2.4\,\mathrm{H} \qquad \text{for } \mathrm{H} < 0.7 \tag{3.50}$$

$$K_H = 2.H^{0.5} \qquad \text{for } 0.7 < H < 5 \tag{3.51}$$

$$K_H = 4.5\,H \qquad \text{for } \mathrm{H} > 5$$

Particle size:

$$K_{D_{50}} = 0.57 \log(2.24.H) \qquad \text{for } D_{50} < 25 \qquad (3.52)$$

$$K_{D_{50}} = 1 \qquad \text{for } D_{50} > 25 \qquad (3.53)$$

Time factor:

$$K_t = \frac{d_s}{d_{se}} = \exp\left[-0.03\left|\frac{u_c}{u} ln\left(\frac{t}{t_e}\right)\right|^{1.6}\right] \qquad (3.54)$$

For computing time factor K_t, it is necessary to compute the value of t_e which is the time to develop equilibrium scour depth. According to the author, t_e can be calculated by means of following relation:

$$t_e(days) = 48.26\frac{b}{u}(U - 0.4) \qquad H > 6 \qquad (3.55)$$

$$t_e(days) = 30.89\frac{b}{u}(U - 0.4)H^{0.25} \qquad H \leq 6 \qquad (3.56)$$

Thus the value of scour depth can be computed by:

$$d_s = K_H.K_U.K_{D_{50}}.K_t \qquad (3.57)$$

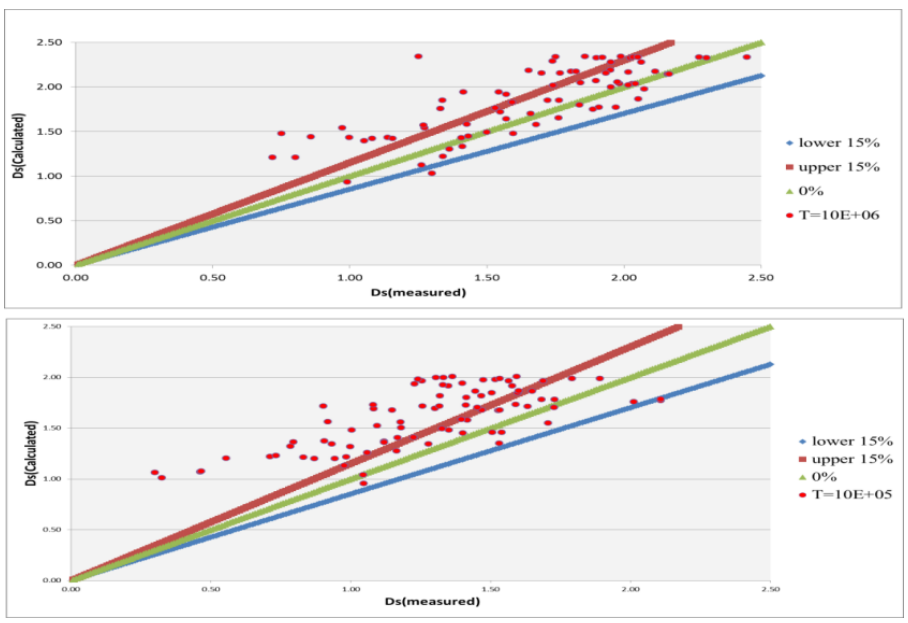

Figure 3.34: Calculated Vs. measured values of D_s at T= 10^6 (up) and T=10^5 (down) using Melville & Chiew (1999)

This model is capable to evaluate the value of D_s for T=10^6 with relatively low amount of error with respect to its measured value (Figure 3.24). 43% of points in figure 3.24, which are mostly related to test with U greater than one, are out of the acceptable range. Unfortunately this model does not show enough accuracy for evaluation of D_s at lower values of dimensionless time. In case with T equal to 10^5, the formula overestimates the measured scour depths, with 67% of points having relative error greater than 15% of their corresponding measured values of D_s.

3.8.2. Lanca et al. (2013)

Lanca also provides the following relation for computing equilibrium scour depth:

$$\frac{d_{se}}{b} = \begin{cases} 7.3{D_{50}}^{-0.29}H^{0.12} & for\ 60 \leq D_{50} \leq 50 \\ 1.2H^{0.12} & for\ D_{50} > 500 \end{cases} \quad (3.58)$$

For evaluating the value of scour depth at time T, following equation can be used:

$$\frac{d_s}{d_{se}} = 1 - exp[-a_1 T^{a_2}] \quad (3.59)$$

Where a_1 and a_2 are defined as:

$$a_1 = 1.22{D_{50}}^{-0.764} \quad (3.60)$$

$$a_2 = 0.09{D_{50}}^{-0.244} \quad (3.61)$$

In this model it is assumed that the flow intensity, u/u_c is near to one so as to maximize the scour depth. As a consequence no factor was defined for flow intensity. On the other hand, the proposed relationship is only valid for tests with D_{50} greater than 60.

According to above restrictions, the mentioned equation provided by Lanca et al. (2013), is only valid for 18 tests out of 86 available test for the case T=10^5 and 15 tests out of 78 for the case T=10^6.

The measured values of scour depth at dimensionless time equal to 10^5 and 10^6 have been plotted versus their corresponding calculated values by using Lanca et.al (2013)'s formula in figure (3.35). It can be seen that 28% of points for T=10^5 and 33% for T=10^6 are not in the acceptable error margin. It is obvious that, Lanca et.al (2013)'s formula shows a bigger amount of relative error for computing the scour depth in cases with low values of flow intensity as a result of disregarding the effect of flow intensity in its prediction.

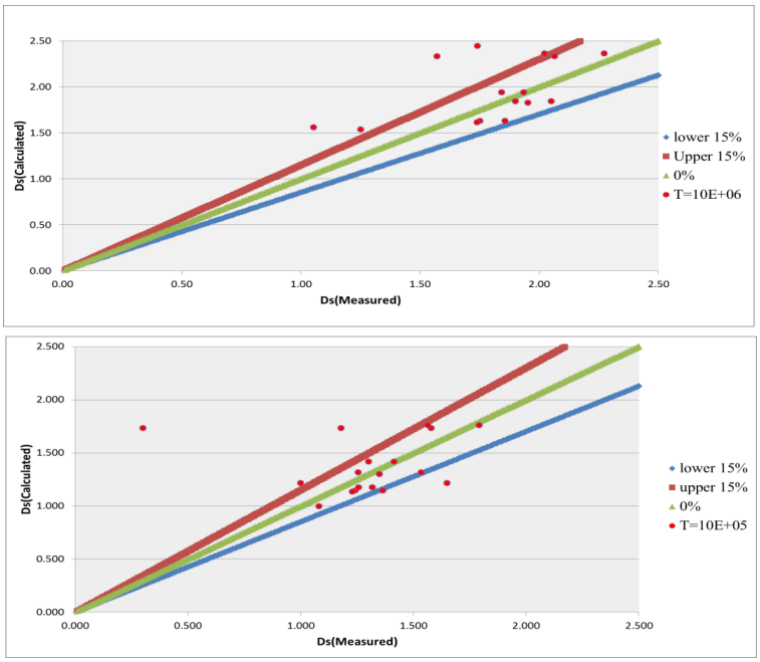

Figure 3.35: Calculated Vs. measured values of D_s at T= 10^6 (up) and T=10^5 (down) using Lanca, et al. (2013)

3.8.3. Sheppard et al. (2014)

The Sheppard and Miller (2006) and Melville (1997) equations were slightly modified to form a new equation:

$$\frac{d_{se}}{b} = 2.5.f_1(H).f_2(U).f_3(D_{50}) \qquad \text{for } 0.4 \leq U < 1 \qquad (3.62)$$

$$\frac{d_{se}}{b} = f_1\left[2.2\left(\frac{U-1}{\frac{u_{1p}}{u_c}-1}\right) + 2.5f_3\left(\frac{\frac{u_{1p}}{u_c}-U}{\frac{u_{1p}}{u_c}-1}\right)\right] \qquad \text{for } 1 \leq U \leq \frac{u_{1p}}{u_c} \qquad (3.63)$$

$$\frac{d_{se}}{b} = 2.2f_1(H) \qquad \text{for } U > \frac{u_{1p}}{u_c} \qquad (3.64)$$

Where:

$$f_1(H) = \tanh(H^{0.4}) \qquad (3.65)$$

$$f_2(U) = 1 - 1.2[\ln(U)]^2 \qquad (3.66)$$

$$f_3(D_{50}) = \frac{D_{50}}{0.4\,{D_{50}}^{1.2} + 10.6{D_{50}}^{-0.13}} \qquad (3.67)$$

$$u_{1p1} = 5u_c \qquad (3.68)$$

$$u_{1p2} = 0.6\sqrt{g.h} \qquad (3.69)$$

$$u_{1p} = \begin{cases} 5u_c & for\ u_{1p1} \geq u_{1p2} \\ 0.6\sqrt{g.h} & for\ \ u_{1p1} \geq u_{1p2} \end{cases} \tag{3.70}$$

Sheppard et al. (2014) model does not provide a general formula for deriving local scour time history. Therefore, only the value of scour depth at equilibrium stage can be computed by the proposed formula.

Figure (3.36) shows that the measured values of D_s using Sheppard et al. (2014) at equilibrium stage are greater than the corresponding measured values in most of the tests at $T=10^5$. This situation is less severe when nondimensional time increased to the value of 10^6. About 91% and 64% of points are out of the acceptable error range for T equal to 10^5 and 10^6 respectively.

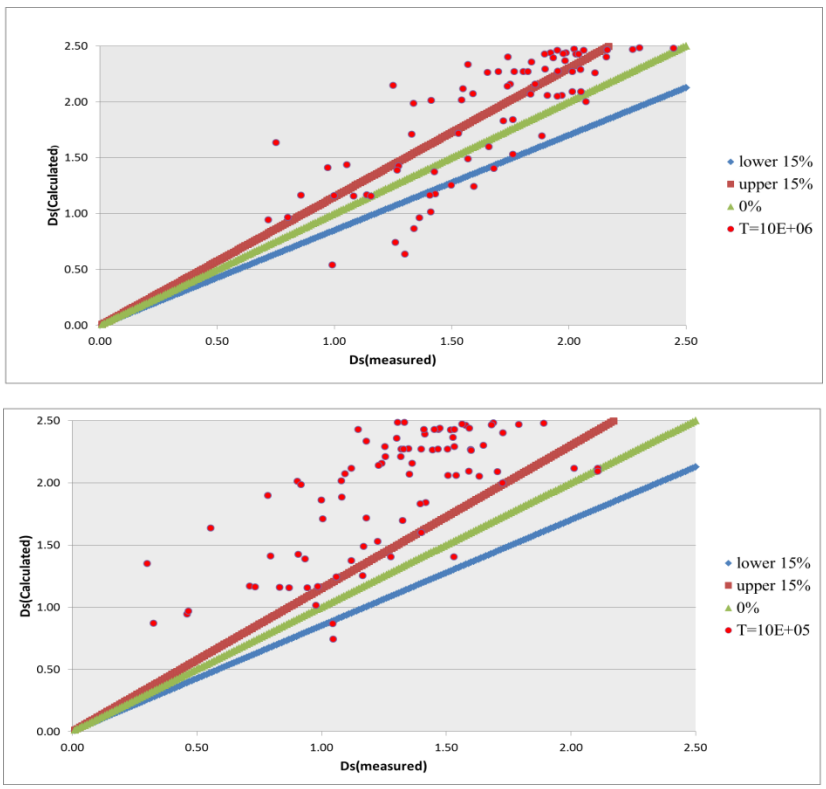

Figure 3.36: Calculated Vs. measured values of D_s at T= 10^6 (up) and $T=10^5$ (down) using Sheppard et al. (2014)

Therefore it can be concluded that, the estimated value of equilibrium scour depth using Sheppard et al. (2014) is an overestimation in most of the cases. Considering the fact that, T equal to 10^6 is reasonably large and according to previous studies and the reports of the conductors of collected experiments, it is fairly near to equilibrium stage.

3.8.4. Oliveto and Hager (2002)

Using similarity arguments and the analogy to flow resistance, an equation for temporal scour evolution was proposed by Oliveto and Hager (2002) in the following form:

$$D_s = 0.068\, N\sigma^{-0.5} Fr^{1.5} \log(T) \qquad (3.71)$$

Where:

N=shape number and is equal to 1 for circular pier;

Fr= Froude number= $u/(g'd_{50})^{1/2}$;

g'= Reduced gravitational acceleration= $g.\Delta$;

T=dimensionless time= $\left\{(g'd_{50})^{\frac{1}{2}}/L_R\right\} t$;

L_R =Reference length= $b^{2/3}h^{1/3}$;

t= Time;

b= Pier width; and

h= Upstream flow depth.

In this model the temporal scour evolution depends on three main parameters, namely:

1. Reference length $b^{2/3}h^{1/3}$ for pier;
2. Densimetric mixture Froude number $\sigma^{-0.5}u/(g'd_{50})^{1/2}$; and
3. Relative time T involving geometry and sediment characteristics.

The values of scour depth at nondimensional times 10^5 and 10^6 were computed by means of Eq.3.71 for all of the valid experiments and the resulting measured versus calculated graphs are plotted in figure 3.37.

It can be concluded from figure 3.37 that the calculated values of scour depth, using Oliveto and Hager (2002)'s fromula, do not respect the threshold of relative error (equal to 15%) in approximately 62% of the tests for both nondimensional cases of 10^5 and 10^6. This formula tends to have an overestiamtion of the measured scour depths.

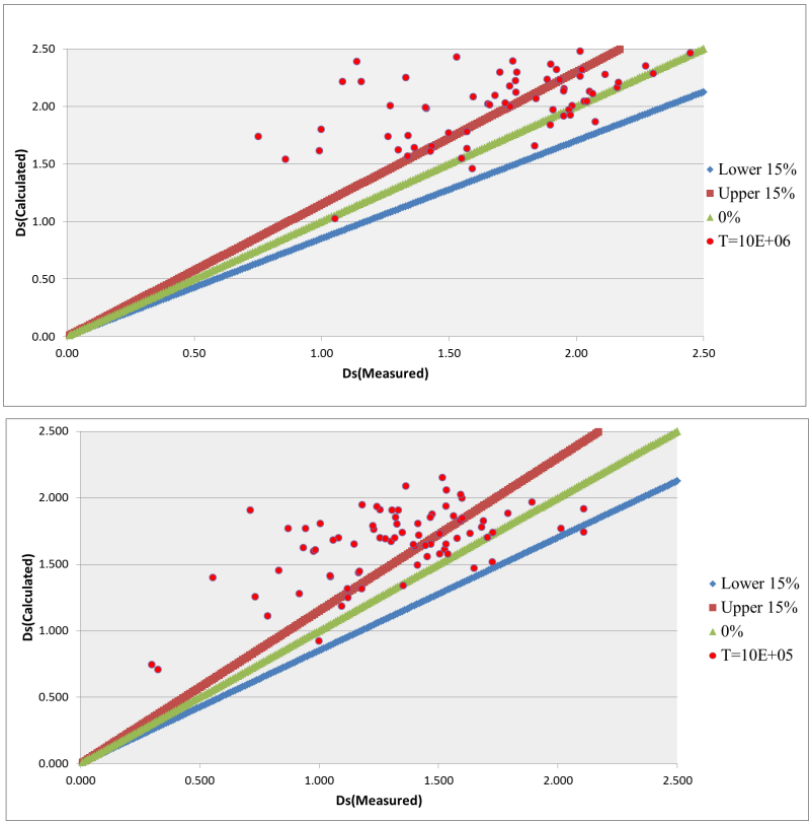

Figure 3.37: Calculated Vs. measured values of D_s at T= 10^6 (up) and T=10^5 (down) using Oliveto and Hager (2002)

In the mentioned comparisons, all the velocities were in term of depth-averaged velocity. In another approach, it was decided to use the velocities decleard by the authors rather than using the converted ones. Thus, the upstream velocities in the database are a mixture of velocities which are given in term of average bulk velocity and the velocities which are given in term of averaged-depth velocity.

Considering Olivet and Hager (2002) formula and using delcread value of velocities by the authors of differnet experiements for computing the Froude number in Eq.3.71, the following measured versus calculated graphs were obtained (Figure 3.8).

Figure 3.38 shows that the predictive capability of the proposed formula is increased by using the declared value of flow velocities instead of their converted ones. In figure 3.38 about 55% of points for the case with T=10^5 and 47% for the case with T=10^6 are having relative error greater than 15%. Thus, it can be concluded that the homogenization of the database velocities can even reduce the accuracy of the formula proposed by Oliveto and Hager (2002).

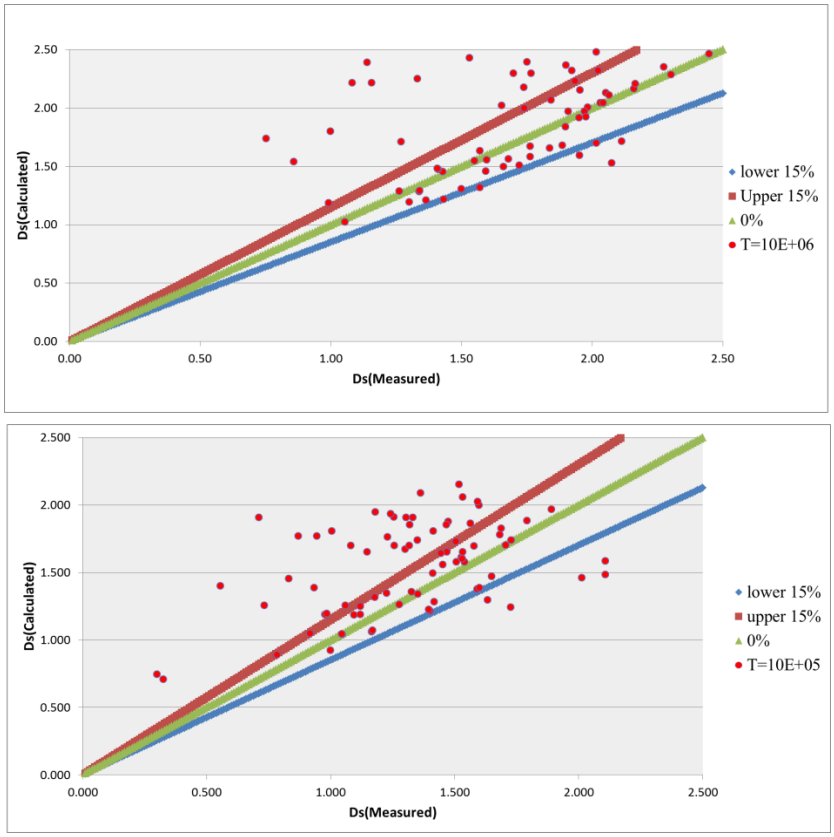

Figure 3.38: Calculated Vs. measured values of D_s at T= 10^6 (up) and T=10^5 (down) using Oliveto and Hager (2002) and velocity proposed by the authors

For conducting the same procedure, using formulae proposed by Sheppard et al. (2014) and Melville and Chiew (1999), it is necessary to know the value of critical velocity declared by the author for all the valid experiments. Due to the fact that the value of the critical velocity is not provided by some of the authors, there is no possibility to use formulae proposed by Sheppard et al. (2014) and Melville and Chiew (1999) for studying of the velocity homogenization effect.

As mentioned before, available restriction in Lanca et al. (2013)'s formula (D50 >60) reduces significantly its range of validity. Verification of the tests which were fulfilling the validity restrictions of the Lanca et al. (2013)'s formula shows that nearly most of these tests are having declared velocities in term of depth-averaged velocity. Thus, due to the absence of experiments with converted upstream flow velocity, studying of velocity homogenization effect seems to be unreasonable, using Lanca et al. (2013)'s formula.

To sum up, it can be clearly concluded that the proposed formula is able to produce more accurate result when compared to the models produced by Sheppard et al. (2014), Melville & Chiew (1999) and Oliveto & Hager (2002). Although Lanca et al. (2013) shows a better

approximation of scour depth quantity, the restriction defined by the author makes the formula invalid for a great range of sediment coarseness (D_{50}). On the other hand, this model does not define a unique factor for considering the effect of the flow intensity and it is based on the assumption that the flow intensity value is near to one so as to maximize the scour depth. Thus, the proposed formula in this study is superior also to Lanca et al. (2013) model because it is able to provide an estimation of scour depth for a bigger range of flow intensity ($0.48 \leq U \leq 1.39$) and sediment coarseness ($2 \leq D50 \leq 325$).

Conclusions

Despite big research efforts in recent decades, predictive capabilities for local scour at bridge piers are still not fully satisfactory and formulae proposed by some authors may fail in representing data from others. Therefore, this thesis has been oriented to a comprehensive analysis of literature data for clear-water scour at cylindrical piers in uniform sand beds, in an attempt to calibrate a formula that could perform better than existing ones. A relatively large amount of local scour data has been used for the purpose of the analysis. Laboratory data are derived from experiments that were well documented by the authors. Suitable criteria were used for selection of appropriate tests among all the available experimental results.

The following conclusions are drawn from this study:

1. An analysis of threshold conditions was conducted and it was concluded that the formula proposed by Melville and Coleman (2000) to estimate the critical velocity could be applied to all the experiments to make them homogeneous with each other.
2. The depth-averaged velocity at mid channel width was considered a better indicator of flow intensity in comparison with the bulk, cross-sectional average velocity. Therefore, all the experiments have been characterized in terms of the former, taking advantage of a conversion formula that was calibrated in a previous thesis work.
3. A dimensionless framework was used based on which the dimensionless scour depth D_s is a function of dimensionless time, flow intensity and sediment coarseness.
4. The dependence of the scour depth on the mentioned control parameters was quantified using the available and selected laboratory data (Figure 3.24 and 3.25).
5. Eq.3.47, which is an exponential function, was proposed to model the influence of sediment coarseness on scour depth at a given time T for the range $2 \leq D50 \leq 325$.
6. It was shown that a 3rd order polynomial (Eq.3.48) can be used for taking into account the effect of flow intensity on scour depth.
7. Two multiplicative constants were introduced for the two dimensionless times considered in the analysis, equal to 10^5 and 10^6 (Eq.3.45 and Eq.3.46).
8. An accurate prediction of scour depth could be obtained through Eq.3.44.
9. A comparison has been made between the proposed equation and some others available in literature, including formulae by Melville & Chiew (1999), Lanca et al. (2013) and Sheppard (2004). It was shown that the proposed formula is able to provide more accurate estimation of the scour depth compared to the mentioned literature ones.

Recommendations for further research

This thesis project has thrown up several questions in need of further investigation. Thus, it is recommended that further research be undertaken in the following areas:

- Choosing more nondimensional times may lead to propose a function for factor $f_1(T)$. By choosing a suitable function and doing the same regression procedure in more choices of dimensionless times, it shall be possible to establish a functional factor for taking into account the effect of nondimensional time on the scour depth rather than just providing constant multipliers.
- In figure 3.31 there are few points that are not following the dominant trend and showing different values of scour depth by having nearly same flow intensity. The characteristics of these test show that they present different values of standard deviation of sediment particle size distribution (σ). Thus, more work shall need to be done to determine the effect of σ on the scour depth evolution.
- The dependence of the scour depth on other dimensionless parameters shall be investigated. In particular, another possible activity of future research would be to investigate the effect of flow shallowness (H) on the scour depth evolution.

References

1. Chabert, J., and Engeldinger, P. (1956), "Etude des affouillements autour des piles des ponts," Laboratoire National d'Hydraulique, Chatou, France.

2. Chang, W.Y, Lai J., S., and Yen C., L. (2004),” Evolution of Scour Depth at Circular Bridge Piers” J. Hydraul. Eng., 130(9), 905-913.

3. Chiew, Y. M. (1995), “Mechanics of Riprap Failure at Bridge Piers”, ASCE Journal of Hydraulic Engineering, 121(9), 635-643

4. Dey et al. (1999) “Time Variation of Scour in The Vicinity of Circular Piers”. Water Maritime and Energy, Volume 136, Issue 2, p. 67 –75

5. Dey, S., Bose, S. K., and Sastry, G. L. N. (1995), “Clear Water Scour at Circular Piers”, J. Hydraul. Eng., 121(12), 869-876.

6. Ettema, R. (1980). “Scour at bridge piers.” Rep. No.216, Scholl of Engrg, University of Auckland, Auckland, New Zealand.

7. Ettema, R., Kirkil, G., Muste, M. (2006), “Similitude of Large-Scale Turbulence in Experiments on Local Scour at Cylinders”, J. Hydraul. Eng., 132(1), 33-40.

8. Franzetti, S., Larcan, E., and Mignosa, P. (1982), “Influence of Tests Duration on The Evaluation of Ultimate Scour Around Circular Piers”, International conference on Hydraul Modeling of Civil engineering Structure, Coventry, England , pp. 381-396.

9. Franzetti, S., Larcan, E. and Mignosa P. (1989), “Erosione alla Base di Pile Circolari di Ponte: Verifica Sperimentale di Esistenza di Una Situazione Finale di Equilibrio”, Estratto da idrotecnica, n. 3 maggio-giugno. Italy.

10. Franzetti, S., Malavasi, S., Piccinin, C. (1994), “Sull’Erosione alla Base delle Pile Di Ponte in Acque Chiare”, XXIV Convegno di Idraulica e Costruzioni Idrauliche. Napoli, p. 1-13

11. Hager, W. H., Oliveto, G. (2002), “Shields’ Entrainment Criterion in Bridge Hydraulics”, Journal of Hydraulic Engineering 128(5): 538-542.

12. Hydraulics & Marine Studies (2013), “Bridge Scour Manual”, Queensland, Canada.

13. Lanca, M. R. et al (2013), “Clear-Water Scour at Comparatively Large Cylindrical Piers”. J. Hydraul Eng., 139(11), 1117-1125.

14. Melville, B. (1997), “Pier and Abutment Scour: Integrated Approach”, J. Hydraul Eng., 123(2), 125-136.

15. Melville, B. W., Coleman, S. E. (2000), “Bridge Scour”, Water Resources Publication

16. Melville, B., and Chiew, Y. M. (1987), “Local Scour around Bridge Piers”, J. Hydraulic Research, 125(1), 59-65.

17. Melville, B., and Chiew, Y. M. (1999), “Time Scale for Local Scour at Bridge Piers”, J. Hydraul Eng., 125(1), 59-65.

18. Mignosa, P. (1980), “Fenomeni di Erosione Locale alla Base delle Pile del Ponti”, Tesi di Laura, Department of hydraulic and Hydraulic structure, Politecnico di Milano. Milan, Italy.

19. Munson, B.R., Okiishi, T.H., Huebsch, W.H., and Rothmayer, A.P. (2013), “Fundamentals of Fluid Mechanics”, 7th Ed, Chapter 7.

20. National Highway institute (2001), “Evaluating Scour At bridge”, Fourth Edition, Hyd. Eng. Circular No.18, Publication No. FHWA NHI 01-001, USA.

21. Neil, C. R. (1967), “Mean-Velocity Criterion for Scour of Coarse Uniform Bed-Material”, Proc. 12th Congress IAHR 3, 46-54. Fort Collins.

22. Oliveto, G., and Hager, W. H. (2002), “Temporal Evolution of Clear-Water Pier and Abutment Scour”, J. Hydraul Eng., 128(9), 811-820.

23. Paleari, R (2014), “Stima Della Profondita di Scavo alla Base delle Pile di Ponti” B.Sc. Thesis, Politecnico di Milano.

24. Raikar, R. V., and Dey, S. (2005), “Clear-water Scour at Bridge Piers in Fine and Medium Gravel Beds” Canadian Journal of Civil Engineering, 32 (4), 775-781,

25. Shen, H.W., Schneider, V.R. and Karaki, S.S. (1969), “Local Scour around Bridge Piers.” Proc. ASCE, J. Hydraulics Div., Vol. 95, No. HY6.

26. Sheppard, D. M, et al (2011) “Scour At Wide Piers and Long Skewed Piers”, NCHRP, Report 682

27. Sheppard, D. M. (2003), “Large Scale and Live Bed Local Pier Scour Experiments, Phase 2, Live Bed Experiments”, Florida Department of Transportation.

28. Sheppard, D. M., Odeh, M., and Glasser, T. (2004), “Large Scale Clearwater Local Pier Scour Experiment”, J. Hydraul Eng., 130(10), 957-963.

29. Sheppard, D., Melville, B., and Demir, H. (2014), “Evaluation of Existing Equations for Local Scour at bridge Pies”, J. Hydraul Eng., 140(1), 14-23.

30. Simarro, G., Fael, M. S., and Cardoso, H. (2011), “Estimating Equilibrium Scour Depth at Cylindrical Piers in Experimental Studies”, J. Hydraul Eng., 137(9), 1089-1093.

31. Simarro, G., Teixeira, L., and Cardoso, H. (2007), “Flow Intensity Parameter in Pier Scour Experiments”, J. Hydraul Eng., 133(11), 1261-1264.

32. Yanmaz, A. M., and Altinbilek H. D. (1991), “Study of Time-Dependent Local Scour around Bridge Piers” J. Hydraul. Eng., 117(10), 1247-1268.

Appendix 1: Summary of full trends and isolated points scour depth data

In the following table, full properties of isolated points and a summary of full trend scour depth tests are provided. These tests are used in analysis and interpolation.

Table notation

Label: Indicate whether the data is provided as isolated data (isolated point) or as full trend (series) by the author.

Test code: Test code provided by author.

Test #: Given code in this study.

h: Upstream flow depth.

u: Velocity of upstream flow.

Velocity label: Indicate the method used in the test for velocity measurement, where M represent average bulk velocity and C stands for average depth velocity. U represents the case in which the author does not indicate the method of velocity measurement in his/her report.

u (transformed): The value of upstream velocity converted to average depth velocity if the velocity is given in terms of average bulk velocity and the test is in fully turbulent regime. Otherwise the original value of velocity is provided for the case of transient regime or the case in which the velocity is given in terms of average depth velocity.

$\boldsymbol{u_c}$ **(Melville):** Critical velocity calculated with formula provided by Melville & Coleman (2000).

$\boldsymbol{d_{50}}$**:** Sediment median size.

ρ (kg/m^3**):** Density of sediment.

σ: Standard deviation of sediment.

b (m): Pier diameter in meter.

$\boldsymbol{l_c}$**(m):** Width of the channel in meter.

t (hr): Experiment duration in hour.

$\boldsymbol{d_s}$ **(m):** Scour depth at the end of the experiment in meter.

$\boldsymbol{D_s}$**:** The ratio between scour depth and pier diameter.

$\boldsymbol{D_{50}}$**:** The ratio between pier size and sediment median size (b/d50) (Coarseness).

U: The ratio between transformed velocity and critical velocity (Flow intensity).

H: The ratio between water depth and pier diameter (h/b) (Flow shallowness).

T: The value of nondimensional time which is equal to t.u/b.

source/paper	label	test code(ref)	test #	h(m)	u(m/s) (data)	Velocity label	u (m/s) transformed	uc (m/s) (Melville)	d50 (mm)	ρ (kg/m^3)	σ	b(m)	l_c (m)	t(hr)	ds(m)	Ds (ds/b)	D50 (b/d50)	U (u/uc) Melville	H (h/b)	T (tu/b)
Yanmaz, Altinbilek (1991)	isolated point	5	1	0.105	0.280	M	0.280	0.399	1.07	2640	1.13	0.067	0.670	3.50	0.064	0.955	62.617	0.701	1.57	5.27E+04
Yanmaz, Altinbilek (1991)	isolated point	6	2	0.085	0.260	M	0.260	0.386	1.07	2640	1.13	0.067	0.670	3.92	0.062	0.925	62.617	0.674	1.27	5.47E+04
Yanmaz, Altinbilek (1991)	isolated point	12	3	0.065	0.230	M	0.230	0.369	1.07	2640	1.13	0.067	0.670	5.00	0.056	0.836	62.617	0.623	0.97	6.18E+04
Yanmaz, Altinbilek (1991)	isolated point	13	4	0.045	0.170	M	0.170	0.346	1.07	2640	1.13	0.067	0.670	4.50	0.039	0.582	62.617	0.492	0.67	4.11E+04
Yanmaz, Altinbilek (1991)	isolated point	17	5	0.121	0.310	M	0.310	0.408	1.07	2640	1.13	0.057	0.670	5.50	0.071	1.246	53.271	0.759	2.12	1.08E+05
Yanmaz, Altinbilek (1991)	isolated point	19	6	0.085	0.260	M	0.260	0.386	1.07	2640	1.13	0.057	0.670	4.00	0.058	1.018	53.271	0.674	1.49	6.57E+04
Yanmaz, Altinbilek (1991)	isolated point	20	7	0.065	0.230	M	0.230	0.369	1.07	2640	1.13	0.057	0.670	5.00	0.051	0.895	53.271	0.623	1.14	7.26E+04
Yanmaz, Altinbilek (1991)	isolated point	21	8	0.045	0.170	M	0.170	0.346	1.07	2640	1.13	0.057	0.670	4.50	0.032	0.561	53.271	0.492	0.79	4.83E+04
Yanmaz, Altinbilek (1991)	isolated point	22	9	0.065	0.230	M	0.230	0.369	1.07	2640	1.13	0.047	0.670	5.00	0.041	0.872	43.925	0.623	1.38	8.81E+04
Yanmaz, Altinbilek (1991)	isolated point	26	10	0.065	0.230	M	0.230	0.320	0.84	2630	1.28	0.067	0.670	5.00	0.077	1.149	79.762	0.718	0.97	6.18E+04
Yanmaz, Altinbilek (1991)	isolated point	28	11	0.105	0.280	M	0.280	0.346	0.84	2630	1.28	0.067	0.670	5.00	0.096	1.433	79.762	0.810	1.57	7.52E+04
Yanmaz, Altinbilek (1991)	isolated point	31	12	0.085	0.260	M	0.260	0.334	0.84	2630	1.28	0.057	0.670	5.00	0.075	1.316	67.857	0.778	1.49	8.21E+04
Yanmaz, Altinbilek (1991)	isolated point	33	13	0.121	0.310	M	0.310	0.353	0.84	2630	1.28	0.057	0.670	5.00	0.088	1.544	67.857	0.878	2.12	9.79E+04
Yanmaz, Altinbilek (1991)	isolated point	35	14	0.085	0.260	M	0.260	0.334	0.84	2630	1.28	0.047	0.670	5.00	0.070	1.489	55.952	0.778	1.81	9.96E+04
Yanmaz, Altinbilek (1991)	isolated point	36	15	0.105	0.280	M	0.280	0.346	0.84	2630	1.28	0.047	0.670	5.00	0.068	1.447	55.952	0.810	2.23	1.07E+05
Melville & Chiew 1987 dato 1992 (Annex A)	isolated point	A1-00	16	0.170	0.265	M	0.265	0.273	0.24	2650	uniform	0.032	0.440	45.00	0.052	1.650	132.292	0.972	5.35	1.35E+06
Melville & Chiew 1987 dato 1992 (Annex A)	isolated point	B1-00	17	0.170	0.220	M	0.220	0.273	0.24	2650	uniform	0.040	0.440	52.00	0.062	1.550	166.667	0.807	4.25	1.03E+06
Melville & Chiew 1987 dato 1992 (Annex A)	isolated point	C1-00	18	0.170	0.307	M	0.307	0.273	0.24	2650	uniform	0.045	0.440	27.00	0.071	1.570	187.500	1.126	3.78	6.63E+05
Melville & Chiew 1987 dato 1992 (Annex A)	isolated point	A2-0A	19	0.170	0.303	M	0.303	0.324	0.60	2650	uniform	0.032	0.440	17.00	0.061	1.910	52.917	0.936	5.35	5.84E+05
Melville & Chiew 1987 dato 1992 (Annex A)	isolated point	A2-0B	20	0.170	0.333	M	0.333	0.324	0.60	2650	uniform	0.032	0.440	29.00	0.066	2.080	52.917	1.029	5.35	1.10E+06
Melville & Chiew 1987 dato 1992 (Annex A)	isolated point	B2-00	21	0.170	0.350	M	0.350	0.324	0.60	2650	uniform	0.038	0.440	17.00	0.085	2.220	63.500	1.082	4.46	5.62E+05
Melville & Chiew 1987 dato 1992 (Annex A)	isolated point	D2-00	22	0.170	0.360	M	0.360	0.324	0.60	2650	uniform	0.051	0.440	16.00	0.097	1.900	84.667	1.113	3.35	4.08E+05
Melville & Chiew 1987 dato 1992 (Annex A)	isolated point	A3-00	23	0.170	0.417	M	0.417	0.521	1.45	2650	uniform	0.032	0.440	70.00	0.073	2.300	21.897	0.800	5.35	3.31E+06
Melville & Chiew 1987 dato 1992 (Annex A)	isolated point	B3-00	24	0.210	0.430	M	0.430	0.538	1.45	2650	uniform	0.038	0.440	51.00	0.091	2.400	26.276	0.799	5.51	2.07E+06
Melville & Chiew 1987 dato 1992 (Annex A)	isolated point	C3-00	25	0.170	0.415	M	0.415	0.521	1.45	2650	uniform	0.045	0.440	68.00	0.102	2.260	31.034	0.796	3.78	2.26E+06
Melville & Chiew 1987 dato 1992 (Annex A)	isolated point	A4-00	26	0.210	0.670	M	0.816	0.773	3.20	2650	uniform	0.032	0.440	42.00	0.044	1.370	9.925	1.056	6.61	3.89E+06
Melville & Chiew 1987 dato 1992 (Annex A)	isolated point	B4-00	27	0.210	0.690	M	0.841	0.773	3.20	2650	uniform	0.045	0.440	47.00	0.071	1.570	14.063	1.088	4.67	3.16E+06
Melville & Chiew 1987 dato 1992 (Annex B)	isolated point	MA1-00	28	0.170	0.350	M	0.350	0.324	0.60	2650	2.00	0.032	0.440	53.00	0.065	2.050	52.917	1.082	5.35	2.10E+06
Melville & Chiew 1987 dato 1992 (Annex B)	isolated point	MB1-00	29	0.170	0.350	M	0.350	0.324	0.60	2650	2.00	0.040	0.440	60.00	0.082	2.050	66.667	1.082	4.25	1.89E+06
Melville & Chiew 1987 dato 1992 (Annex B)	isolated point	MC1-00	30	0.170	0.350	M	0.350	0.324	0.60	2650	2.00	0.045	0.440	48.00	0.076	1.690	75.000	1.082	3.78	1.34E+06
Melville & Chiew 1987 dato 1992 (Annex B)	isolated point	MA2-00	31	0.170	0.490	M	0.490	0.364	0.80	2650	2.80	0.032	0.440	42.00	0.039	1.230	39.688	1.344	5.35	2.33E+06
Melville & Chiew 1987 dato 1992 (Annex B)	isolated point	MA2-01	32	0.170	0.410	M	0.410	0.364	0.80	2650	2.80	0.032	0.440	20.00	0.028	0.880	39.688	1.125	5.35	9.30E+05
Melville & Chiew 1987 dato 1992 (Annex B)	isolated point	MA3-00	33	0.170	0.370	M	0.370	0.324	0.60	2650	5.50	0.032	0.440	17.00	0.015	0.480	52.917	1.143	5.35	7.13E+05
Melville & Chiew 1987 dato 1992 (Annex B)	isolated point	MA3-01	34	0.170	0.500	M	0.500	0.324	0.60	2650	5.50	0.032	0.440	24.00	0.027	0.850	52.917	1.545	5.35	1.36E+06
Melville & Chiew 1987 dato 1992 (Annex B)	isolated point	MB-00	35	0.170	0.350	M	0.350	0.324	0.60	2650	5.50	0.045	0.440	45.00	0.022	0.480	75.000	1.082	3.78	1.26E+06
Melville & Chiew 1987 dato 1992 (Annex B)	isolated point	MB3-01	36	0.170	0.480	M	0.480	0.324	0.60	2650	5.50	0.045	0.440	113.00	0.039	0.870	75.000	1.483	3.78	4.34E+06
Melville & Chiew 1987 dato 1992 (Annex B)	isolated point	MB3-02	37	0.170	0.610	M	0.610	0.324	0.60	2650	5.50	0.045	0.440	47.00	0.054	1.210	75.000	1.885	3.78	2.29E+06
Melville & Chiew 1987 dato 1992 (Annex B)	isolated point	MC3-01	38	0.170	0.590	M	0.590	0.324	0.60	2650	5.50	0.070	0.440	47.00	0.110	1.570	116.667	1.823	2.43	1.43E+06
Melville & Chiew 1987 dato 1992 (Annex B)	isolated point	MA4-00	39	0.170	0.530	M	0.530	0.521	1.45	2650	4.30	0.032	0.440	22.00	0.022	0.690	21.897	1.017	5.35	1.32E+06
Melville & Chiew 1987 dato 1992 (Annex B)	isolated point	MA4-01	40	0.170	0.680	M	0.680	0.521	1.45	2650	4.30	0.032	0.440	25.00	0.029	0.910	21.897	1.304	5.35	1.93E+06
Melville & Chiew 1987 dato 1992 (Annex B)	isolated point	MB4-00	41	0.170	0.500	M	0.500	0.521	1.45	2650	4.30	0.045	0.440	24.00	0.021	0.470	31.034	0.959	3.78	9.60E+05
Melville & Chiew 1987 dato 1992 (Annex B)	isolated point	MB4-01	42	0.170	0.680	M	0.680	0.521	1.45	2650	4.30	0.045	0.440	27.00	0.050	1.110	31.034	1.304	3.78	1.47E+06
Chiew (1995)	isolated point	C1	43	0.200	0.215	M	0.215	0.410	0.96	2650	1.25	0.070	0.600	4.00	0.021	0.300	72.917	0.524	2.86	4.42E+04
Chiew (1995)	isolated point	C2	44	0.200	0.257	M	0.257	0.410	0.96	2650	1.25	0.070	0.600	68.00	0.041	0.586	72.917	0.627	2.86	9.00E+05
Chiew (1995)	isolated point	C3	45	0.200	0.326	M	0.326	0.410	0.96	2650	1.25	0.070	0.600	150.25	0.070	1.000	72.917	0.795	2.86	2.52E+06

source/paper	label	test code (ref)	test #	h(m)	u(m/s) (data)	Velocity label	u (m/s) transformed	uc (m/s) (Melville)	d50 (mm)	ρ (kg/m^3)	σ	b(m)	I_c (m)	t(hr)	ds(m)	Ds (ds/b)	D50 (b/d50)	U (u/uc) Melville	H (h/b)	T (tu/b)
Chiew (1995)	isolated point	C4	46	0.200	0.431	M	0.431	0.410	0.96	2650	1.25	0.070	0.600	192.00	0.144	2.057	72.917	1.050	2.86	4.25E+06
Chiew (1995)	isolated point	C5	47	0.200	0.220	M	0.220	0.410	0.96	2650	1.25	0.070	0.600	24.00	0.023	0.329	72.917	0.536	2.86	2.72E+05
Chiew (1995)	isolated point	C6	48	0.200	0.378	M	0.378	0.410	0.96	2650	1.25	0.070	0.600	188.00	0.106	1.514	72.917	0.922	2.86	3.66E+06
Chiew (1995)	isolated point	C7	49	0.200	0.500	M	0.500	0.410	0.96	2650	1.25	0.070	0.600	170.00	0.151	2.157	72.917	1.219	2.86	4.37E+06
Chiew (1995)	isolated point	C8	50	0.150	0.456	M	0.456	0.394	0.96	2650	1.25	0.070	0.600	168.58	0.148	2.114	72.917	1.159	2.14	3.95E+06
Chiew (1995)	isolated point	C9	51	0.150	0.449	M	0.449	0.394	0.96	2650	1.25	0.070	0.600	166.08	0.143	2.043	72.917	1.142	2.14	3.84E+06
Chiew (1995)	isolated point	C10	52	0.150	0.449	M	0.449	0.394	0.96	2650	1.25	0.070	0.600	72.00	0.141	2.014	72.917	1.142	2.14	1.66E+06
Chiew (1995)	isolated point	C11	53	0.150	0.422	M	0.422	0.394	0.96	2650	1.25	0.070	0.600	72.00	0.134	1.914	72.917	1.073	2.14	1.56E+06
Chiew (1995)	isolated point	C12	54	0.150	0.374	M	0.374	0.394	0.96	2650	1.25	0.070	0.600	72.00	0.099	1.414	72.917	0.951	2.14	1.39E+06
Chiew (1995)	isolated point	C13	55	0.150	0.295	M	0.295	0.394	0.96	2650	1.25	0.070	0.600	72.00	0.046	0.657	72.917	0.750	2.14	1.09E+06
Chiew (1984) from NCHRP	isolated point	CN1	56	0.170	0.351	M	0.351	0.327	0.60	2680	1.20	0.038	0.800	17.00	0.085	2.224	63.500	1.073	4.46	5.63E+05
Chiew (1984) from NCHRP	isolated point	CN2	57	0.170	0.341	M	0.341	0.327	0.60	2680	1.20	0.045	0.800	20.00	0.095	2.108	75.184	1.045	3.77	5.45E+05
Chiew (1984) from NCHRP	isolated point	CN3	58	0.340	1.609	M	1.899	0.582	1.45	2680	1.20	0.045	0.800	3.00	0.079	1.757	31.111	3.261	7.53	4.55E+05
Chiew (1984) from NCHRP	isolated point	CN4	59	0.170	0.360	M	0.360	0.327	0.60	2680	1.20	0.050	0.800	16.00	0.095	1.902	83.312	1.101	3.40	4.14E+05
Graf from Melville & Chiew (1999)	isolated point	G1	60	0.170	0.579	C	0.579	0.627	2.10	2650	1.30	0.110	1.000	79.67	0.174	1.582	52.381	0.924	1.55	1.51E+06
Graf from Melville & Chiew (1999)	isolated point	G2	61	0.232	0.609	C	0.609	0.658	2.10	2650	1.30	0.100	1.000	103.33	0.195	1.950	47.619	0.925	2.32	2.27E+06
Graf from Melville & Chiew (1999)	isolated point	G3	62	0.232	0.609	C	0.609	0.658	2.10	2650	1.30	0.150	1.000	104.67	0.259	1.727	71.429	0.925	1.55	1.53E+06
Melville & Chiew (1999)	isolated point	N1	63	0.200	0.231	M	0.231	0.410	0.96	2650	1.30	0.070	1.000	52.37	0.094	1.343	72.917	0.563	2.86	6.22E+05
Melville & Chiew (1999)	isolated point	N2	64	0.070	0.245	M	0.245	0.349	0.96	2650	1.30	0.070	1.000	45.05	0.077	1.100	72.917	0.702	1.00	5.68E+05
Melville & Chiew (1999)	isolated point	N3	65	0.070	0.218	M	0.218	0.349	0.96	2650	1.30	0.070	1.000	48.00	0.069	0.986	72.917	0.624	1.00	5.38E+05
Melville & Chiew (1999)	isolated point	N4	66	0.070	0.231	M	0.231	0.349	0.96	2650	1.30	0.070	1.000	46.95	0.079	1.129	72.917	0.662	1.00	5.58E+05
Melville & Chiew (1999)	isolated point	N5	67	0.070	0.198	M	0.198	0.349	0.96	2650	1.30	0.070	1.000	25.62	0.039	0.557	72.917	0.567	1.00	2.61E+05
Melville & Chiew (1999)	isolated point	N6	68	0.070	0.231	M	0.231	0.349	0.96	2650	1.30	0.050	1.000	43.50	0.060	1.200	52.083	0.662	1.40	7.23E+05
Melville & Chiew (1999)	isolated point	N7	69	0.200	0.231	M	0.231	0.410	0.96	2650	1.30	0.050	1.000	51.50	0.060	1.200	52.083	0.563	4.00	8.57E+05
Melville & Chiew (1999)	isolated point	N8	70	0.200	0.243	M	0.243	0.410	0.96	2650	1.30	0.038	1.000	67.25	0.054	1.421	39.583	0.592	5.26	1.55E+06
Melville & Chiew (1999)	isolated point	N9	71	0.200	0.231	M	0.231	0.410	0.96	2650	1.30	0.038	1.000	29.02	0.045	1.184	39.583	0.563	5.26	6.35E+05
Melville & Chiew (1999)	isolated point	AU1	72	0.200	0.213	M	0.213	0.373	0.80	2650	1.30	0.016	1.000	29.22	0.024	1.500	20.000	0.571	12.50	1.40E+06
Melville & Chiew (1999)	isolated point	AU2	73	0.200	0.213	M	0.213	0.373	0.80	2650	1.30	0.025	1.000	44.92	0.025	1.000	31.250	0.571	8.00	1.38E+06
Melville & Chiew (1999)	isolated point	N10	74	0.095	0.278	M	0.278	0.367	0.96	2650	1.30	0.070	1.000	54.20	0.116	1.657	72.917	0.758	1.36	7.75E+05
Melville & Chiew (1999)	isolated point	N11	75	0.095	0.278	M	0.278	0.367	0.96	2650	1.30	0.070	1.000	69.90	0.118	1.686	72.917	0.758	1.36	9.99E+05
Melville & Chiew (1999)	isolated point	N12	76	0.050	0.269	M	0.269	0.330	0.96	2650	1.30	0.070	1.000	67.58	0.107	1.529	72.917	0.816	0.71	9.35E+05
Melville & Chiew (1999)	isolated point	N13	77	0.070	0.304	M	0.304	0.349	0.96	2650	1.30	0.070	1.000	68.15	0.121	1.729	72.917	0.871	1.00	1.07E+06
Melville & Chiew (1999)	isolated point	N14	78	0.070	0.298	M	0.298	0.349	0.96	2650	1.30	0.050	1.000	53.58	0.089	1.780	52.083	0.853	1.40	1.15E+06
Melville & Chiew (1999)	isolated point	N15	79	0.200	0.278	M	0.278	0.410	0.96	2650	1.30	0.038	1.000	70.50	0.077	2.026	39.583	0.678	5.26	1.86E+06
Melville & Chiew (1999)	isolated point	N16	80	0.200	0.324	M	0.324	0.410	0.96	2650	1.30	0.038	1.000	75.50	0.097	2.553	39.583	0.790	5.26	2.32E+06
Melville & Chiew (1999)	isolated point	N17	81	0.070	0.317	M	0.317	0.349	0.96	2650	1.30	0.050	1.000	69.38	0.091	1.820	52.083	0.908	1.40	1.58E+06
Melville & Chiew (1999)	isolated point	AU3	82	0.200	0.250	M	0.250	0.373	0.80	2650	1.30	0.016	1.000	29.00	0.032	2.000	20.000	0.671	12.50	1.63E+06
Melville & Chiew (1999)	isolated point	AU4	83	0.200	0.250	M	0.250	0.373	0.80	2650	1.30	0.025	1.000	48.25	0.048	1.920	31.250	0.671	8.00	1.74E+06
Melville & Chiew (1999)	isolated point	AU5	84	0.200	0.294	M	0.294	0.373	0.80	2650	1.30	0.016	1.000	34.42	0.038	2.375	20.000	0.789	12.50	2.28E+06
Melville & Chiew (1999)	isolated point	AU6	85	0.200	0.294	M	0.294	0.373	0.80	2650	1.30	0.025	1.000	44.83	0.064	2.560	31.250	0.789	8.00	1.90E+06
Melville & Chiew (1999)	isolated point	N18	86	0.200	0.271	M	0.271	0.410	0.96	2650	1.30	0.070	1.000	71.00	0.133	1.900	72.917	0.661	2.86	9.90E+05
Melville & Chiew (1999)	isolated point	N19	87	0.077	0.271	M	0.271	0.355	0.96	2650	1.30	0.070	1.000	51.67	0.107	1.529	72.917	0.764	1.10	7.20E+05
Melville & Chiew (1999)	isolated point	N20	88	0.070	0.251	M	0.251	0.349	0.96	2650	1.30	0.070	1.000	70.17	0.091	1.300	72.917	0.719	1.00	9.06E+05
Melville & Chiew (1999)	isolated point	N21	89	0.070	0.265	M	0.265	0.349	0.96	2650	1.30	0.050	1.000	69.30	0.079	1.580	52.083	0.759	1.40	1.32E+06
Melville & Chiew (1999)	isolated point	N22	90	0.070	0.179	M	0.179	0.349	0.96	2650	1.30	0.070	1.000	22.30	0.025	0.357	72.917	0.513	1.00	2.05E+05

source/paper	label	test code (ref)	test #	h(m)	u(m/s) (data)	Velocity label	u (m/s) transformed	u c (m/s) (Melville)	d50 (mm)	ρ (kg/m^3)	σ	b(m)	lc (m)	t (hr)	ds (m)	Ds (ds/b)	D50 (b/d50)	U(u/uc) Melville	H (h/b)	T (tu/b)
Melville & Chiew (1999)	isolated point	N23	91	0.200	0.197	M	0.197	0.410	0.96	2650	1.30	0.050	1.000	23.75	0.026	0.520	52.083	0.480	4.00	3.37E+05
Melville & Chiew (1999)	isolated point	N24	92	0.200	0.197	M	0.197	0.410	0.96	2650	1.30	0.070	1.000	30.25	0.043	0.614	72.917	0.480	2.86	3.06E+05
Melville & Chiew (1999)	isolated point	N25	93	0.070	0.185	M	0.185	0.349	0.96	2650	1.30	0.070	1.000	40.48	0.037	0.529	72.917	0.530	1.00	3.85E+05
Melville & Chiew (1999)	isolated point	N26	94	0.070	0.185	M	0.185	0.349	0.96	2650	1.30	0.070	1.000	23.88	0.035	0.500	72.917	0.530	1.00	2.27E+05
Melville & Chiew (1999)	isolated point	N27	95	0.070	0.198	M	0.198	0.349	0.96	2650	1.30	0.050	1.000	29.47	0.029	0.580	52.083	0.567	1.40	4.20E+05
Melville & Chiew (1999)	isolated point	N28	96	0.070	0.165	M	0.165	0.349	0.96	2650	1.30	0.070	1.000	5.00	0.007	0.100	72.917	0.473	1.00	4.24E+04
Melville & Chiew (1999)	isolated point	N29	97	0.200	0.171	M	0.171	0.410	0.96	2650	1.30	0.070	1.000	21.63	0.020	0.286	72.917	0.417	2.86	1.90E+05
Melville & Chiew (1999)	isolated point	N30	98	0.200	0.185	M	0.185	0.410	0.96	2650	1.30	0.070	1.000	21.67	0.028	0.400	72.917	0.451	2.86	2.06E+05
Melville & Chiew (1999)	isolated point	N31	99	0.200	0.174	M	0.174	0.410	0.96	2650	1.30	0.050	1.000	7.50	0.011	0.220	52.083	0.424	4.00	9.40E+04
Melville & Chiew (1999)	isolated point	N32	100	0.200	0.174	M	0.174	0.410	0.96	2650	1.30	0.038	1.000	3.33	0.004	0.105	39.583	0.424	5.26	5.49E+04
Melville & Chiew (1999)	isolated point	AU7	101	0.200	0.175	M	0.175	0.396	0.90	2650	1.30	0.016	1.000	5.33	0.010	0.625	17.778	0.442	12.50	2.10E+05
Melville & Chiew (1999)	isolated point	AU8	102	0.200	0.175	M	0.175	0.396	0.90	2650	1.30	0.025	1.000	20.58	0.017	0.680	27.778	0.442	8.00	5.19E+05
Melville & Chiew (1999)	isolated point	AU9	103	0.135	0.269	M	0.269	0.374	0.90	2650	1.30	0.200	1.000	119.00	0.237	1.185	222.222	0.719	0.68	5.76E+05
Melville & Chiew (1999)	isolated point	AU10	104	0.120	0.291	M	0.291	0.367	0.90	2650	1.30	0.200	1.000	92.00	0.209	1.045	222.222	0.792	0.60	4.82E+05
Melville & Chiew (1999)	isolated point	AU11	105	0.120	0.228	M	0.228	0.367	0.90	2650	1.30	0.200	1.000	63.00	0.109	0.545	222.222	0.620	0.60	2.59E+05
Melville & Chiew (1999)	isolated point	AU12	106	0.230	0.186	M	0.186	0.404	0.90	2650	1.30	0.200	1.000	14.00	0.059	0.295	222.222	0.461	1.15	4.69E+04
Melville & Chiew (1999)	isolated point	AU13	107	0.181	0.320	M	0.320	0.390	0.90	2650	1.30	0.200	1.000	43.50	0.235	1.175	222.222	0.820	0.91	2.51E+05
Melville & Chiew (1999)	isolated point	MC46	108	0.600	0.571	M	0.571	0.720	1.90	2650	1.30	0.051	1.000	61.00	0.115	2.264	26.737	0.793	11.81	2.47E+06
Melville & Chiew (1999)	isolated point	MC47	109	0.600	0.428	M	0.428	0.440	0.84	2650	1.30	0.150	1.000	250.00	0.225	1.500	178.571	0.972	4.00	2.57E+06
Melville & Chiew (1999)	isolated point	MC48	110	0.600	0.399	M	0.399	0.429	0.80	2650	1.30	0.102	1.000	166.67	0.227	2.234	127.000	0.929	5.91	2.36E+06
Melville & Chiew (1999)	isolated point	MC49	111	0.600	0.405	M	0.405	0.440	0.84	2650	1.30	0.102	1.000	175.00	0.227	2.234	120.952	0.920	5.91	2.51E+06
Melville & Chiew (1999)	isolated point	MC50	112	0.600	0.399	M	0.399	0.429	0.80	2650	1.30	0.150	1.000	250.00	0.315	2.100	187.500	0.929	4.00	2.39E+06
Melville & Chiew (1999)	isolated point	MC51	113	0.600	0.405	M	0.405	0.440	0.84	2650	1.30	0.150	1.000	250.00	0.314	2.093	178.571	0.920	4.00	2.43E+06
Melville & Chiew (1999) from NCHRP	isolated point	MCN1	114	0.200	0.232	M	0.232	0.410	0.96	2650	1.30	0.070	1.000	85.95	0.099	1.413	73.025	0.565	2.85	1.02E+06
Melville & Chiew (1999) from NCHRP	isolated point	MCN2	115	0.095	0.277	M	0.277	0.367	0.96	2650	1.30	0.070	1.000	92.68	0.122	1.739	73.025	0.756	1.36	1.32E+06
Melville & Chiew (1999) from NCHRP	isolated point	MCN3	116	0.050	0.268	M	0.268	0.330	0.96	2650	1.30	0.070	1.000	108.50	0.111	1.583	73.025	0.814	0.71	1.49E+06
Melville & Chiew (1999) from NCHRP	isolated point	MCN4	117	0.070	0.305	M	0.305	0.349	0.96	2650	1.30	0.070	1.000	87.80	0.125	1.783	73.025	0.873	1.00	1.37E+06
Melville & Chiew (1999) from NCHRP	isolated point	MCN5	118	0.070	0.290	M	0.290	0.349	0.96	2650	1.30	0.050	1.000	75.87	0.091	1.823	52.070	0.829	1.40	1.58E+06
Melville & Chiew (1999) from NCHRP	isolated point	MCN6	119	0.070	0.317	M	0.317	0.349	0.96	2650	1.30	0.050	1.000	65.25	0.091	1.823	52.070	0.908	1.40	1.49E+06
Melville & Chiew (1999) from NCHRP	isolated point	MCN7	120	0.200	0.271	M	0.271	0.410	0.96	2650	1.30	0.070	1.000	127.30	0.142	2.026	73.025	0.661	2.85	1.77E+06
Melville & Chiew (1999) from NCHRP	isolated point	MCN8	121	0.077	0.271	M	0.271	0.355	0.96	2650	1.30	0.070	1.000	76.23	0.112	1.596	73.025	0.765	1.10	1.06E+06
Melville & Chiew (1999) from NCHRP	isolated point	MCN9	122	0.070	0.244	M	0.244	0.349	0.96	2650	1.30	0.070	1.000	79.25	0.085	1.213	73.025	0.698	1.00	9.92E+05
Melville & Chiew (1999) from NCHRP	isolated point	MCN10	123	0.070	0.180	M	0.180	0.349	0.96	2650	1.30	0.070	1.000	38.25	0.027	0.387	73.025	0.515	1.00	3.53E+05
Melville & Chiew (1999) from NCHRP	isolated point	MCN11	124	0.070	0.186	M	0.186	0.349	0.96	2650	1.30	0.070	1.000	43.02	0.037	0.526	73.025	0.532	1.00	4.11E+05
Melville & Chiew (1999) from NCHRP	isolated point	MCN12	125	0.070	0.198	M	0.198	0.349	0.96	2650	1.30	0.050	1.000	49.75	0.029	0.579	52.070	0.567	1.40	7.10E+05
Melville & Chiew (1999) from NCHRP	isolated point	MCN13	126	0.070	0.219	M	0.219	0.349	0.96	2650	1.30	0.070	1.000	79.92	0.073	1.043	73.025	0.628	1.00	9.01E+05
Melville & Chiew (1999) from NCHRP	isolated point	MCN14	127	0.070	0.232	M	0.232	0.349	0.96	2650	1.30	0.070	1.000	76.80	0.083	1.183	73.025	0.663	1.00	9.14E+05
Melville & Chiew (1999) from NCHRP	isolated point	MCN15	128	0.070	0.198	M	0.198	0.349	0.96	2650	1.30	0.070	1.000	56.73	0.044	0.626	73.025	0.567	1.00	5.77E+05
Melville & Chiew (1999) from NCHRP	isolated point	MCN16	129	0.070	0.232	M	0.232	0.349	0.96	2650	1.30	0.050	1.000	77.37	0.062	1.238	52.070	0.663	1.40	1.29E+06
Melville & Chiew (1999) from NCHRP	isolated point	MCN17	130	0.200	0.232	M	0.232	0.410	0.96	2650	1.30	0.038	1.000	35.85	0.046	1.208	39.688	0.565	5.25	7.85E+05
Dey et al (1995)	isolated point	D1	131	0.050	0.262	U	0.262	0.267	0.58	2650	1.31	0.076	0.810	12.00	0.096	1.265	130.854	0.982	0.66	1.49E+05
Dey et al (1995)	isolated point	D2	132	0.050	0.262	U	0.262	0.267	0.58	2650	1.31	0.065	0.810	12.00	0.086	1.324	111.935	0.982	0.77	1.74E+05
Dey et al (1995)	isolated point	D3	133	0.050	0.262	U	0.262	0.267	0.58	2650	1.31	0.057	0.810	12.00	0.079	1.385	98.272	0.982	0.88	1.99E+05
Dey et al (1995)	isolated point	D4	134	0.041	0.226	U	0.226	0.258	0.58	2650	1.31	0.076	0.810	12.00	0.080	1.052	130.854	0.873	0.54	1.28E+05
Dey et al (1995)	isolated point	D5	135	0.041	0.226	U	0.226	0.258	0.58	2650	1.31	0.065	0.810	12.00	0.068	1.047	111.935	0.873	0.63	1.50E+05

source/paper	label	test code(ref)	test #	h(m)	u(m/s) (data)	Velocity label	u (m/s) transformed	uc (m/s) (Melville)	d50 (mm)	ρ (kg/m^3)	σ	b(m)	Ic (m)	t (hr)	ds(m)	Ds (ds/b)	D50 (b/d50)	U(u/uc) Melville	H (h/b)	T (tu/b)
Dey et al (1995)	isolated point	D6	136	0.041	0.226	U	0.226	0.258	0.58	2650	1.31	0.057	0.810	12.00	0.060	1.053	98.272	0.873	0.72	1.71E+05
Dey et al (1995)	isolated point	D7	137	0.035	0.186	U	0.186	0.252	0.58	2650	1.31	0.076	0.810	12.00	0.072	0.948	130.854	0.739	0.46	1.06E+05
Dey et al (1995)	isolated point	D8	138	0.035	0.186	U	0.186	0.252	0.58	2650	1.31	0.065	0.810	12.00	0.062	0.953	111.935	0.739	0.54	1.24E+05
Dey et al (1995)	isolated point	D9	139	0.035	0.186	U	0.186	0.252	0.58	2650	1.31	0.057	0.810	12.00	0.054	0.947	98.272	0.739	0.61	1.41E+05
Dey et al (1995)	isolated point	D10	140	0.050	0.232	U	0.232	0.233	0.26	2650	1.39	0.076	0.810	12.00	0.093	1.225	291.905	0.994	0.66	1.32E+05
Dey et al (1995)	isolated point	D11	141	0.050	0.232	U	0.232	0.233	0.26	2650	1.39	0.065	0.810	12.00	0.084	1.296	249.702	0.994	0.77	1.54E+05
Dey et al (1995)	isolated point	D12	142	0.050	0.232	U	0.232	0.233	0.26	2650	1.39	0.057	0.810	12.00	0.076	1.332	219.222	0.994	0.88	1.76E+05
Dey et al (1995)	isolated point	D13	143	0.041	0.204	U	0.204	0.227	0.26	2650	1.39	0.076	0.810	12.00	0.070	0.924	291.905	0.901	0.54	1.16E+05
Dey et al (1995)	isolated point	D14	144	0.041	0.204	U	0.204	0.227	0.26	2650	1.39	0.065	0.810	12.00	0.063	0.972	249.702	0.901	0.63	1.36E+05
Dey et al (1995)	isolated point	D15	145	0.041	0.204	U	0.204	0.227	0.26	2650	1.39	0.057	0.810	12.00	0.056	0.984	219.222	0.901	0.72	1.55E+05
Dey et al (1995)	isolated point	D16	146	0.035	0.171	U	0.171	0.221	0.26	2650	1.39	0.076	0.810	12.00	0.060	0.791	291.905	0.771	0.46	9.72E+04
Dey et al (1995)	isolated point	D17	147	0.035	0.171	U	0.171	0.221	0.26	2650	1.39	0.065	0.810	12.00	0.056	0.864	249.702	0.771	0.54	1.14E+05
Dey et al (1995)	isolated point	D18	148	0.035	0.171	U	0.171	0.221	0.26	2650	1.39	0.057	0.810	12.00	0.052	0.914	219.222	0.771	0.61	1.29E+05
ETTE-RAUD	isolated point	ER1	149	0.600	0.695	C	0.695	0.720	1.90	2650	1.34	0.045	0.457	49.12	0.093	2.070	23.684	0.966	13.33	2.73E+06
Ettema 80 da NCHRP	isolated point	EN1	150	0.100	0.436	C	0.436	0.547	1.90	2650	1.30	0.240	--	0.48	0.271	1.131	126.251	0.797	0.42	3.16E+03
Ettema 80 da NCHRP	isolated point	EN2	151	0.600	0.433	C	0.433	0.429	0.80	2650	1.30	0.051	--	95.73	0.123	2.425	63.627	1.008	11.79	2.93E+06
Ettema Kirkil Muste 2006	isolated point	EKM1	152	1.000	0.460	C	0.460	0.536	1.05	2650	1.30	0.406	3.000	48.00	0.435	1.071	387.048	0.858	2.46	1.96E+05
Ettema Kirkil Muste 2006	isolated point	EKM2	153	1.000	0.460	C	0.460	0.536	1.05	2650	1.30	0.341	3.000	24.00	0.368	1.081	324.571	0.858	2.93	1.17E+05
Ettema Kirkil Muste 2006	isolated point	EKM3	154	1.000	0.460	C	0.460	0.536	1.05	2650	1.30	0.241	3.000	24.00	0.313	1.299	229.810	0.858	4.14	1.65E+05
Ettema Kirkil Muste 2006	isolated point	EKM4	155	1.000	0.460	C	0.460	0.536	1.05	2650	1.30	0.172	3.000	24.00	0.258	1.504	163.333	0.858	5.83	2.32E+05
Ettema Kirkil Muste 2006	isolated point	EKM5	156	1.000	0.460	C	0.460	0.536	1.05	2650	1.30	0.114	3.000	24.00	0.185	1.615	108.857	0.858	8.75	3.48E+05
Ettema Kirkil Muste 2006	isolated point	EKM6	157	1.000	0.460	C	0.460	0.536	1.05	2650	1.30	0.064	3.000	24.00	0.111	1.740	60.476	0.858	15.75	6.26E+05
Lee, S. L., and Sturm, W., (2009)	isolated point	FB/1:45	158	0.183	0.333	C	0.333	0.314	0.53	2650	1.17	0.406	1.100	10.00	0.082	0.202	766.038	1.061	0.45	2.95E+04
Lee, S. L., and Sturm, W., (2009)	isolated point	RM/1:45	159	0.181	0.312	C	0.312	0.444	1.10	2650	1.33	0.406	4.300	98.00	0.083	0.204	369.091	0.703	0.45	2.71E+05
Lee, S. L., and Sturm, W., (2009)	isolated point	RM/1:45	160	0.191	0.336	C	0.336	0.447	1.10	2650	1.33	0.406	4.300	92.00	0.089	0.219	369.091	0.751	0.47	2.74E+05
Lee, S. L., and Sturm, W., (2009)	isolated point	RM/1:45	161	0.203	0.350	C	0.350	0.451	1.10	2650	1.33	0.406	4.300	92.00	0.084	0.207	369.091	0.776	0.50	2.86E+05
Raikar, R. V., and Dey, S., (2005)	isolated point	RAJ5	162	0.250	1.102	M	1.350	1.310	14.25	2650	1.09	0.032	0.600	24.00	0.032	0.991	2.246	1.031	7.81	3.65E+06
Raikar, R. V., and Dey, S., (2005)	isolated point	RAJ10	163	0.250	1.102	M	1.350	1.310	14.25	2650	1.09	0.038	0.600	24.00	0.049	1.300	2.667	1.031	6.58	3.07E+06
Raikar, R. V., and Dey, S., (2005)	isolated point	RAJ15	164	0.250	1.102	M	1.350	1.310	14.25	2650	1.09	0.060	0.600	24.00	0.082	1.363	4.211	1.031	4.17	1.94E+06
Raikar, R. V., and Dey, S., (2005)	isolated point	RAJ20	165	0.250	1.102	M	1.350	1.310	14.25	2650	1.09	0.077	0.600	24.00	0.110	1.431	5.404	1.031	3.25	1.52E+06
ETTEMA (1980) APPENDIX1 Tab A1-4	isolated point	E11	166	0.600	0.246	C	0.246	0.429	0.80	2650	1.33	0.051	1.524	9.42	0.016	0.310	63.500	0.573	11.81	1.64E+05
ETTEMA (1980) APPENDIX1 Tab A1-4	isolated point	E12	167	0.600	0.341	C	0.341	0.720	1.90	2650	1.34	0.051	1.524	9.67	0.016	0.310	26.737	0.473	11.81	2.33E+05
ETTEMA (1980) APPENDIX1 Tab A1-4	isolated point	E13	168	0.600	0.583	C	0.583	1.113	5.35	2650	1.24	0.051	1.524	5.70	0.016	0.320	9.495	0.524	11.81	2.35E+05
Sheppard Miller (2006)	isolated point	P1	169	0.420	0.170	C	0.170	0.305	0.27	2650	1.33	0.152	1.500	29.00	0.110	0.724	562.963	0.557	2.76	1.17E+05
Sheppard Miller (2006)	isolated point	P2	170	0.420	0.620	C	0.620	0.305	0.27	2650	1.33	0.152	1.500	5.12	0.240	1.579	562.963	2.030	2.76	7.51E+04
Sheppard Miller (2006)	isolated point	P3	171	0.430	0.880	C	0.880	0.306	0.27	2650	1.33	0.152	1.500	7.37	0.340	2.237	562.963	2.874	2.83	1.54E+05
Sheppard Miller (2006)	isolated point	P4	172	0.400	1.100	C	1.100	0.304	0.27	2650	1.33	0.152	1.500	7.75	0.260	1.711	562.963	3.621	2.63	2.02E+05
Sheppard Miller (2006)	isolated point	P22	173	0.430	0.250	C	0.250	0.423	0.84	2650	1.32	0.152	1.500	332.00	0.160	1.053	180.952	0.592	2.83	1.97E+06
Sheppard Miller (2006)	isolated point	P5A	174	0.400	1.260	C	1.260	0.304	0.27	2650	1.33	0.152	1.500	4.28	0.300	1.974	562.963	4.148	2.63	1.28E+05
Sheppard Miller (2006)	isolated point	P5B	175	0.400	1.430	C	1.430	0.304	0.27	2650	1.33	0.152	1.500	1.57	0.290	1.908	562.963	4.708	2.63	5.31E+04
Sheppard Miller (2006)	isolated point	P6	176	0.400	1.640	C	1.640	0.304	0.27	2650	1.33	0.152	1.500	1.73	0.320	2.105	562.963	5.399	2.63	6.73E+04
Sheppard Miller (2006)	isolated point	P7A	177	0.200	0.550	C	0.550	0.280	0.27	2650	1.33	0.152	1.500	1.72	0.180	1.184	562.963	1.962	1.32	2.24E+04
Sheppard Miller (2006)	isolated point	P7B	178	0.200	0.720	C	0.720	0.280	0.27	2650	1.33	0.152	1.500	1.12	0.240	1.579	562.963	2.568	1.32	1.90E+04
Sheppard Miller (2006)	isolated point	P8	179	0.430	0.690	C	0.690	0.306	0.27	2650	1.33	0.152	1.500	24.50	0.330	2.171	562.963	2.253	2.83	4.00E+05
Sheppard Miller (2006)	isolated point	P9	180	0.490	0.250	C	0.250	0.311	0.27	2650	1.33	0.152	1.500	46.00	0.140	0.921	562.963	0.805	3.22	2.72E+05

source/paper	label	test code(ref)	test #	h(m)	u(m/s) (data)	Velocity label	u (m/s) transformed	u c (m/s) (Melville)	d50 (mm)	ρ (kg/m^3)	σ	b(m)	lc (m)	t (hr)	ds(m)	Ds (ds/b)	D50 (b/d50)	U (u/uc) Melville	H (h/b)	T (tu/b)
Sheppard Miller (2006)	isolated point	P10	181	0.430	0.370	C	0.370	0.423	0.84	2650	1.32	0.152	1.500	18.83	0.200	1.316	180.952	0.875	2.83	1.65E+05
Sheppard Miller (2006)	isolated point	P11	182	0.380	0.580	C	0.580	0.416	0.84	2650	1.32	0.152	1.500	50.88	0.190	1.250	180.952	1.394	2.50	6.99E+05
Sheppard Miller (2006)	isolated point	P12	183	0.380	0.740	C	0.740	0.416	0.84	2650	1.32	0.152	1.500	16.98	0.270	1.776	180.952	1.779	2.50	2.98E+05
Sheppard Miller (2006)	isolated point	P13	184	0.380	1.050	C	1.050	0.416	0.84	2650	1.32	0.152	1.500	16.10	0.290	1.908	180.952	2.524	2.50	4.00E+05
Sheppard Miller (2006)	isolated point	P14	185	0.380	1.210	C	1.210	0.416	0.84	2650	1.32	0.152	1.500	1.68	0.290	1.908	180.952	2.908	2.50	4.82E+04
Sheppard Miller (2006)	isolated point	P15	186	0.380	1.370	C	1.370	0.416	0.84	2650	1.32	0.152	1.500	1.00	0.290	1.908	180.952	3.293	2.50	3.24E+04
Sheppard Miller (2006)	isolated point	P16	187	0.380	1.520	C	1.520	0.416	0.84	2650	1.32	0.152	1.500	1.00	0.310	2.039	180.952	3.653	2.50	3.60E+04
Sheppard Miller (2006)	isolated point	P17	188	0.300	1.520	C	1.520	0.403	0.84	2650	1.32	0.152	1.500	1.08	0.310	2.039	180.952	3.767	1.97	3.90E+04
Sheppard Miller (2006)	isolated point	P18	189	0.300	1.760	C	1.760	0.403	0.84	2650	1.32	0.152	1.500	1.25	0.300	1.974	180.952	4.362	1.97	5.21E+04
Sheppard Miller (2006)	isolated point	P19	190	0.300	1.850	C	1.850	0.403	0.84	2650	1.32	0.152	1.500	0.50	0.280	1.842	180.952	4.585	1.97	2.19E+04
Sheppard Miller (2006)	isolated point	P20	191	0.300	1.990	C	1.990	0.403	0.84	2650	1.32	0.152	1.500	0.33	0.320	2.105	180.952	4.932	1.97	1.57E+04
Sheppard Miller (2006)	isolated point	P21	192	0.300	2.160	C	2.160	0.403	0.84	2650	1.32	0.152	1.500	0.33	0.340	2.237	180.952	5.353	1.97	1.71E+04
Sheppard, D., et al. (2002)	series	S2002-1	193	1.190	0.290	C	0.290	0.335	0.22	2650	1.510	0.114	6.100	89.00	0.133	1.170	518.182	0.867	10.40	8.15E+05
Sheppard, D., et al. (2002)	series	S2002-2	194	1.190	0.310	C	0.310	0.335	0.22	2650	1.510	0.305	6.100	163.00	0.257	0.840	1386.364	0.927	3.90	5.96E+05
Sheppard, D., et al. (2002)	series	S2002-3	195	1.270	0.400	C	0.400	0.468	0.80	2650	1.290	0.915	6.100	360.00	1.112	1.220	1143.750	0.854	1.40	5.67E+05
Sheppard, D., et al. (2002)	series	S2002-4	196	0.870	0.390	C	0.390	0.449	0.80	2650	1.290	0.915	6.100	143.00	0.638	0.700	1143.750	0.869	1.00	2.19E+05
Sheppard ,D., et al. (2002)	series	S2002-5	197	1.270	0.390	C	0.390	0.468	0.80	2650	1.290	0.305	6.100	88.00	0.416	1.360	381.250	0.833	4.20	4.05E+05
Sheppard, D., et al. (2002)	series	S2002-6	198	1.270	0.410	C	0.410	0.468	0.80	2650	1.290	0.114	6.100	41.00	0.185	1.620	142.500	0.876	11.10	5.31E+05
Sheppard, D., et al. (2002)	series	S2002-7	199	1.220	0.760	C	0.760	0.962	2.90	2650	1.210	0.915	6.100	188.00	1.270	1.390	315.517	0.790	1.30	5.62E+05
Sheppard, D., et al. (2002)	series	S2002-8	200	0.560	0.650	C	0.650	0.865	2.90	2650	1.210	0.915	6.100	330.00	1.058	1.160	315.517	0.751	0.60	8.44E+05
Sheppard, D., et al. (2002)	series	S2002-9	201	0.290	0.570	C	0.570	0.784	2.90	2650	1.210	0.915	6.100	448.00	0.896	0.980	315.517	0.727	0.30	1.00E+06
Sheppard, D., et al. (2002)	series	S2002-10	202	0.170	0.500	C	0.500	0.717	2.90	2650	1.210	0.915	6.100	616.00	0.659	0.720	315.517	0.697	0.20	1.21E+06
Sheppard, D., et al. (2002)	series	S2002-11	203	1.900	0.700	C	0.700	1.017	2.90	2650	1.210	0.915	6.100	350.00	1.004	1.100	315.517	0.688	2.10	9.64E+05
Sheppard, D., et al. (2002)	series	S2002-12	204	1.220	0.400	C	0.400	0.335	0.22	2650	1.510	0.305	6.100	256.00	0.377	1.240	1386.364	1.193	4.00	1.21E+06
Sheppard ,D., et al. (2002)	series	S2002-13	205	0.180	0.300	C	0.300	0.273	0.22	2650	1.510	0.305	6.100	216.00	0.296	0.970	1386.364	1.098	0.60	7.65E+05
Sheppard ,D., et al. (2002)	series	S2002-14	206	1.810	0.300	C	0.300	0.348	0.22	2650	1.510	0.915	6.100	580.00	0.787	0.860	4159.091	0.862	2.00	6.85E+05
Yanmaz & Altinbilek (1991) (digitization)	series	1	207	0.165	0.360	M	0.360	0.428	1.07	2640	1.13	0.067	0.670	6.00	0.102	1.522	62.617	0.841	2.46	1.16E+05
Yanmaz & Altinbilek (1991) (digitization)	series	2	208	0.152	0.340	M	0.340	0.423	1.07	2640	1.13	0.067	0.670	5.50	0.095	1.418	62.617	0.804	2.27	1.00E+05
Yanmaz & Altinbilek (1991) (digitization)	series	3	209	0.135	0.330	M	0.330	0.415	1.07	2640	1.13	0.067	0.670	6.00	0.092	1.373	62.617	0.795	2.01	1.06E+05
Yanmaz & Altinbilek (1991) (digitization)	series	4	210	0.121	0.310	M	0.310	0.408	1.07	2640	1.13	0.067	0.670	5.50	0.078	1.164	62.617	0.759	1.81	9.16E+04
Yanmaz & Altinbilek (1991) (digitization)	series	14	211	0.165	0.360	M	0.360	0.428	1.07	2640	1.13	0.057	0.670	6.00	0.098	1.719	53.271	0.841	2.89	1.36E+05
Yanmaz & Altinbilek (1991) (digitization)	series	15	212	0.152	0.340	M	0.340	0.423	1.07	2640	1.13	0.057	0.670	5.50	0.090	1.579	53.271	0.804	2.67	1.18E+05
Yanmaz & Altinbilek (1991) (digitization)	series	16	213	0.135	0.330	M	0.330	0.415	1.07	2640	1.13	0.057	0.670	5.33	0.083	1.456	53.271	0.795	2.37	1.11E+05
Yanmaz & Altinbilek (1991) (digitization))	series	18	214	0.105	0.280	M	0.280	0.399	1.07	2640	1.13	0.057	0.670	4.00	0.061	1.070	53.271	0.701	1.84	7.07E+04
Yanmaz & Altinbilek (1991) (digitization)	series	23	215	0.105	0.280	M	0.280	0.399	1.07	2640	1.13	0.047	0.670	4.00	0.059	1.255	43.925	0.701	2.23	8.58E+04
Yanmaz & Altinbilek (1991) (digitization)	series	24	216	0.135	0.330	M	0.330	0.415	1.07	2640	1.13	0.047	0.670	5.50	0.077	1.638	43.925	0.795	2.87	1.39E+05
Yanmaz & Altinbilek (1991) (digitization)	series	25	217	0.165	0.360	M	0.360	0.428	1.07	2640	1.13	0.047	0.670	6.00	0.095	2.021	43.925	0.841	3.51	1.65E+05
Yanmaz & Altinbilek (1991) (digitization)	series	27	218	0.085	0.260	M	0.260	0.334	0.84	2630	1.28	0.067	0.670	5.00	0.091	1.358	79.762	0.778	1.27	6.99E+04
Yanmaz & Altinbilek (1991) (digitization)	series	29	219	0.121	0.310	M	0.310	0.353	0.84	2630	1.28	0.067	0.670	5.00	0.101	1.507	79.762	0.878	1.81	8.33E+04
Yanmaz & Altinbilek (1991) (digitization)	series	30	220	0.135	0.330	M	0.330	0.359	0.84	2630	1.28	0.067	0.670	5.00	0.107	1.597	79.762	0.920	2.01	8.87E+04
Yanmaz & Altinbilek (1991) (digitization)	series	32	221	0.105	0.280	M	0.280	0.346	0.84	2630	1.28	0.057	0.670	5.00	0.083	1.456	67.857	0.810	1.84	8.84E+04
Yanmaz & Altinbilek (1991) (digitization)	series	34	222	0.135	0.330	M	0.330	0.359	0.84	2630	1.28	0.057	0.670	5.00	0.095	1.667	67.857	0.920	2.37	1.04E+05
Yanmaz & Altinbilek (1991) (digitization)	series	37	223	0.121	0.150	M	0.150	0.353	0.84	2630	1.28	0.047	0.670	5.00	0.077	1.638	55.952	0.425	2.57	5.74E+04
Yanmaz & Altinbilek (1991) (digitization)	series	38	224	0.135	0.330	M	0.330	0.359	0.84	2630	1.28	0.047	0.670	5.00	0.085	1.809	55.952	0.920	2.87	1.26E+05
Chang, W.,Y., et al, (2004) (digitization)	series	S1	225	0.200	0.390	C	0.390	0.420	1.00	2650	1.20	0.100	1.000	19.00	0.186	1.860	100.000	0.928	2.00	2.67E+05

source/paper	label	test code(ref)	test #	h(m)	u(m/s) (data)	Velocity label	u (m/s) transformed	u c (m/s) (Melville)	d50 (mm)	ρ (kg/m3)	σ	b(m)	lc(m)	t(hr)	ds(m)	Ds (ds/b)	D50 (b/d50)	U(u/uc) Melville	H (h/b)	T (tu/b)
Chang, W.,Y., et al, (2004) (digitization)	series	S2	226	0.200	0.280	C	0.280	0.420	1.00	2650	1.20	0.100	1.000	19.00	0.118	1.180	100.000	0.667	2.00	1.92E+05
Chang, W.,Y., et al, (2004) (digitization)	series	S3	227	0.200	0.280	C	0.280	0.420	1.00	2650	2.00	0.100	1.000	56.00	0.043	0.430	100.000	0.667	2.00	5.64E+05
Chang, W.,Y., et al, (2004) (digitization)	series	S4	228	0.200	0.280	C	0.280	0.420	1.00	2650	3.00	0.100	1.000	28.00	0.029	0.290	100.000	0.667	2.00	2.82E+05
Chang, W.,Y., et al, (2004) (digitization)	series	S5	229	0.300	0.355	C	0.355	0.373	0.71	2650	1.20	0.100	1.000	7.00	0.154	1.540	140.845	0.953	3.00	8.95E+04
Chang, W.,Y., et al, (2004) (digitization)	series	S6	230	0.150	0.227	C	0.227	0.339	0.71	2650	1.20	0.100	1.000	7.00	0.066	0.660	140.845	0.669	1.50	5.72E+04
Chang, W.,Y., et al, (2004) (digitization)	series	S7	231	0.300	0.355	C	0.355	0.373	0.71	2650	2.00	0.100	1.000	72.00	0.083	0.830	140.845	0.953	3.00	9.20E+05
Chang, W.,Y., et al, (2004) (digitization)	series	S8	232	0.150	0.227	C	0.227	0.339	0.71	2650	2.00	0.100	1.000	47.00	0.024	0.240	140.845	0.669	1.50	3.84E+05
Chang, W.,Y., et al, (2004) (digitization)	series	S9	233	0.300	0.355	C	0.355	0.373	0.71	2650	3.00	0.100	1.000	38.00	0.068	0.680	140.845	0.953	3.00	4.86E+05
Chang, W.,Y., et al, (2004) (digitization)	series	S10	234	0.150	0.227	C	0.227	0.339	0.71	2650	3.00	0.100	1.000	27.00	0.015	0.150	140.845	0.669	1.50	2.21E+05
ETTEMA (1980) (digitization)	series	e4.1.1	235	0.600	0.301	C	0.301	0.314	0.24	2650	1.18	0.029	1.524	33.86	0.039	1.385	118.750	0.957	21.05	1.29E+06
ETTEMA (1980) (digitization)	series	e4.1.2	236	0.600	0.329	C	0.329	0.334	0.38	2650	1.29	0.029	1.524	13.62	0.044	1.533	75.000	0.987	21.05	5.67E+05
ETTEMA (1980) (digitization)	series	e4.1.3	237	0.600	0.438	C	0.438	0.440	0.84	2650	1.17	0.029	1.524	31.82	0.070	2.454	33.929	0.996	21.05	1.76E+06
ETTEMA (1980) (digitization)	series	e4.1.4	238	0.600	0.624	C	0.624	0.720	1.90	2650	1.34	0.029	1.524	30.53	0.057	2.017	15.000	0.866	21.05	2.41E+06
ETTEMA (1980) (digitization)	series	e4.1.5	239	0.600	1.105	C	1.105	1.113	5.35	2650	1.24	0.029	1.524	45.24	0.032	1.115	5.327	0.993	21.05	6.32E+06
ETTEMA (1980) (digitization)	series	e4.1.6	240	0.600	1.661	C	1.661	1.275	7.80	2650	1.10	0.029	1.524	31.17	0.023	0.790	3.654	1.303	21.05	6.54E+06
ETTEMA (1980) (digitization)	series	e4.1.7	241	0.600	0.463	C	0.463	0.440	0.84	2650	1.17	0.029	1.524	26.41	0.072	2.537	33.929	1.051	21.05	1.54E+06
ETTEMA (1980) (digitization)	series	e4.1.8	242	0.600	0.658	C	0.658	0.720	1.90	2650	1.34	0.029	1.524	44.06	0.061	2.157	15.000	0.915	21.05	3.66E+06
ETTEMA (1980) (digitization)	series	e4.1.9	243	0.600	1.167	C	1.167	1.113	5.35	2650	1.24	0.029	1.524	35.91	0.040	1.389	5.327	1.048	21.05	5.29E+06
ETTEMA (1980) (digitization)	series	e4.1.10	244	0.600	1.753	C	1.753	1.275	7.80	2650	1.12	0.029	1.524	47.82	0.030	1.037	3.654	1.375	21.05	1.06E+07
ETTEMA (1980) (digitization)	series	e4.1.11	245	0.600	0.624	C	0.624	0.720	1.90	2650	1.34	0.045	0.457	43.71	0.094	2.080	23.684	0.866	13.33	2.18E+06
ETTEMA (1980) (digitization)	series	e4.1.12	246	0.600	0.438	C	0.438	0.440	0.84	2650	1.17	0.045	0.457	108.31	0.098	2.180	53.571	0.996	13.33	3.80E+06
ETTEMA (1980) (digitization)	series	e4.1.13	247	0.600	0.984	C	0.984	0.987	3.80	2686	1.07	0.045	0.457	70.38	0.071	1.580	11.842	0.997	13.33	5.54E+06
ETTEMA (1980) (digitization)	series	e4.1.14	248	0.600	0.329	C	0.329	0.334	0.38	2650	1.29	0.045	0.457	68.80	0.075	1.670	118.421	0.987	13.33	1.81E+06
ETTEMA (1980) (digitization)	series	e4.1.15	249	0.600	0.301	C	0.301	0.314	0.24	2650	1.18	0.045	0.457	30.40	0.061	1.350	187.500	0.957	13.33	7.31E+05
ETTEMA (1980) (digitization)	series	e4.1.16	250	0.600	0.658	C	0.658	0.720	1.90	2650	1.34	0.045	0.457	58.70	0.098	2.174	23.684	0.915	13.33	3.09E+06
ETTEMA (1980) (digitization)	series	e4.1.17	251	0.600	0.463	C	0.463	0.440	0.84	2650	1.17	0.045	0.457	135.89	0.104	2.302	53.571	1.051	13.33	5.03E+06
ETTEMA (1980) (digitization)	series	e4.1.18	252	0.600	0.348	C	0.348	0.334	0.38	2650	1.29	0.045	0.457	38.15	0.077	1.719	118.421	1.042	13.33	1.06E+06
ETTEMA (1980) (digitization)	series	e4.1.19	253	0.600	1.038	C	1.038	0.977	3.80	2650	1.08	0.045	0.457	44.71	0.085	1.887	11.842	1.063	13.33	3.71E+06
ETTEMA (1980) (digitization)	series	e4.1.20	254	0.600	0.317	C	0.317	0.314	0.24	2650	uniform	0.045	0.457	29.72	0.073	1.621	187.500	1.010	13.33	7.55E+05
ETTEMA (1980) (digitization)	series	e4.1.21	255	0.600	0.624	C	0.624	0.720	1.90	2650	1.34	0.051	1.524	74.43	0.113	2.225	26.737	0.866	11.81	3.29E+06
ETTEMA (1980) (digitization)	series	e4.1.22	256	0.600	0.419	C	0.419	0.429	0.80	2650	1.33	0.051	1.524	67.29	0.111	2.190	63.500	0.975	11.81	2.00E+06
ETTEMA (1980) (digitization)	series	e4.1.23	257	0.600	0.438	C	0.438	0.440	0.84	2650	1.17	0.051	1.524	82.32	0.112	2.199	60.476	0.996	11.81	2.56E+06
ETTEMA (1980) (digitization)	series	e4.1.24	258	0.600	1.105	C	1.105	1.113	5.35	2650	1.24	0.051	1.524	94.79	0.081	1.587	9.495	0.993	11.81	7.42E+06
ETTEMA (1980) (digitization)	series	e4.1.25	259	0.600	0.329	C	0.329	0.334	0.38	2650	1.29	0.051	1.524	41.49	0.073	1.436	133.684	0.987	11.81	9.68E+05
ETTEMA (1980) (digitization)	series	e4.1.26	260	0.600	0.301	C	0.301	0.314	0.24	2650	1.18	0.051	1.524	21.77	0.069	1.356	211.667	0.957	11.81	4.64E+05
ETTEMA (1980) (digitization)	series	e4.1.27	261	0.600	1.661	C	1.661	1.275	7.80	2650	1.10	0.051	1.524	21.33	0.051	1.011	6.513	1.303	11.81	2.51E+06
ETTEMA (1980) (digitization)	series	e4.1.28	262	0.600	0.463	C	0.463	0.440	0.84	2650	1.33	0.051	1.524	190.53	0.123	2.412	60.476	1.051	11.81	6.25E+06
ETTEMA (1980) (digitization)	series	e4.1.29	263	0.600	0.658	C	0.658	0.720	1.90	2650	1.34	0.051	1.524	99.79	0.116	2.286	26.737	0.915	11.81	4.66E+06
ETTEMA (1980) (digitization)	series	e4.1.30	264	0.600	0.348	C	0.348	0.334	0.38	2650	uniform	0.051	1.524	17.52	0.086	1.702	133.684	1.042	11.81	4.32E+05
ETTEMA (1980) (digitization)	series	e4.1.31	265	0.600	1.167	C	1.167	1.113	5.35	2650	1.24	0.051	1.524	52.27	0.086	1.702	9.495	1.048	11.81	4.32E+06
ETTEMA (1980) (digitization)	series	e4.1.32	266	0.600	1.753	C	1.753	1.275	7.80	2650	1.12	0.051	1.524	44.71	0.075	1.479	6.513	1.375	11.81	5.55E+06
ETTEMA (1980) (digitization)	series	e4.1.33	267	0.600	0.984	C	0.984	0.977	3.80	2650	1.07	0.102	1.524	31.96	0.209	2.057	26.737	1.007	5.91	1.11E+06
ETTEMA (1980) (digitization)	series	e4.1.34	268	0.600	1.105	C	1.105	1.113	5.35	2650	1.24	0.102	1.524	35.53	0.177	1.744	18.991	0.993	5.91	1.39E+06
ETTEMA (1980) (digitization)	series	e4.1.35	269	0.600	0.624	C	0.624	0.720	1.90	2650	1.34	0.102	1.524	96.11	0.223	2.196	53.474	0.866	5.91	2.12E+06
ETTEMA (1980) (digitization)	series	e4.1.36	270	0.600	0.438	C	0.438	0.440	0.84	2650	1.17	0.102	1.524	233.87	0.227	2.232	120.952	0.996	5.91	3.63E+06

source/paper	label	test code(ref)	test #	h(m)	u(m/s) (data)	Velocity label	u (m/s) transformed	u c (m/s) (Melville)	d50 (mm)	ρ (kg/m^3)	σ	b(m)	lc(m)	t(hr)	ds(m)	Ds (ds/b)	D50 (b/d50)	U(u/uc) Melville	H (h/b)	T (tu/b)
ETTEMA (1980) (digitization)	series	e4.1.37	271	0.600	0.419	C	0.419	0.429	0.80	2650	1.33	0.102	1.524	197.43	0.227	2.232	127.000	0.975	5.91	2.93E+06
ETTEMA (1980) (digitization)	series	e4.1.38	272	0.600	0.329	C	0.329	0.334	0.38	2650	1.29	0.102	1.524	43.91	0.143	1.411	267.368	0.987	5.91	5.12E+05
ETTEMA (1980) (digitization)	series	e4.1.39	273	0.600	1.661	C	1.661	1.275	7.80	2650	1.10	0.102	1.524	46.79	0.163	1.605	13.026	1.303	5.91	2.75E+06
ETTEMA (1980) (digitization)	series	e4.1.40	274	0.600	0.301	C	0.301	0.314	0.24	2650	1.18	0.102	1.524	111.46	0.172	1.688	423.333	0.957	5.91	1.19E+06
ETTEMA (1980) (digitization)	series	e4.1.41	275	0.600	1.167	C	1.167	1.113	5.35	2650	1.24	0.102	1.524	46.20	0.213	2.093	18.991	1.048	5.91	1.91E+06
ETTEMA (1980) (digitization)	series	e4.1.42	276	0.600	0.658	C	0.658	0.720	1.90	2650	1.34	0.102	1.524	83.82	0.230	2.262	53.474	0.915	5.91	1.96E+06
ETTEMA (1980) (digitization)	series	e4.1.43	277	0.600	0.463	C	0.463	0.440	0.84	2650	1.17	0.102	1.524	182.66	0.228	2.242	120.952	1.051	5.91	3.00E+06
ETTEMA (1980) (digitization)	series	e4.1.44	278	0.600	1.753	C	1.753	1.275	7.80	2650	1.12	0.102	1.524	66.66	0.185	1.825	13.026	1.375	5.91	4.14E+06
ETTEMA (1980) (digitization)	series	e4.1.45	279	0.600	0.317	C	0.317	0.314	0.24	2650	unif	0.102	1.524	28.55	0.159	1.567	423.333	1.010	5.91	3.21E+05
ETTEMA (1980) (digitization)	series	e4.1.46	280	0.600	1.105	C	1.105	1.113	5.35	2650	1.24	0.150	1.524	81.19	0.306	2.037	28.037	0.993	4.00	2.15E+06
ETTEMA (1980) (digitization)	series	e4.1.47	281	0.600	1.661	C	1.661	1.275	7.80	2650	1.10	0.150	1.524	49.88	0.284	1.893	19.231	1.303	4.00	1.99E+06
ETTEMA (1980) (digitization)	series	e4.1.48	282	0.600	0.624	C	0.624	0.720	1.90	2650	1.34	0.150	1.524	258.99	0.315	2.099	78.947	0.866	4.00	3.88E+06
ETTEMA (1980) (digitization)	series	e4.1.49	283	0.600	0.438	C	0.438	0.440	0.84	2650	1.17	0.150	1.524	495.91	0.310	2.068	178.571	0.996	4.00	5.22E+06
ETTEMA (1980) (digitization)	series	e4.1.50	284	0.600	0.419	C	0.419	0.429	0.80	2650	1.33	0.150	1.524	431.47	0.312	2.078	187.500	0.975	4.00	4.34E+06
ETTEMA (1980) (digitization)	series	e4.1.51	285	0.600	0.301	C	0.301	0.314	0.24	2650	1.18	0.150	1.524	215.12	0.239	1.595	625.000	0.957	4.00	1.55E+06
ETTEMA (1980) (digitization)	series	e4.1.52	286	0.600	1.167	C	1.167	1.113	5.35	2650	1.24	0.150	1.524	55.55	0.306	2.039	28.037	1.048	4.00	1.56E+06
ETTEMA (1980) (digitization)	series	e4.1.53	287	0.600	1.753	C	1.753	1.275	7.80	2650	1.12	0.150	1.524	45.01	0.286	1.906	19.231	1.375	4.00	1.89E+06
ETTEMA (1980) (digitization)	series	e4.1.54	288	0.600	0.658	C	0.658	0.720	1.90	2650	1.34	0.150	1.524	285.33	0.341	2.275	78.947	0.915	4.00	4.51E+06
ETTEMA (1980) (digitization)	series	e4.1.55	289	0.600	0.463	C	0.463	0.440	0.84	2650	1.17	0.150	1.524	631.73	0.347	2.316	178.571	1.051	4.00	7.02E+06
ETTEMA (1980) (digitization)	series	e4.1.56	290	0.600	0.317	C	0.317	0.314	0.24	2650	uniform	0.150	1.524	88.66	0.241	1.609	625.000	1.010	4.00	6.75E+05
ETTEMA (1980) (digitization)	series	e4.1.57	291	0.600	0.301	C	0.301	0.314	0.24	2650	1.18	0.240	1.524	32.61	0.216	0.901	1000.000	0.957	2.50	1.47E+05
ETTEMA (1980) (digitization)	series	e4.1.58	292	0.600	0.329	C	0.329	0.334	0.38	2650	1.29	0.240	1.524	34.69	0.199	0.827	631.579	0.987	2.50	1.71E+05
ETTEMA (1980) (digitization)	series	e4.1.59	293	0.600	0.429	C	0.429	0.429	0.80	2650	1.33	0.240	1.524	13.14	0.250	1.041	300.000	0.998	2.50	8.45E+04
ETTEMA (1980) (digitization)	series	e4.1.60	294	0.600	0.624	C	0.624	0.720	1.90	2650	1.34	0.240	1.524	13.98	0.328	1.366	126.316	0.866	2.50	1.31E+05
ETTEMA (1980) (digitization)	series	e4.1.61	295	0.600	1.105	C	1.105	1.113	5.35	2650	1.24	0.240	1.524	14.28	0.348	1.450	44.860	0.993	2.50	2.37E+05
ETTEMA (1980) (digitization)	series	E4.2.1	296	0.600	0.274	C	0.274	0.334	0.38	2650	1.29	0.051	1.524	65.82	0.072	1.423	133.684	0.822	11.81	1.28E+06
ETTEMA (1980) (digitization)	series	E4.2.2	297	0.600	0.921	C	0.921	1.113	5.35	2650	1.24	0.051	1.524	43.94	0.043	0.856	9.495	0.827	11.81	2.87E+06
ETTEMA (1980) (digitization)	series	E4.2.3	298	0.600	0.349	C	0.349	0.429	0.80	2650	1.33	0.051	1.524	61.95	0.082	1.609	63.500	0.812	11.81	1.53E+06
ETTEMA (1980) (digitization)	series	E4.2.4	299	0.600	0.520	C	0.520	0.720	1.90	2650	1.34	0.051	1.524	54.88	0.085	1.674	26.737	0.722	11.81	2.02E+06
ETTEMA (1980) (digitization)	series	e4.3.1	300	0.600	0.233	C	0.233	0.429	0.80	2650	1.33	0.051	1.524	9.94	0.017	0.333	63.500	0.542	11.81	1.64E+05
ETTEMA (1980) (digitization)	series	e4.3.2	301	0.600	0.347	C	0.347	0.720	1.90	2650	1.34	0.051	1.524	7.30	0.016	0.325	26.737	0.481	11.81	1.79E+05
ETTEMA (1980) (digitization)	series	e4.3.3	302	0.600	0.614	C	0.614	1.113	5.35	2650	1.24	0.051	1.524	5.90	0.017	0.342	9.495	0.551	11.81	2.57E+05
ETTEMA (1980) (digitization)	series	E4.17.1	303	0.600	1.105	C	1.105	1.113	5.35	2650	1.24	0.029	1.524	46.79	0.034	1.208	5.327	0.993	21.05	6.53E+06
ETTEMA (1980) (digitization)	series	E4.17.2	304	0.200	0.934	C	0.934	0.923	5.35	2650	1.24	0.029	1.524	35.91	0.030	1.062	5.327	1.012	7.02	4.24E+06
ETTEMA (1980) (digitization)	series	E4.17.3	305	0.100	0.826	C	0.826	0.803	5.35	2650	1.24	0.029	1.524	51.10	0.027	0.962	5.327	1.029	3.51	5.33E+06
ETTEMA (1980) (digitization)	series	E4.17.4	306	0.050	0.718	C	0.718	0.683	5.35	2650	1.24	0.029	1.524	46.79	0.019	0.654	5.327	1.051	1.75	4.24E+06
ETTEMA (1980) (digitization)	series	E4.17.5	307	0.600	0.624	C	0.624	0.720	1.90	2650	1.34	0.029	1.524	32.90	0.058	2.019	15.000	0.866	21.05	2.59E+06
ETTEMA (1980) (digitization)	series	E4.17.6	308	0.200	0.540	C	0.540	0.614	1.90	2650	1.34	0.029	1.524	55.61	0.057	2.006	15.000	0.879	7.02	3.79E+06
ETTEMA (1980) (digitization)	series	E4.17.7	309	0.100	0.486	C	0.486	0.547	1.90	2650	1.34	0.029	1.524	35.62	0.049	1.713	15.000	0.889	3.51	2.19E+06
ETTEMA (1980) (digitization)	series	E4.17.8	310	0.050	0.433	C	0.433	0.480	1.90	2650	1.34	0.029	1.524	37.36	0.042	1.462	15.000	0.902	1.75	2.05E+06
ETTEMA (1980) (digitization)	series	E4.17.9	311	0.100	1.035	C	1.035	0.268	0.38	2650	1.29	0.029	1.524	23.97	0.038	1.349	75.000	3.866	3.51	3.14E+06
ETTEMA (1980) (digitization)	series	E4.17.10	312	0.200	1.127	C	1.127	0.293	0.38	2650	1.29	0.029	1.524	5.31	0.046	1.609	75.000	3.841	7.02	7.55E+05
ETTEMA (1980) (digitization)	series	E4.17.11	313	0.600	1.272	C	1.272	0.334	0.38	2650	1.29	0.029	1.524	14.50	0.046	1.625	75.000	3.811	21.05	2.33E+06
ETTEMA (1980) (digitization)	series	E4.17.12	314	0.050	0.718	C	0.718	0.683	5.35	2650	1.24	0.102	1.524	39.09	0.101	0.990	18.991	1.051	0.49	9.95E+05
ETTEMA (1980) (digitization)	series	E4.17.13	315	0.100	0.826	C	0.826	0.803	5.35	2650	1.24	0.102	1.524	38.49	0.130	1.278	18.991	1.029	0.98	1.13E+06

source/paper	label	test code(ref)	test #	h(m)	u(m/s) (data)	Velocity label	u (m/s) transformed	u c (m/s) (Melville)	d50 (mm)	ρ (kg/m^3)	σ	b(m)	lc(m)	t(hr)	ds(m)	Ds (ds/b)	D50 (b/d50)	U(u/uc) Melville	H (h/b)	T (tu/b)
ETTEMA (1980) (digitization)	series	E4.17.14	316	0.200	0.934	C	0.934	0.923	5.35	2650	1.24	0.102	1.524	30.07	0.145	1.430	18.991	1.012	1.97	9.95E+05
ETTEMA (1980) (digitization)	series	E4.17.15	317	0.300	0.997	C	0.997	0.993	5.35	2650	1.24	0.102	1.524	31.49	0.168	1.656	18.991	1.004	2.95	1.11E+06
ETTEMA (1980) (digitization)	series	E4.17.16	318	0.400	1.042	C	1.042	1.043	5.35	2650	1.24	0.102	1.524	25.38	0.179	1.759	18.991	0.999	3.94	9.37E+05
ETTEMA (1980) (digitization)	series	E4.17.17	319	0.600	1.105	C	1.105	1.113	5.35	2650	1.24	0.102	1.524	30.07	0.180	1.773	18.991	0.993	5.91	1.18E+06
ETTEMA (1980) (digitization)	series	E4.17.18	320	0.050	0.433	C	0.433	0.480	1.90	2650	1.34	0.102	1.524	82.37	0.149	1.467	53.474	0.902	0.49	1.26E+06
ETTEMA (1980) (digitization)	series	E4.17.19	321	0.100	0.486	C	0.486	0.547	1.90	2650	1.34	0.102	1.524	82.37	0.177	1.740	53.474	0.889	0.98	1.42E+06
ETTEMA (1980) (digitization)	series	E4.17.20	322	0.200	0.540	C	0.540	0.614	1.90	2650	1.34	0.102	1.524	80.39	0.202	1.983	53.474	0.879	1.97	1.54E+06
ETTEMA (1980) (digitization)	series	E4.17.21	323	0.300	0.571	C	0.571	0.653	1.90	2650	1.34	0.102	1.524	90.78	0.210	2.067	53.474	0.874	2.95	1.84E+06
ETTEMA (1980) (digitization)	series	E4.17.22	324	0.400	0.593	C	0.593	0.681	1.90	2650	1.34	0.102	1.524	90.78	0.217	2.135	53.474	0.871	3.94	1.91E+06
ETTEMA (1980) (digitization)	series	E4.17.23	325	0.600	0.624	C	0.624	0.720	1.90	2650	1.34	0.102	1.524	88.60	0.222	2.181	53.474	0.866	5.91	1.96E+06
ETTEMA (1980) (digitization)	series	E4.17.24	326	0.050	0.244	C	0.244	0.242	0.38	2650	1.29	0.102	1.524	21.01	0.086	0.848	267.368	1.009	0.49	1.82E+05
ETTEMA (1980) (digitization)	series	E4.17.25	327	0.100	0.268	C	0.268	0.268	0.38	2650	1.29	0.102	1.524	39.60	0.130	1.276	267.368	1.001	0.98	3.76E+05
ETTEMA (1980) (digitization)	series	E4.17.26	328	0.200	0.292	C	0.292	0.293	0.38	2650	12.29	0.102	1.524	44.81	0.128	1.262	267.368	0.995	1.97	4.63E+05
ETTEMA (1980) (digitization)	series	E4.17.27	329	0.300	0.306	C	0.306	0.308	0.38	2650	1.29	0.102	1.524	43.45	0.146	1.441	267.368	0.992	2.95	4.70E+05
ETTEMA (1980) (digitization)	series	E4.17.28	330	0.300	0.306	C	0.306	0.308	0.38	2650	1.29	0.102	1.524	43.45	0.146	1.441	267.368	0.992	2.95	4.70E+05
ETTEMA (1980) (digitization)	series	E4.17.29	331	0.400	0.315	C	0.315	0.319	0.38	2650	1.29	0.102	1.524	40.84	0.151	1.483	267.368	0.989	3.94	4.56E+05
ETTEMA (1980) (digitization)	series	E4.17.30	332	0.600	0.624	C	0.624	0.720	1.90	2650	1.34	0.102	1.524	36.09	0.147	1.448	53.474	0.866	5.91	7.98E+05
ETTEMA (1980) (digitization)	series	E4.17.31	333	0.100	0.486	C	0.486	0.547	1.90	2650	1.34	0.240	1.524	45.84	0.266	1.110	126.316	0.889	0.42	3.35E+05
ETTEMA (1980) (digitization)	series	E4.17.32	334	0.600	0.624	C	0.624	0.720	1.90	2650	1.34	0.240	1.524	13.76	0.312	1.299	126.316	0.866	2.50	1.29E+05
ETTEMA (1980) (digitization)	series	E4.17.33	335	0.100	0.268	C	0.268	0.268	0.38	2650	1.29	0.240	1.524	28.69	0.169	0.704	631.579	1.001	0.42	1.15E+05
ETTEMA (1980) (digitization)	series	E4.17.34	336	0.600	0.329	C	0.329	0.334	0.38	2650	1.29	0.240	1.524	32.53	0.209	0.870	631.579	0.987	2.50	1.61E+05
ETTEMA (1980) (digitization)	series	E4.17.35	337	0.050	0.718	C	0.718	0.683	5.35	2650	1.24	0.240	1.524	38.93	0.260	1.083	44.860	1.051	0.21	4.19E+05
ETTEMA (1980) (digitization)	series	E4.17.36	338	0.100	0.826	C	0.826	0.803	5.35	2650	1.24	0.240	1.524	23.97	0.283	1.178	44.860	1.029	0.42	2.97E+05
ETTEMA (1980) (digitization)	series	E4.17.37	339	0.600	1.105	C	1.105	1.113	5.35	2650	1.24	0.240	1.524	7.80	0.325	1.354	44.860	0.993	2.50	1.29E+05
Lanca et al. (2013)	series	L1	340	0.055	0.280	M	0.280	0.317	0.86	2650	1.36	0.110	2.000	170.00	0.154	1.396	127.900	0.884	0.50	1.56E+06
Lanca et al. (2013)	series	L2	341	0.080	0.290	M	0.290	0.337	0.86	2650	1.36	0.160	2.000	168.00	0.195	1.219	186.000	0.860	0.50	1.10E+06
Lanca et al. (2013)	series	L3	342	0.100	0.290	M	0.290	0.349	0.86	2650	1.36	0.200	2.000	170.00	0.225	1.125	232.600	0.831	0.50	8.87E+05
Lanca et al. (2013)	series	L4	343	0.125	0.300	M	0.300	0.361	0.86	2650	1.36	0.250	2.000	168.00	0.250	0.998	290.700	0.831	0.50	7.26E+05
Lanca et al. (2013)	series	L5	344	0.158	0.290	M	0.290	0.374	0.86	2650	1.36	0.315	2.000	223.00	0.315	1.001	366.300	0.776	0.50	7.39E+05
Lanca et al. (2013)	series	L6	345	0.175	0.330	M	0.330	0.379	0.86	2650	1.36	0.350	2.000	306.00	0.335	0.958	407.000	0.870	0.50	1.04E+06
Lanca et al. (2013)	series	L7	346	0.200	0.310	M	0.310	0.387	0.86	2650	1.36	0.400	2.000	288.00	0.377	0.942	465.100	0.802	0.50	8.04E+05
Lanca et al. (2013)	series	L8	347	0.050	0.270	M	0.270	0.312	0.86	2650	1.36	0.050	2.000	168.00	0.104	2.084	58.100	0.866	1.00	3.27E+06
Lanca et al. (2013)	series	L9	348	0.075	0.280	M	0.280	0.334	0.86	2650	1.36	0.075	2.000	168.00	0.143	1.900	87.200	0.839	1.00	2.26E+06
Lanca et al. (2013)	series	L10	349	0.110	0.290	M	0.290	0.354	0.86	2650	1.36	0.110	2.000	168.00	0.180	1.635	127.900	0.819	1.00	1.59E+06
Lanca et al. (2013)	series	L11	350	0.160	0.300	M	0.300	0.375	0.86	2650	1.36	0.160	1.000	285.00	0.223	1.391	186.000	0.801	1.00	1.92E+06
Lanca et al. (2013)	series	L12	351	0.200	0.310	M	0.310	0.387	0.86	2650	1.36	0.200	1.000	261.00	0.283	1.417	232.600	0.802	1.00	1.46E+06
Lanca et al. (2013)	series	L13	352	0.250	0.320	M	0.320	0.399	0.86	2650	1.36	0.250	2.000	263.00	0.324	1.296	290.700	0.803	1.00	1.21E+06
Lanca et al. (2013)	series	L14	353	0.315	0.330	M	0.330	0.411	0.86	2650	1.36	0.315	2.000	186.00	0.352	1.117	366.300	0.803	1.00	7.01E+05
Lanca et al. (2013)	series	L15	354	0.350	0.330	M	0.330	0.417	0.86	2650	1.36	0.350	2.000	291.00	0.373	1.065	407.000	0.792	1.00	9.88E+05
Lanca et al. (2013)	series	L16	355	0.400	0.330	M	0.330	0.424	0.86	2650	1.36	0.400	2.000	224.00	0.406	1.014	465.100	0.778	1.00	6.65E+05
Lanca et al. (2013)	series	L17	356	0.075	0.280	M	0.280	0.334	0.86	2650	1.36	0.050	2.000	168.00	0.105	2.108	58.100	0.839	1.50	3.39E+06
Lanca et al. (2013)	series	L18	357	0.113	0.300	M	0.300	0.356	0.86	2650	1.36	0.075	2.000	168.00	0.159	2.121	87.200	0.843	1.51	2.42E+06
Lanca et al. (2013)	series	L19	358	0.165	0.300	M	0.300	0.376	0.86	2650	1.36	0.110	1.000	241.00	0.180	1.637	127.900	0.798	1.50	2.37E+06
Lanca et al. (2013)	series	L20	359	0.225	0.330	M	0.330	0.393	0.86	2650	1.36	0.160	2.000	267.00	0.272	1.701	186.000	0.840	1.41	1.98E+06
Lanca et al. (2013)	series	L21	360	0.300	0.330	M	0.330	0.408	0.86	2650	1.36	0.200	2.000	262.00	0.309	1.544	232.600	0.808	1.50	1.56E+06

source/paper	label	test code(ref)	test #	h(m)	u(m/s) (data)	Velocity label	u (m/s) transformed	u c (m/s) (Melville)	d50 (mm)	ρ (kg/m^3)	σ	b(m)	lc(m)	t(hr)	ds(m)	Ds (ds/b)	D50 (b/d50)	U(u/uc) Melville	H (h/b)	T (tu/b)
Lanca et al. (2013)	series	L22	361	0.375	0.330	M	0.330	0.420	0.86	2650	1.36	0.250	2.000	221.00	0.339	1.355	290.700	0.785	1.50	1.05E+06
Lanca et al. (2013)	series	L23	362	0.100	0.290	M	0.290	0.349	0.86	2650	1.36	0.050	2.000	170.00	0.115	2.292	58.100	0.830	2.00	3.55E+06
Lanca et al. (2013)	series	L24	363	0.150	0.300	M	0.300	0.371	0.86	2650	1.36	0.075	2.000	169.00	0.154	2.053	87.200	0.809	2.00	2.43E+06
Lanca et al. (2013)	series	L25	364	0.220	0.330	M	0.330	0.392	0.86	2650	1.36	0.110	2.000	216.00	0.198	1.795	127.900	0.842	2.00	2.33E+06
Lanca et al. (2013)	series	L26	365	0.300	0.330	M	0.330	0.408	0.86	2650	1.36	0.160	2.000	330.00	0.247	1.545	186.000	0.808	1.88	2.45E+06
Lanca et al. (2013)	series	L27	366	0.400	0.330	M	0.330	0.424	0.86	2650	1.36	0.200	2.000	219.00	0.299	1.494	232.600	0.778	2.00	1.30E+06
Lanca et al. (2013)	series	L28	367	0.125	0.300	M	0.300	0.361	0.86	2650	1.36	0.050	2.000	168.00	0.112	2.236	58.100	0.830	2.50	3.63E+06
Lanca et al. (2013)	series	L29	368	0.188	0.310	M	0.310	0.383	0.86	2650	1.36	0.075	1.000	191.00	0.138	1.844	87.200	0.809	2.51	2.84E+06
Lanca et al. (2013)	series	L30	369	0.275	0.330	M	0.330	0.404	0.86	2650	1.36	0.110	2.000	184.00	0.216	1.962	127.900	0.817	2.50	1.99E+06
Lanca et al. (2013)	series	L31	370	0.375	0.330	M	0.330	0.421	0.86	2650	1.36	0.160	2.000	313.00	0.241	1.507	186.000	0.785	2.34	2.32E+06
Lanca et al. (2013)	series	L32	371	0.150	0.300	M	0.300	0.371	0.86	2650	1.36	0.050	1.000	173.00	0.095	1.890	58.100	0.808	3.00	3.74E+06
Lanca et al. (2013)	series	L33	372	0.225	0.330	M	0.330	0.393	0.86	2650	1.36	0.075	2.000	197.00	0.156	2.084	87.200	0.840	3.00	3.12E+06
Lanca et al. (2013)	series	L34	373	0.330	0.330	M	0.330	0.414	0.86	2650	1.36	0.110	2.000	169.00	0.193	1.755	127.900	0.798	3.00	1.83E+06
Lanca et al. (2013)	series	L35	374	0.200	0.310	M	0.310	0.387	0.86	2650	1.36	0.050	2.000	170.00	0.116	2.318	58.100	0.802	4.00	3.79E+06
Lanca et al. (2013)	series	L36	375	0.300	0.330	M	0.330	0.408	0.86	2650	1.36	0.075	2.000	314.00	0.174	2.316	87.200	0.808	4.00	4.97E+06
Lanca et al. (2013)	series	L37	376	0.250	0.330	M	0.330	0.399	0.86	2650	1.36	0.050	2.000	237.00	0.100	2.006	58.100	0.828	5.00	5.63E+06
Lanca et al. (2013)	series	L38	377	0.375	0.330	M	0.330	0.421	0.86	2650	1.36	0.075	2.000	315.00	0.162	2.153	87.200	0.785	5.00	4.99E+06
Simmaro, G. (from Lanca (2013))	series	Si1	378	0.160	0.270	M	0.270	0.374	0.86	2650	1.36	0.075	0.820	34.90	0.168	2.240	87.209	0.721	2.13	4.52E+05
Simmaro, G. (from Lanca (2013))	series	Si2	379	0.160	0.300	M	0.300	0.374	0.86	2650	1.36	0.080	0.820	45.60	0.196	2.450	93.023	0.801	2.00	6.16E+05
Simmaro, G. (from Lanca (2013))	series	Si3	380	0.160	0.340	M	0.340	0.481	1.28	2650	1.46	0.080	0.820	29.70	0.130	1.625	62.500	0.708	2.00	4.54E+05
Simmaro, G. (from Lanca (2013))	series	Si4	381	0.150	0.340	M	0.340	0.476	1.28	2650	1.46	0.075	0.820	24.90	0.139	1.853	58.594	0.715	2.00	4.06E+05
Simmaro, G. (from Lanca (2013))	series	Si5	382	0.130	0.340	M	0.340	0.465	1.28	2650	1.46	0.063	0.820	29.00	0.129	2.048	49.219	0.731	2.06	5.63E+05
Grimaldi (2005) (from Lanca (2013))	series	Gr1	383	0.150	0.400	M	0.400	0.476	1.28	2650	1.46	0.075	0.800	4.00	0.121	1.613	58.594	0.841	2.00	7.68E+04
Grimaldi (2005) (from Lanca (2013))	series	Gr2	384	0.250	0.340	M	0.340	0.399	0.86	2650	1.36	0.090	2.000	6.20	0.179	1.989	104.651	0.853	2.78	8.43E+04
Grimaldi (2005) (from Lanca (2013))	series	Gr3	385	0.250	0.340	M	0.340	0.399	0.86	2650	1.36	0.120	2.000	6.10	0.225	1.875	139.535	0.853	2.08	6.22E+04
Oliveto & Hager (1999)	series	OH1	386	0.153	0.780	M	0.891	0.846	4.80	2650	1.25	0.064	1.000	22.73	0.133	2.087	13.229	1.054	2.41	1.15E+06
Oliveto & Hager (1999)	series	OH2	387	0.203	0.620	M	0.719	0.891	4.80	2650	1.25	0.064	1.000	22.00	0.071	1.110	13.229	0.806	3.19	8.96E+05
Oliveto & Hager (1999)	series	OH3	388	0.153	0.690	M	0.788	0.846	4.80	2650	1.25	0.064	1.000	22.83	0.086	1.354	13.229	0.933	2.41	1.02E+06
Oliveto & Hager (1999)	series	OH4	389	0.101	0.530	M	0.592	0.777	4.80	2650	1.25	0.064	1.000	18.33	0.036	0.567	13.229	0.762	1.58	6.16E+05
Oliveto & Hager (1999)	series	OH5	390	0.094	0.760	M	0.846	0.765	4.80	2650	1.25	0.110	1.000	22.00	0.188	1.709	22.917	1.106	0.85	6.09E+05
Oliveto & Hager (1999)	series	OH6	391	0.096	0.570	M	0.635	0.769	4.80	2650	1.25	0.110	1.000	14.08	0.126	1.145	22.917	0.826	0.87	2.93E+05
Oliveto & Hager (1999)	series	OH7	392	0.046	0.680	M	0.727	0.651	4.80	2650	1.25	0.257	1.000	27.17	0.230	0.895	53.542	1.117	0.18	2.77E+05
Oliveto & Hager (1999)	series	OH8	393	0.051	0.530	M	0.569	0.664	4.80	2650	1.25	0.257	1.000	2.33	0.128	0.496	53.542	0.857	0.20	1.86E+04
Oliveto & Hager (1999)	series	OH9	394	0.054	0.390	M	0.420	0.674	4.80	2650	1.25	0.257	1.000	44.95	0.051	0.198	53.542	0.624	0.21	2.65E+05
Oliveto & Hager (1999)	series	OH10	395	0.061	0.500	M	0.543	0.694	4.80	2650	1.25	0.500	1.000	11.02	0.221	0.442	104.167	0.782	0.12	4.31E+04
Oliveto & Hager (1999)	series	OH11	396	0.154	0.330	M	0.330	0.310	0.55	2650	1.37	0.110	1.000	0.95	0.106	0.959	200.000	1.064	1.40	1.03E+04
Oliveto & Hager (1999)	series	OH12	397	0.149	0.240	M	0.240	0.309	0.55	2650	1.37	0.110	1.000	22.33	0.116	1.055	200.000	0.777	1.35	1.75E+05
Oliveto & Hager (1999)	series	OH13	398	0.302	0.250	M	0.250	0.339	0.55	2650	1.37	0.110	1.000	10.67	0.097	0.877	200.000	0.738	2.75	8.73E+04
Oliveto & Hager (1999)	series	OH14	399	0.149	0.210	M	0.210	0.309	0.55	2650	1.37	0.064	1.000	4.68	0.044	0.688	116.364	0.680	2.32	5.53E+04
Oliveto & Hager (1999)	series	OH15	400	0.201	0.250	M	0.250	0.321	0.55	2650	1.37	0.064	1.000	0.75	0.052	0.805	116.364	0.778	3.13	1.05E+04
Oliveto & Hager (1999)	series	OH16	401	0.300	0.250	M	0.250	0.338	0.55	2650	1.37	0.064	1.000	21.35	0.081	1.258	116.364	0.739	4.69	3.00E+05
Oliveto & Hager (1999)	series	OH17	402	0.050	0.190	M	0.190	0.263	0.55	2650	1.37	0.257	1.000	14.10	0.035	0.134	467.273	0.723	0.19	3.75E+04
Oliveto & Hager (1999)	series	OH18	403	0.102	0.210	M	0.210	0.293	0.55	2650	1.37	0.257	1.000	70.50	0.178	0.693	467.273	0.718	0.39	2.07E+05
Oliveto & Hager (1999)	series	OH19	404	0.100	0.190	M	0.190	0.292	0.55	2650	1.37	0.257	1.000	66.17	0.061	0.235	467.273	0.651	0.39	1.76E+05
Oliveto & Hager (1999)	series	OH20	405	0.300	0.220	M	0.220	0.338	0.55	2650	1.37	0.257	1.000	45.42	0.155	0.603	467.273	0.650	1.17	1.40E+05

source/paper	label	test code(ref)	test #	h(m)	u(m/s) (data)	Velocity label	u (m/s) transformed	u c (m/s) (Melville)	d50 (mm)	ρ (kg/m^3)	σ	b(m)	lc(m)	t(hr)	ds(m)	Ds (ds/b)	D50 (b/d50)	U(u/uc) Melville	H (h/b)	T (tu/b)
Oliveto & Hager (1999)	series	OH21	406	0.098	0.260	M	0.260	0.291	0.55	2650	1.37	0.257	1.000	5.33	0.152	0.589	467.273	0.894	0.38	1.94E+04
Oliveto & Hager (1999)	series	OH22	407	0.201	0.220	M	0.220	0.321	0.55	2650	1.37	0.110	1.000	505.50	0.174	1.582	200.000	0.685	1.82	3.64E+06
Oliveto & Hager (2000)	series	OH23	408	0.092	0.710	M	0.790	0.786	5.30	2650	1.43	0.110	1.000	40.67	0.141	1.282	20.755	1.005	0.84	1.05E+06
Oliveto & Hager (2000)	series	OH24	409	0.080	1.080	M	1.193	0.762	5.30	2650	1.43	0.110	1.000	0.58	0.171	1.555	20.755	1.565	0.73	2.28E+04
Oliveto & Hager (2000)	series	OH25	410	0.077	0.980	M	1.080	0.756	5.30	2650	1.43	0.110	1.000	4.58	0.177	1.609	20.755	1.429	0.70	1.62E+05
Oliveto & Hager (2000)	series	OH26	411	0.153	0.670	M	0.767	0.874	5.30	2650	1.43	0.110	1.000	47.00	0.105	0.955	20.755	0.877	1.39	1.18E+06
Oliveto & Hager (2000)	series	OH27	412	0.145	0.820	M	0.936	0.865	5.30	2650	1.43	0.110	1.000	71.33	0.190	1.727	20.755	1.082	1.32	2.18E+06
Oliveto & Hager (2000)	series	OH28	413	0.049	0.710	M	0.762	0.678	5.30	2650	1.43	0.110	1.000	46.93	0.113	1.027	20.755	1.124	0.45	1.17E+06
Oliveto & Hager (2000)	series	OH29	414	0.053	0.690	M	0.744	0.691	5.30	2650	1.43	0.257	1.000	46.53	0.192	0.747	48.491	1.076	0.21	4.85E+05
Oliveto & Hager (2000)	series	OH30	415	0.045	0.430	M	0.459	0.663	5.30	2650	1.43	0.257	1.000	26.17	0.016	0.062	48.491	0.692	0.18	1.68E+05
Oliveto & Hager (2000)	series	OH31	416	0.092	0.670	M	0.746	0.786	5.30	2650	1.43	0.257	1.000	68.17	0.255	0.992	48.491	0.949	0.36	7.12E+05
Oliveto & Hager (2000)	series	OH32	417	0.100	0.540	M	0.604	0.801	5.30	2650	1.43	0.257	1.000	46.68	0.074	0.288	48.491	0.754	0.39	3.95E+05
Oliveto & Hager (2000)	series	OH33	418	0.088	0.950	M	1.055	0.779	5.30	2650	1.43	0.257	1.000	5.38	0.322	1.253	48.491	1.355	0.34	7.95E+04
Oliveto & Hager (2000)	series	OH34	419	0.099	0.730	M	0.816	0.799	5.30	2650	1.43	0.257	1.000	17.22	0.274	1.066	48.491	1.021	0.39	1.97E+05
Oliveto & Hager (2000)	series	OH35	420	0.153	0.620	M	0.709	0.874	5.30	2650	1.43	0.257	1.000	70.60	0.141	0.549	48.491	0.812	0.60	7.02E+05
Oliveto & Hager (2000)	series	OH36	421	0.047	0.710	M	0.760	0.671	5.30	2650	1.43	0.400	1.000	46.53	0.232	0.580	75.472	1.133	0.12	3.18E+05
Oliveto & Hager (2000)	series	OH37	422	0.143	0.660	M	0.753	0.862	5.30	2650	1.43	0.400	1.000	7.75	0.283	0.708	75.472	0.873	0.36	5.25E+04
Oliveto & Hager (2000)	series	OH38	423	0.151	0.500	M	0.572	0.872	5.30	2650	1.43	0.400	1.000	22.60	0.068	0.170	75.472	0.656	0.38	1.16E+05
Oliveto & Hager (2000)	series	OH39	424	0.050	0.680	M	0.731	0.681	5.30	2650	1.43	0.050	1.000	45.53	0.037	0.740	9.434	1.072	1.00	2.40E+06
Oliveto & Hager (2000)	series	OH40	425	0.046	0.950	M	1.016	0.667	5.30	2650	1.43	0.050	1.000	23.64	0.067	1.340	9.434	1.523	0.92	1.73E+06
Oliveto & Hager (2000)	series	OH41	426	0.200	0.650	M	0.789	0.920	5.30	2650	1.43	0.110	0.500	113.65	0.111	1.009	20.755	0.857	1.82	2.93E+06
Oliveto & Hager (2000)	series	OH42	427	0.048	0.260	M	0.260	0.377	1.20	2650	1.80	0.110	1.000	21.23	0.038	0.345	91.667	0.689	0.44	1.81E+05
Oliveto & Hager (2000)	series	OH43	428	0.051	0.300	M	0.300	0.382	1.20	2650	1.80	0.110	1.000	22.67	0.046	0.418	91.667	0.786	0.46	2.23E+05
Oliveto & Hager (2000)	series	OH44	429	0.204	0.270	M	0.270	0.478	1.20	2650	1.80	0.110	1.000	21.25	0.031	0.282	91.667	0.564	1.85	1.88E+05
Oliveto & Hager (2000)	series	OH45	430	0.203	0.320	M	0.320	0.478	1.20	2650	1.80	0.110	1.000	22.93	0.066	0.600	91.667	0.669	1.84	2.40E+05
Oliveto & Hager (2000)	series	OH46	431	0.203	0.240	M	0.240	0.478	1.20	2650	1.80	0.110	1.000	70.57	0.030	0.273	91.667	0.502	1.84	5.54E+05
Oliveto & Hager (2000)	series	OH47	432	0.048	0.270	M	0.270	0.377	1.20	2650	1.80	0.400	1.000	22.77	0.031	0.078	333.333	0.715	0.12	5.53E+04
Oliveto & Hager (2000)	series	OH48	433	0.048	0.330	M	0.330	0.377	1.20	2650	1.80	0.400	1.000	23.12	0.112	0.280	333.333	0.874	0.12	6.87E+04
Oliveto & Hager (2000)	series	OH49	434	0.199	0.280	M	0.280	0.477	1.20	2650	1.80	0.400	1.000	22.43	0.048	0.120	333.333	0.587	0.50	5.65E+04
Oliveto & Hager (2000)	series	OH50	435	0.201	0.320	M	0.320	0.477	1.20	2650	1.80	0.400	1.000	22.40	0.153	0.383	333.333	0.670	0.50	6.45E+04
Oliveto & Hager (2000)	series	OH51	436	0.199	0.240	M	0.240	0.477	1.20	2650	1.80	0.400	1.000	70.77	0.019	0.048	333.333	0.503	0.50	1.53E+05
Oliveto & Hager (2000)	series	OH52	437	0.049	0.310	M	0.310	0.379	1.20	2650	1.80	0.064	1.000	78.54	0.042	0.656	53.333	0.818	0.77	1.37E+06
Oliveto & Hager (2000)	series	OH53	438	0.085	0.870	M	0.958	0.648	3.10	2650	2.15	0.110	1.000	3.01	0.178	1.618	35.484	1.480	0.78	9.44E+04
Oliveto & Hager (2000)	series	OH54	439	0.101	0.590	M	0.656	0.670	3.10	2650	2.15	0.110	1.000	42.00	0.089	0.809	35.484	0.979	0.92	9.01E+05
Oliveto & Hager (2000)	series	OH55	440	0.196	0.500	M	0.574	0.754	3.10	2650	2.15	0.500	1.000	21.50	0.197	0.394	161.290	0.761	0.39	8.89E+04
Oliveto & Hager (2000)	series	OH56	441	0.046	0.580	M	0.617	0.568	3.10	2650	2.15	0.500	1.000	757.10	0.224	0.448	161.290	1.086	0.09	3.37E+06
Oliveto & Hager(2001)	series	OH57	442	0.103	0.590	M	0.659	0.753	4.30	2650	2.35	0.110	1.000	42.87	0.047	0.427	25.581	0.875	0.94	9.25E+05
Oliveto & Hager(2001)	series	OH58	443	0.100	0.710	M	0.792	0.749	4.30	2650	2.35	0.110	1.000	47.45	0.080	0.727	25.581	1.058	0.91	1.23E+06
Oliveto & Hager(2001)	series	OH59	444	0.072	1.130	M	1.238	0.698	4.30	2650	2.35	0.110	1.000	23.50	0.171	1.555	25.581	1.774	0.65	9.52E+05
Oliveto & Hager(2001)	series	OH60	445	0.058	0.520	M	0.563	0.665	4.30	2650	2.35	0.110	1.000	169.23	0.058	0.527	25.581	0.847	0.53	3.12E+06
Oliveto & Hager(2001)	series	OH61	446	0.055	0.650	M	0.701	0.657	4.30	2650	2.35	0.110	1.000	48.32	0.097	0.882	25.581	1.068	0.50	1.11E+06
Oliveto & Hager(2001)	series	OH62	447	0.065	0.650	M	0.708	0.682	4.30	2650	2.35	0.110	1.000	24.90	0.094	0.855	25.581	1.038	0.59	5.77E+05
Oliveto & Hager(2002)	series	OH63	448	0.091	0.540	M	0.599	0.734	4.30	2650	2.35	0.257	1.000	89.00	0.126	0.490	59.767	0.816	0.35	7.47E+05
Oliveto & Hager(2002)	series	OH64	449	0.094	0.680	M	0.756	0.739	4.30	2650	2.35	0.257	1.000	89.83	0.213	0.829	59.767	1.023	0.37	9.51E+05
Oliveto & Hager(2002)	series	OH65	450	0.195	0.570	M	0.658	0.852	4.30	2650	2.35	0.257	1.000	138.25	0.143	0.556	59.767	0.773	0.76	1.28E+06

source/paper	label	test code(ref)	test #	h(m)	u(m/s) (data)	Velocity label	u (m/s) transformed	u c (m/s) (Melville)	d50 (mm)	ρ (kg/m^3)	σ	b(m)	lc (m)	t (hr)	ds(m)	Ds (ds/b)	D50 (b/d50)	U(u/uc) Melville	H (h/b)	T (t.u/b)
Oliveto & Hager (1999)	series	OH66	451	0.150	0.370	M	0.420	0.372	3.30	1420	1.00	0.022	1.000	5.35	0.035	1.555	6.724	1.129	6.76	3.65E+05
Oliveto & Hager (1999)	series	OH67	452	0.101	0.330	M	0.367	0.345	3.30	1420	1.00	0.022	1.000	18.68	0.029	1.307	6.724	1.063	4.55	1.11E+06
Oliveto & Hager (1999)	series	OH68	453	0.051	0.290	M	0.311	0.299	3.30	1420	1.00	0.022	1.000	22.12	0.031	1.374	6.724	1.039	2.28	1.11E+06
Oliveto & Hager (1999)	series	OH69	454	0.250	0.280	M	0.280	0.406	3.30	1420	1.00	0.050	1.000	94.75	0.063	1.258	15.170	0.689	4.99	1.91E+06
Oliveto & Hager (1999)	series	OH70	455	0.151	0.340	M	0.386	0.373	3.30	1420	1.00	0.050	1.000	6.20	0.104	2.068	15.170	1.036	3.02	1.72E+05
Oliveto & Hager (1999)	series	OH71	456	0.150	0.360	M	0.409	0.372	3.30	1420	1.00	0.050	1.000	22.12	0.125	2.487	15.170	1.098	3.00	6.50E+05
Oliveto & Hager (1999)	series	OH72	457	0.102	0.340	M	0.378	0.346	3.30	1420	1.00	0.050	1.000	18.87	0.127	2.527	15.170	1.094	2.03	5.13E+05
Oliveto & Hager (1999)	series	OH73	458	0.148	0.230	M	0.230	0.371	3.30	1420	1.00	0.050	1.000	44.33	0.031	0.609	15.170	0.620	2.95	7.33E+05
Oliveto & Hager (1999)	series	OH74	459	0.050	0.230	M	0.230	0.298	3.30	1420	1.00	0.050	1.000	23.00	0.063	1.258	15.170	0.771	1.00	3.80E+05
Oliveto & Hager (1999)	series	OH75	460	0.100	0.390	M	0.434	0.345	3.30	1420	1.00	0.110	1.000	2.53	0.197	1.786	33.333	1.258	0.91	3.59E+04
Oliveto & Hager (1999)	series	OH76	461	0.103	0.340	M	0.379	0.347	3.30	1420	1.00	0.110	1.000	22.12	0.192	1.745	33.333	1.092	0.94	2.74E+05
Oliveto & Hager (1999)	series	OH77	462	0.053	0.320	M	0.344	0.302	3.30	1420	1.00	0.110	1.000	21.83	0.175	1.586	33.333	1.138	0.48	2.46E+05
Oliveto & Hager (1999)	series	OH78	463	0.150	0.290	M	0.290	0.372	3.30	1420	1.00	0.110	1.000	21.03	0.164	1.491	33.333	0.779	1.36	2.00E+05
Oliveto & Hager (1999)	series	OH79	464	0.106	0.290	M	0.290	0.349	3.30	1420	1.00	0.110	1.000	1125.00	0.213	1.936	33.333	0.832	0.96	1.07E+07
Oliveto & Hager (1999)	series	OH80	465	0.050	0.270	M	0.270	0.298	3.30	1420	1.00	0.110	1.000	17.08	0.146	1.327	33.333	0.906	0.45	1.51E+05
Oliveto & Hager (1999)	series	OH81	466	0.100	0.230	M	0.230	0.344	3.30	1420	1.00	0.110	1.000	65.00	0.088	0.800	33.333	0.668	0.90	4.89E+05
Oliveto & Hager (1999)	series	OH82	467	0.035	0.290	M	0.304	0.274	3.30	1420	1.00	0.110	1.000	20.77	0.145	1.314	33.333	1.109	0.32	2.07E+05
Oliveto & Hager (1999)	series	OH83	468	0.019	0.250	M	0.252	0.233	3.30	1420	1.00	0.110	1.000	43.62	0.098	0.891	33.333	1.082	0.17	3.60E+05
Oliveto & Hager (1999)	series	OH84	469	0.150	0.350	M	0.397	0.372	3.30	1420	1.00	0.257	1.000	21.83	0.321	1.249	77.879	1.068	0.58	1.21E+05
Oliveto & Hager (1999)	series	OH85	470	0.040	0.280	M	0.296	0.283	3.30	1420	1.00	0.257	1.000	22.42	0.207	0.804	77.879	1.045	0.16	9.29E+04
Oliveto & Hager (1999)	series	OH86	471	0.150	0.220	M	0.220	0.372	3.30	1420	1.00	0.257	1.000	21.20	0.082	0.319	77.879	0.591	0.58	6.53E+04
Oliveto & Hager (1999)	series	OH87	472	0.049	0.230	M	0.230	0.297	3.30	1420	1.00	0.257	1.000	23.00	0.178	0.693	77.879	0.775	0.19	7.41E+04
Oliveto & Hager (1999)	series	OH88	473	0.041	0.170	M	0.170	0.284	3.30	1420	1.00	0.257	1.000	70.00	0.030	0.115	77.879	0.599	0.16	1.67E+05
Chabert & Engeldinger (1952)	series	500	474	0.350	0.325	M	0.325	0.596	1.50	2680	1.39	0.050	0.800	233.83	0.114	2.271	33.333	0.545	7.00	5.47E+06
Chabert & Engeldinger (1952)	series	501	475	0.100	0.375	M	0.375	0.492	1.50	2680	1.39	0.050	0.800	139.13	0.112	2.246	33.333	0.763	2.00	3.76E+06
Chabert & Engeldinger (1952)	series	502	476	0.200	0.350	M	0.350	0.549	1.50	2680	1.39	0.050	0.800	210.75	0.124	2.483	33.333	0.637	4.00	5.31E+06
Chabert & Engeldinger (1952)	series	503	477	0.200	0.350	M	0.350	0.549	1.50	2680	1.39	0.100	0.800	227.25	0.191	1.912	66.667	0.637	2.00	2.86E+06
Chabert & Engeldinger (1952)	series	504	478	0.350	0.375	M	0.375	0.596	1.50	2680	1.39	0.050	0.800	116.13	0.114	2.275	33.333	0.629	7.00	3.14E+06
Chabert & Engeldinger (1952)	series	505	479	0.350	0.375	M	0.375	0.596	1.50	2680	1.39	0.100	0.800	113.81	0.194	1.941	66.667	0.629	3.50	1.54E+06
Chabert & Engeldinger (1952)	series	506	480	0.200	0.245	M	0.245	0.319	0.52	2680	1.39	0.050	0.800	156.28	0.080	1.603	96.154	0.769	4.00	2.76E+06
Chabert & Engeldinger (1952)	series	507	481	0.200	0.245	M	0.245	0.319	0.52	2680	1.39	0.075	0.800	156.28	0.113	1.511	144.231	0.769	2.67	1.84E+06
Chabert & Engeldinger (1952)	series	508	482	0.200	0.325	M	0.325	0.319	0.52	2680	1.39	0.050	0.800	72.73	0.110	2.199	96.154	1.020	4.00	1.70E+06
Chabert & Engeldinger (1952)	series	509	483	0.350	0.305	M	0.305	0.342	0.52	2680	1.39	0.050	0.800	119.25	0.103	2.056	96.154	0.892	7.00	2.62E+06
Chabert & Engeldinger (1952)	series	510	484	0.200	0.325	M	0.325	0.319	0.52	2680	1.39	0.100	0.800	73.85	0.136	1.356	192.308	1.020	2.00	8.64E+05
Chabert & Engeldinger (1952)	series	511	485	0.200	0.325	M	0.325	0.319	0.52	2680	1.39	0.050	0.800	143.11	0.103	2.056	96.154	1.020	4.00	3.35E+06
Mignosa, P. (1979/1980)	series	MI1	486	0.126	0.136	M	0.136	0.215	2.60	1180	1.32	0.027	0.495	216.00	0.056	2.079	10.269	0.632	4.72	3.96E+06
Mignosa, P. (1979/1980)	series	MI2	487	0.126	0.136	M	0.136	0.215	2.60	1180	1.32	0.048	0.495	216.00	0.080	1.656	18.462	0.632	2.63	2.20E+06
Mignosa, P. (1979/1980)	series	MI3	488	0.125	0.141	M	0.141	0.215	2.60	1180	1.32	0.027	0.495	213.50	0.055	2.041	10.269	0.656	4.66	4.06E+06
Mignosa, P. (1979/1980)	series	MI4	489	0.126	0.139	M	0.139	0.215	2.60	1180	1.32	0.027	0.495	71.00	0.053	1.966	10.269	0.646	4.72	1.33E+06
Mignosa, P. (1979/1980)	series	MI5	490	0.126	0.139	M	0.139	0.215	2.60	1180	1.32	0.048	0.495	71.00	0.072	1.500	18.462	0.646	2.63	7.40E+05
Mignosa, P. (1979/1980)	series	MI6	491	0.125	0.150	M	0.150	0.215	2.60	1180	1.32	0.027	0.495	190.50	0.064	2.404	10.269	0.698	4.68	3.85E+06
Mignosa, P. (1979/1980)	series	MI7	492	0.125	0.150	M	0.150	0.215	2.60	1180	1.32	0.048	0.495	190.50	0.086	1.781	18.462	0.698	2.60	2.14E+06
Mignosa, P. (1979/1980)	series	MI8	493	0.127	0.161	M	0.161	0.216	2.60	1180	1.32	0.048	0.495	166.50	0.094	1.958	18.462	0.745	2.65	2.00E+06
Mignosa, P. (1979/1980)	series	MI9	494	0.125	0.141	M	0.141	0.215	2.60	1180	1.32	0.048	0.495	213.50	0.064	1.329	18.462	0.656	2.59	2.26E+06
Mignosa, P. (1979/1980)	series	MI10	495	0.127	0.170	M	0.170	0.216	2.60	1180	1.32	0.048	0.495	95.50	0.046	0.954	18.462	0.789	2.65	1.22E+06

source/paper	label	test code(ref)	test #	h(m)	u(m/s) (data)	Velocity label	u (m/s) transformed	u c (m/s) (Melville)	d50 (mm)	ρ (kg/m^3)	σ	b(m)	lc (m)	t (hr)	ds(m)	Ds (ds/b)	D50 (b/d50)	U(u/uc) Melville	H (h/b)	T (t.u/b)
Mignosa, P. (1979/1980)	series	MI11	496	0.127	0.170	M	0.170	0.216	2.60	1180	1.32	0.048	0.495	95.50	0.098	2.042	18.462	0.789	2.65	1.22E+06
Mignosa, P. (1979/1980)	series	MI12	497	0.127	0.183	M	0.183	0.216	2.60	1180	1.32	0.048	0.495	237.50	0.042	0.879	18.462	0.849	2.65	3.26E+06
Mignosa, P. (1979/1980)	series	MI13	498	0.126	0.185	M	0.185	0.215	2.60	1180	1.32	0.048	0.800	237.50	0.096	2.000	18.462	0.857	2.63	3.29E+06
Franzetti, S. (1989)	series	FRANZ89	499	0.144	0.146	M	0.146	0.220	2.60	1180	1.32	0.048	0.495	1395.92	0.080	1.667	18.462	0.662	3.00	1.53E+07
Azzaroli, D. (1983)	series	AZAROLI	500	0.098	0.285	M	0.285	0.371	0.98	2635	1.320	0.030	0.500	96.17	0.072	2.400	30.612	0.768	3.27	3.29E+06
Raikar, V. R., Dey, S. (2005)	series	32C	501	0.250	0.761	M	0.920	0.875	4.10	2650	1.13	0.032	0.600	24.00	0.059	1.834	7.805	1.052	7.81	2.48E+06
Raikar, V. R., Dey, S. (2005)	series	38C	502	0.250	0.761	M	0.920	0.875	4.10	2650	1.13	0.038	0.600	24.00	0.074	1.958	9.268	1.052	6.58	2.09E+06
Raikar, V. R., Dey, S. (2005)	series	60c	503	0.250	0.761	M	0.920	0.875	4.10	2650	1.13	0.060	0.600	24.00	0.122	2.040	14.634	1.052	4.17	1.32E+06
Raikar, V. R., Dey, S. (2005)	series	77c	504	0.250	0.761	M	0.920	0.875	4.10	2650	1.13	0.077	0.600	24.00	0.163	2.119	18.780	1.052	3.25	1.03E+06
Raikar, V. R., Dey, S. (2005)	series	32C	505	0.250	0.833	M	1.011	0.973	5.53	2650	1.10	0.032	0.600	24.00	0.054	1.688	5.787	1.040	7.81	2.73E+06
Raikar, V. R., Dey, S. (2005)	series	38C	506	0.250	0.833	M	1.011	0.973	5.53	2650	1.10	0.038	0.600	24.00	0.066	1.739	6.872	1.040	6.58	2.30E+06
Raikar, V. R., Dey, S. (2005)	series	60c	507	0.250	0.833	M	1.011	0.973	5.53	2650	1.10	0.060	0.600	24.00	0.107	1.782	10.850	1.040	4.17	1.46E+06
Raikar, V. R., Dey, S. (2005)	series	77c	508	0.250	0.833	M	1.011	0.973	5.53	2650	1.10	0.077	0.600	24.00	0.150	1.951	13.924	1.040	3.25	1.13E+06
Raikar, V. R., Dey, S. (2005)	series	32C	509	0.250	0.905	M	1.102	1.060	7.15	2650	1.08	0.032	0.600	24.00	0.046	1.444	4.476	1.040	7.81	2.98E+06
Raikar, V. R., Dey, S. (2005)	series	38C	510	0.250	0.905	M	1.102	1.060	7.15	2650	1.08	0.038	0.600	24.00	0.055	1.447	5.315	1.040	6.58	2.51E+06
Raikar, V. R., Dey, S. (2005)	series	60c	511	0.250	0.905	M	1.102	1.060	7.15	2650	1.08	0.060	0.600	24.00	0.100	1.663	8.392	1.040	4.17	1.59E+06
Raikar, V. R., Dey, S. (2005)	series	77c	512	0.250	0.905	M	1.102	1.060	7.15	2650	1.08	0.077	0.600	24.00	0.132	1.716	10.769	1.040	3.25	1.24E+06
Raikar, V. R., Dey, S. (2005)	series	32C	513	0.250	1.010	M	1.235	1.188	10.25	2650	1.16	0.032	0.600	24.00	0.042	1.303	3.122	1.039	7.81	3.33E+06
Raikar, V. R., Dey, S. (2005)	series	38C	514	0.250	1.010	M	1.235	1.188	10.25	2650	1.16	0.038	0.600	24.00	0.053	1.387	3.707	1.039	6.58	2.81E+06
Raikar, V. R., Dey, S. (2005)	series	60c	515	0.250	1.010	M	1.235	1.188	10.25	2650	1.16	0.060	0.600	24.00	0.090	1.505	5.854	1.039	4.17	1.78E+06
Raikar, V. R., Dey, S. (2005)	series	77c	516	0.250	1.010	M	1.235	1.188	10.25	2650	1.16	0.077	0.600	24.00	0.121	1.570	7.512	1.039	3.25	1.39E+06

Appendix 2: Interpolation further attempts

In this part the formula obtained for f_1 (T), f_2 (D_{50}) and f_3 (U) in attempt number 2 and 3 for reaching to final results are presented. Then the measured vs. calculated diagram for each of these steps are also provided.

Attempt 2:

$$f_1(\mathrm{T} = 10^6) = 25.292 \tag{5.1}$$
$$f_1(\mathrm{T} = 10^5) = 18.925 \tag{5.2}$$

$$f_2(D_{50}) = {D_{50}}^{-0.43}.\exp\left(-5.1\,{D_{50}}^{-0.464}\right) \qquad 2 \leq D_{50} \leq 187 \tag{5.3}$$

$$f_3(U) = 103.5 - 293.26\,U^2 - 277.43 - U - 86.623 \qquad 0.8 \leq \mathrm{U} \leq 1.2 \tag{5.4}$$

Attempt 3:

$$f_1(\mathrm{T} = 10^6) = 20.978 \tag{5.5}$$
$$f_1(\mathrm{T} = 10^5) = 15.861 \tag{5.6}$$
$$f_2(D_{50}) = {D_{50}}^{-0.43}.exp\left(-5.1\,{D_{50}}^{-0.464}\right) \qquad 2 \leq D_{50} \leq 325 \tag{5.7}$$

$$f_3(U) = -5.226\,U^3 + 11.436\,U^2 - 5.947\,U + 1.1046 \qquad 0.48 \leq \mathrm{U} \leq 1.39 \tag{5.8}$$

Measured vs. Calculated graph

Attempt 2: (0.8<U<1.2):

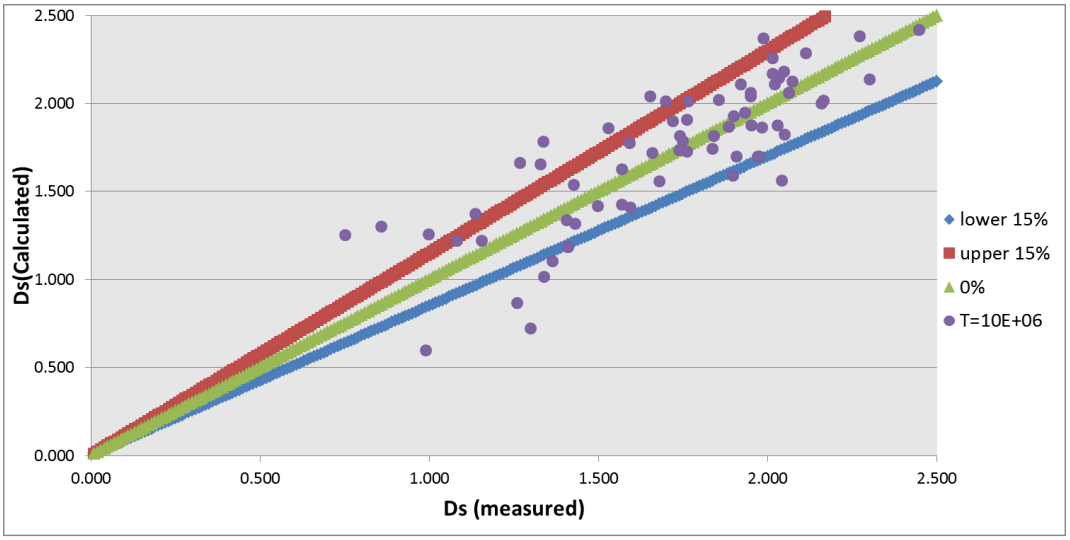

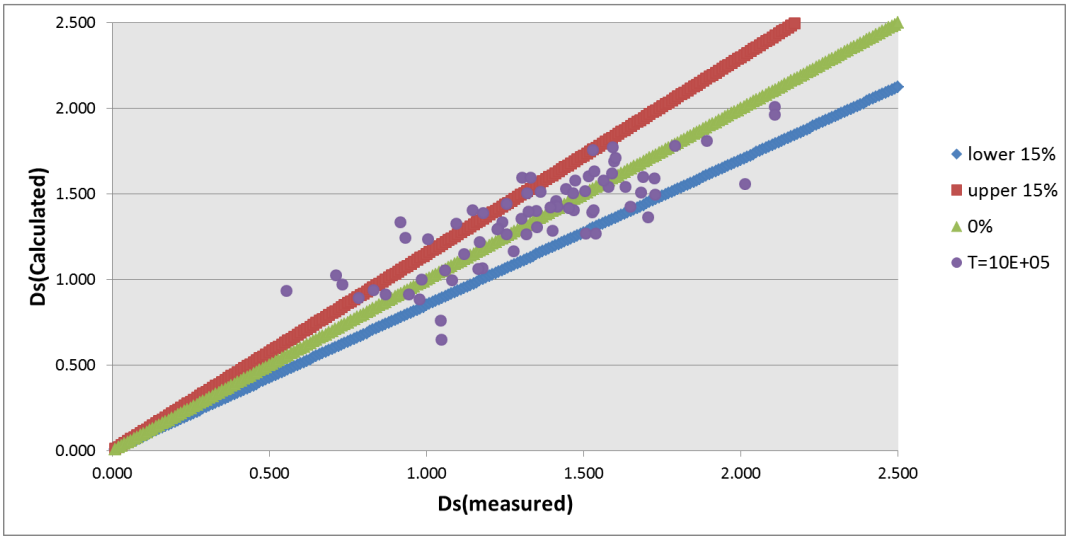
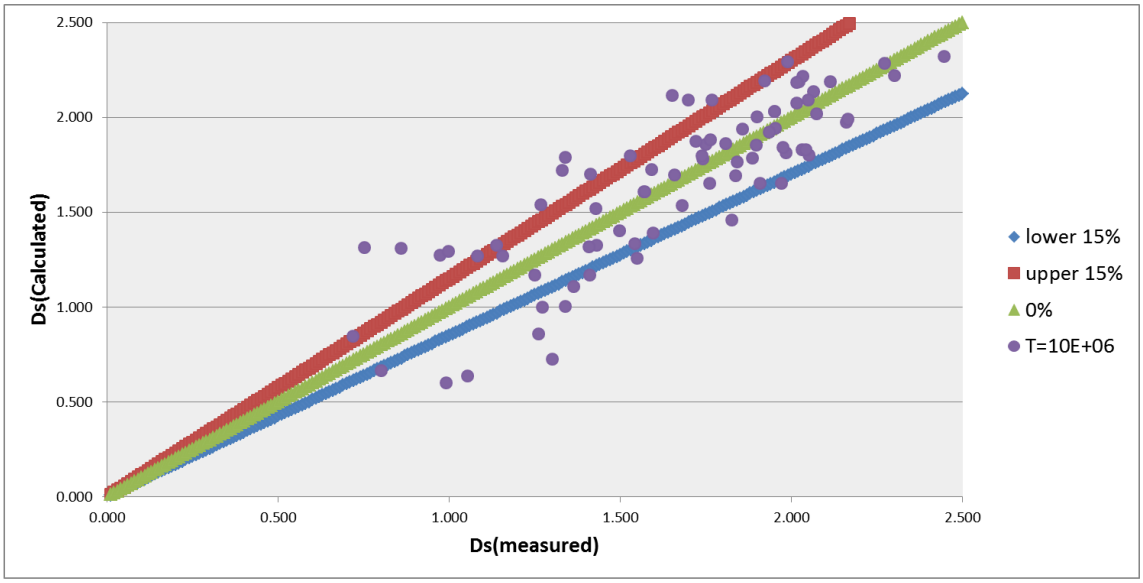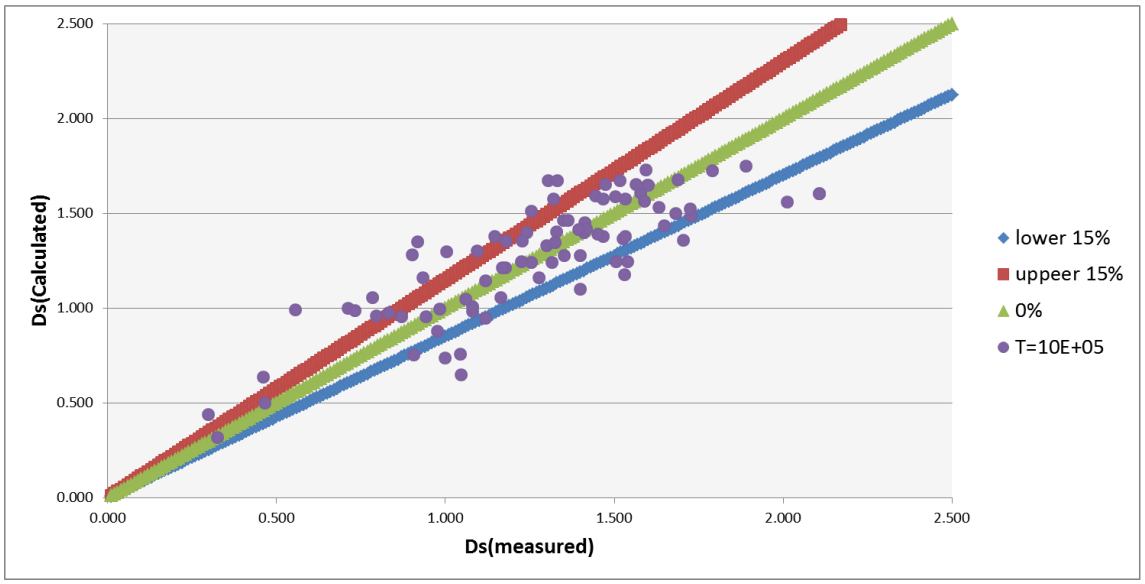
Attempt 3 (0.48<U<1.39):